



UNIVERSITÀ  
DI SIENA  
1240

University of Siena – Department of Medical Biotechnologies  
Doctorate in Genetics, Oncology and Clinical Medicine (GenOMeC)

XXXIII cycle (2017-2020)

Coordinator: Prof. Francesca Ariani

**Modeling of cancer immune phenotype by new epigenetic drugs:  
a strategy to improve efficacy of immunotherapy**

Scientific disciplinary sector: MED/06 – Medical Oncology

Tutor

Prof. Michele Maio

PhD Candidate

Sara Cannito

**Academic Year 2019/2020**

## Table of contents

### **RIASSUNTO**

### **ABSTRACT**

<b>1. INTRODUCTION .....</b>	<b>1</b>
1.1. Epigenetic regulation in health and disease .....	1
1.1.1. Epigenetic control of the gene expression.....	1
1.1.2. The role of epigenetics in cancer initiation and progression.....	7
1.1.2.1. DNA methylation in cancer and DNMT inhibitors .....	8
1.1.2.2. Histone acetylation and inhibition of HDACs in cancer .....	11
1.1.2.3. Targeting the lysine methyltransferase EZH2 .....	14
1.2. Malignant Mesothelioma biology .....	17
1.2.1. Risk factors and pathogenesis .....	17
1.2.2. The genetic and epigenetic landscape of mesothelioma.....	19
1.2.3. Epithelial-to-Mesenchymal Transition in mesothelioma .....	21
1.2.4. Standard treatments and novel immunotherapeutic strategies .....	23
<b>2. AIM OF THE THESIS .....</b>	<b>27</b>
<b>3. MATERIALS AND METHODS.....</b>	<b>28</b>
3.1. Cell lines.....	28
3.2. Total RNA isolation .....	28
3.3. Multiplexed gene expression analysis.....	29
3.4. Cell proliferation assay.....	30
3.5. Compounds preparation and schedule of treatments.....	30
3.6. Flow cytometry analysis and antibodies .....	31
3.7. DNase I treatment of RNA samples and reverse transcription.....	32
3.8. Real-time polymerase chain reaction (RT-PCR).....	32
3.9. Statistical analysis .....	33
<b>4. RESULTS.....</b>	<b>34</b>
4.1. nCounter gene expression panel analysis .....	34
4.2. Cytofluorimetric analysis of HLA class I antigens and ICAM-1 surface expression on MPM cell lines treated with combined epigenetic drugs .....	42

4.3.	Molecular analysis of gene expression of CTA expression on MPM cell lines treated with combined epigenetic drugs .....	43
4.4.	Molecular analysis of gene expression of PD-L1 expression on MPM cell lines treated with combined epigenetic drugs .....	45
4.5.	Molecular analysis of gene expression of NKG2DLs expression on MPM cell lines treated with combined epigenetic drugs .....	46
4.6.	Molecular analysis of gene expression of EMT-regulating genes on MPM cell lines treated with combined epigenetic drugs .....	47
<b>5.</b>	<b>DISCUSSION.....</b>	<b>50</b>
<b>6.</b>	<b>REFERENCES .....</b>	<b>55</b>
<b>7.</b>	<b>ACKNOWLEDGEMENTS .....</b>	<b>65</b>

## RIASSUNTO

Il mesotelioma pleurico maligno (MPM) è un tumore molto aggressivo e rapidamente progressivo che si sviluppa a livello del mesotelio che compone la pleura; questa neoplasia può assumere diversi sottotipi istologici (epitelioide, bifasico e sarcomatoide), i quali sono strettamente correlati alla prognosi. Le modificazioni epigenetiche che avvengono nelle fasi di iniziazione e progressione del MPM possono svolgere un ruolo fondamentale nel regolare negativamente il crosstalk tra tumore e sistema immunitario, contribuendo a mantenere un microambiente tumorale immunosoppressivo. Conoscere più dettagliatamente il panorama epigenetico del MPM può contribuire a definire il razionale per nuove terapie antitumorali e porre le basi per studi di combinazione che prevedano l'utilizzo di farmaci epigenetici con farmaci immunoterapeutici.

Con il presente studio abbiamo voluto valutare, in un primo momento, le modificazioni nel profilo di espressione genica di 10 linee di MPM, di diverso istotipo, trattate con la guadecitabina, un agente demetilante il DNA di seconda generazione, tramite la piattaforma nCounter di Nanostring. I risultati ottenuti tramite Ingenuity Pathway Analysis (IPA) hanno mostrato che la guadecitabina era in grado di indurre l'attivazione dei geni coinvolti nel crosstalk tra cellule dendritiche e natural killer nel 50% delle linee cellulari di MPM indagate, accompagnata dall'attivazione di altre componenti coinvolte nella risposta immunitaria a infezioni e infiammazioni. I fattori trascrizionali "upstream" più frequentemente attivati appartenevano al pathway di segnalazione dell'interferon (IFN)- $\gamma$ . Inoltre, è stata riscontrata l'up-regolazione (fold change medio (mFC)  $\geq 1.5$ ) di molecole immuno-relate, come NY-ESO-1 (mFC=13.16), MAGE-B2 (mFC=13.09), CD70 (mFC=5.27) e CTLA-4 (mFC=4.81). Abbiamo inoltre effettuato analisi istotipo-specifiche per esplorare le modificazioni molecolari indotte dalla guadecitabina nei 3 sottotipi di MPM. La guadecitabina ha indotto l'up-regolazione dell'espressione di marcatori del fenotipo epiteliale (es. CDH1, EPCAM e PECAM1), osservata ad alti livelli nelle linee cellulari sarcomatoidi; ciò è stato associato alla down-regolazione di molecole di origine mesenchimale (es. CDH2 e NCAM) e induttori della cascata metastatica (es. CDH11).

Successivamente abbiamo comparato gli effetti immunomodulatori della guadecitabina con quelli di altri farmaci epigenetici (gli inibitori delle iston acetiltransferasi (HDAC) VPA e SAHA o l'inibitore di EZH2 EPZ-6438) da soli o in combinazione con la guadecitabina in 5 linee cellulari di MPM (2 sarcomatoidi, 1 bifasica e 2 epitelioidi). Analisi citofluorimetriche e molecolari hanno rivelato che la guadecitabina up-regolava l'espressione delle molecole immuno-relate, quali HLA di classe I (mFC=1.59), ICAM-1 (mFC=3.27), PD-L1 (mFC=2.13), e NKG2DL (MICA mFC=1.88, MICB mFC=2.42, ULBP2 mFC=3.16), inducendo/up-regolando l'espressione dei Cancer Testis Antigens (CTA) NY-ESO-1, MAGE-A1 e MAGE-A3; il VPA up-regolava l'espressione degli antigeni di HLA di classe I (mFC=1.50), PD-L1 (mFC=2.76), NKG2DL (MICA mFC=1.69, MICB mFC=2.67, ULBP2 mFC=3.26) e quella dei CTA MAGE-A1 e MAGE-A3, rispettivamente in 2/5 e 3/5 linee cellulari di

MPM; il SAHA up-regolava l'espressione di MICA (mFC=1.57), MICB (mFC=4.05) e MAGE-A1 e MAGE-A3, rispettivamente in 2/5 e 4/5 linee cellulari; per contro, l'EPZ-6438 ha mostrato minime capacità immunomodulanti, inducendo solamente NY-ESO-1 e up-regolando l'espressione di PD-L1, MICB e ULBP2 in 1 linea cellulare ciascuno. Contrariamente ai risultati eterogenei ottenuti dai singoli farmaci, l'associazione di VPA, SAHA o EPZ-6438 alla guadecitabine ha rafforzato le capacità immunomodulanti di quest'ultima, influenzando l'espressione di tutte le molecole indagate. Specificatamente, le combinazioni di guadecitabine con VPA, SAHA o EPZ-6438 up-regolavano l'espressione degli antigeni HLA di classe I (mFC=2.21, 2.03, o 2.29 rispettivamente), di ICAM-1 (mFC=4.09, 4.63, o 5.33), di PD-L1 (mFC=6.95, 2.42, o 2.50), di MIC-A (mFC=3.48, 2.00, o 2.23), di MIC-B (mFC=6.80, 2.48, o 2.81) e di ULBP2 (mFC=13.45, 3.40, o 4.11). Infine, livelli di up-regolazione/induzione maggiori sono stati osservati per i CTA a seguito di tutti e 3 i trattamenti combinati rispetto alla guadecitabina in singolo. La modulazione delle caderine è stata influenzata dal sottotipo istologico di MPM: l'espressione di CDH1 è stata indotta dalla guadecitabina in singolo e dalla sua combinazione con VPA, SAHA e EPZ-6438 nelle 2 linee cellulari sarcomatoidi, costitutivamente negative per l'espressione del gene; l'espressione di CDH2 è stata up-regolata dal VPA e dal SAHA singoli in 1/5 linee cellulari e dalle combinazioni di guadecitabina con VPA o SAHA, rispettivamente in 3/5 o 1/5 linee cellulari di MPM; ciononostante, non è stata osservata alcuna up-regolazione del gene nelle 2 linee cellulari epiteliodi, costitutivamente negative per l'espressione di CDH2.

In conclusione, dalle analisi approfondite del pannello di espressione genica abbiamo confermato che la guadecitabina è in grado di up-regolare/indurre l'espressione di molecole immunitarie e immuno-relate cruciali per il crosstalk tra il tumore e il sistema immunitario; inoltre, abbiamo dimostrato che essa induce l'attivazione di geni correlati all'IFN, soprattutto nel fenotipo sarcomatoide, supportando l'ipotesi che i demetilanti possano aumentare la risposta immunitaria contro il MPM, potenzialmente anche del tipo istologico più aggressivo; la modulazione delle molecole di adesione tendente verso il fenotipo epitelioide suggerisce la possibilità di revertire la transizione epitelio-mesenchima, cruciale nel processo di metastatizzazione. Infine, combinando la guadecitabina con farmaci inibitori delle HDAC/EZH2 ha rafforzato la sua attività immunomodulante, fornendo il razionale per studi di associazione di farmaci epigenetici e agenti immunoterapici in modo da aumentare l'efficacia di questi ultimi nel trattamento del mesotelioma.

## ABSTRACT

Malignant pleural mesothelioma (MPM) is a highly aggressive and rapidly progressive tumor that affect the mesothelium composing the pleura; it can acquire different histological subtypes (mainly epithelioid, biphasic, and sarcomatoid MPM), which are of prognostic significance. Epigenetic modifications occurring during MPM initiation and progression may play a relevant role in negatively regulating the crosstalk between the tumor and the immune system, as well as contributing to the highly immunosuppressive microenvironment. A better understanding of MPM epigenetics will contribute to refine antitumor strategies, laying the ground for epigenetic-based immunotherapy.

The present study evaluated, in the first instance, changes in the gene expression fingerprint of 10 MPM cell lines of different phenotype treated with the second-generation DNA hypomethylating agent (DHA) guadecitabine, through the Nanostring Oncology panel with nCounter readout. Ingenuity pathway analysis results revealed that guadecitabine induced the activation of natural killer and dendritic cells signaling pathways in 50% of MPM cell lines, followed by the activation of other components involved in the immune system response to infections and inflammation. Besides, the most frequently activated upstream regulators belonging to the interferon (IFN)- $\gamma$  signaling pathway. Also, the up- regulation (mean fold change (mFC)  $\geq 1.5$ ) of key immune-related molecules, such as the NY-ESO-1 (mFC=13.16), MAGE-B2 (mFC=13.09), CD70 (mFC=5.27), and CTLA-4 (mFC=4.81) was reported.

We also performed histological type-specific investigations to explore molecular changes induced by guadecitabine among the 3 histotypes. Guadecitabine induced the up-regulation of the expression of epithelial markers (*e.g.*, CDH1, EPCAM, PECAM1), observed at higher levels in sarcomatoid cell lines; this was accompanied by the down-regulation of mesenchymal origin molecules (*e.g.*, CDH2, NCAM), and inductor of metastatic signals (*e.g.*, CDH11).

Secondly, the immunomodulatory effects of guadecitabine were compared to those of different epigenetic drugs (the histone deacetylase (HDAC) inhibitors VPA and SAHA, or the EZH2 EPZ-6438), alone or in combination with guadecitabine, in 5 MPM cell lines (two sarcomatoid, one biphasic, and two epithelioid). We performed cytofluorimetric and molecular qRT-PCR analyses and, in this regard, results showed that guadecitabine up-regulated the expression of immune-related molecules, such as HLA class I antigens (mFC=1.59), ICAM-1 (mFC=3.27), PD-L1 (mFC=2.13), and NKG2DLs (MIC-A mFC=1.88, MIC-B mFC=2.42, and ULBP2 mFC=3.16), and up-regulated/induced Cancer Testis Antigens (CTA: NY-ESO-1, MAGE-A1, and MAGE-A3) expression; VPA up-regulated the expression of HLA class I antigens (mFC=1.50), PD-L1 (mFC=2.76), NKG2DLs (MIC-A mFC=1.69, MIC-B mFC=2.67, and ULBP2 mFC=3.26), and the expression of CTA MAGE-A1 and MAGE-A3 in 2/5 and 3/5 MPM cell lines, respectively; SAHA up-regulated the expression of MICA (mFC=1.57), MICB (mFC=4.05), MAGE-A1 and MAGE-A3 in 2/5 and 4/5 MPM

cell lines, respectively; conversely, EPZ-6438 induced minimal immunomodulatory effects, inducing only NY-ESO-1 and up-regulating PD-L1, MIC-B, and ULBP2 expression in 1 MPM cell line each. Despite the heterogeneous activities of single epigenetic drugs, the addition of both VPA, SAHA, and EPZ-6438 to guadecitabine strengthened the immunomodulatory effects of the latter, by affecting the expression of all investigated molecules. Specifically, guadecitabine plus VPA, SAHA, or EPZ-6438 upregulated the expression of HLA class I antigens mFC=2.21, 2.03, or 2.29; ICAM-1 mFC=4.09, 4.63, or 5.33; PD-L1 mFC=6.95, 2.42, or 2.50; MIC-A mFC=3.48, 2.00, or 2.23; MIC-B mFC=6.80, 2.48, or 2.81; ULBP2 mFC=13.45, 3.40, or 4.11, respectively. Lastly, higher levels of upregulated/induced CTA expression were observed after all 3 combination treatments versus guadecitabine alone. Cadherins modulation was MPM histotype-related: CDH1 expression was induced in the 2 constitutive-negative sarcomatoid MPM cell lines by guadecitabine alone or combined with VPA, SAHA, or EPZ-6438; CDH2 expression was upregulated by VPA or SAHA in 1/5 cell lines, and by guadecitabine plus VPA or SAHA in 3/5 or in 1/5 MPM cell lines, respectively; however, no induction of CDH2 have been reported in the constitutive negative epithelioid cell lines. Overall, from comprehensive gene expression panel analyses, we confirmed that guadecitabine induced/up-regulated the expression of immune and immune-related molecules, pivotal in the tumor-immune system crosstalk; also, we highlighted that guadecitabine-induced activation of IFN-related genes, especially in the sarcomatoid phenotype, supporting the hypothesis that DHA could increase the immune response against MPM, potentially also with sarcomatoid features; moreover, the modulation of adhesion molecules towards the epithelial type suggests the possibility to revert the epithelial-to-mesenchymal transition (EMT) event, crucial in the invasion-metastasis cascade. Also, combining guadecitabine with HDACi/EZH2i strengthened its immunomodulatory capabilities, laying the rationale for epigenetic drugs-based immunotherapies, to enhance efficacy of these strategy in the MPM clinic.

# 1. Introduction

## 1.1. Epigenetic regulation in health and disease

### 1.1.1. Epigenetic control of the gene expression

Epigenetic mechanisms refer to a series of potentially reversible and heritable changes in the chromatin structure and in the gene expression, which address the tissue-specific transcription and conserve cell identity, inducing changes in the phenotype, without altering the underlying nucleotide sequence (Esteller, 2008). Through interconnected biochemical modifications of DNA and histone/non-histone proteins, as well as by the activity of highly controlled remodellers/regulators, genes can be switched “on” or “off”, determining which proteins are transcribed at a specific time and in a particular cell type, in response to extracellular signals. The epigenetic landscape of complex organisms is set out during cell differentiation processes, playing a pivotal role in embryogenesis, but also involving a dynamical pattern of responses during critical stages such as pregnancy, the post-natal period and, to a lower extent, in later life. Epigenetic modifications are responsible, for example, for genomic imprinting processes, as well as for the inactivation of the X chromosome in female mammals, through events of initiation, spreading and maintenance of gene silencing (Hassler, 2012). In addition, epigenetic regulation plays as an interface between the genome and the environment, being characterized by plasticity in response to several factors, such as aging and environment/lifestyle. These mechanisms are potential source of missing heritability in complex traits. Theoretically, only germline heritable epigenetic events may contribute to the missing heritability, as opposed to the non-germline heritable components (inherited through mitosis or somatic epigenetic events). Identical twins, developed from a single fertilized egg, have the same genome, so any differences between twins are due to their epigenetics, not genetics. Since epigenetic modifications are involved in gene regulation during differentiation and homeostasis with the ability to integrate environmental stimuli, it is not surprising that abnormalities in these mechanisms have been linked to a wide range of diseases (Portela, 2010). In higher-order eukaryotes, epigenetic marks include principally DNA methylation, post-translational modifications (PTMs) of histone proteins, chromatin remodelling components, histone variant exchange, and non-coding RNAs. The most studied mechanism of epigenetic regulation is the DNA methylation, elicited by the addition of a methyl (-CH<sub>3</sub>) group to the 5' carbon of cytosine to become 5-methylcytosines (Fig. 1). It affects especially small regions of DNA (<500 bp) enriched in cytosine-guanosine dinucleotides, known as CpG islands, owning a CG content greater than 55%. CpG-rich DNA is usually clustered around the promoter region of the gene and the methylation process can affect the transcriptional regulation of this gene. CpG sites

are methylated by the DNA methyltransferase (DNMT) enzymes, epigenetic “writers” that establish the mark, crucial for the normal development as evidenced by studies of embryology (Li, 1992; Egger, 2004). DNMTs are mainly grouped in enzymes performing de novo methylation, and those in charge to stably maintain the methylation patterns; all of them catalyse the reaction of methylation using the S-adenosyl-L-methionine (SAM) as the methyl groups donor. Currently, there are five known mammalian DNMTs and DNMT-like proteins: DNMT1, DNMT2, DNMT3A, DNMT3B, and DNMT3L (Robertson, 2002). The most abundant is the DNMT1, responsible for the maintenance of the methylation patterns on hemi-methylated replicating DNA within cell division, while de novo DNMTs, such as DNMT3A and DNMT3B, define the methylation fingerprint on unmethylated DNA (Morris, 2014). Methylation at CpG sites can be recognized by “readers” such as the methyl-CpG binding domain protein 1 (MBD1) and the methyl-CpG binding protein 2 (MeCP2), inducing repression. Besides classic CpG methylation, non-CpG methylation has been detected in embryonic stem cells at high levels (Pulverer, 2012). CpGs are hot spots for mutation, as 5-methylcytosine (5mC) can spontaneously undergo hydrolytic deamination to thymine (Smith, 2013), resulting in a mismatch with guanine opposite to the original 5mC. Conversely, methyl groups can be erased within active/passive demethylation pathways, followed by glycosylation and replacement with an unmethylated cytosine (Emran, 2019). Indeed, ten-eleven translocation (TET) cytosine oxygenases have been found to oxidase 5mC to 5-hydroxymethylcytosine (5hmC) (Fig. 1), present prevalently in neurons and embryonic stem cells, and further products. This methylation state has been defined as a demethylation intermediate, but some studies underline its role as an active epigenetic mark (Szulwach, 2011), associated with transcriptional activation, even though specific involvements in different contexts is yet to be elucidated (Branco, 2012).

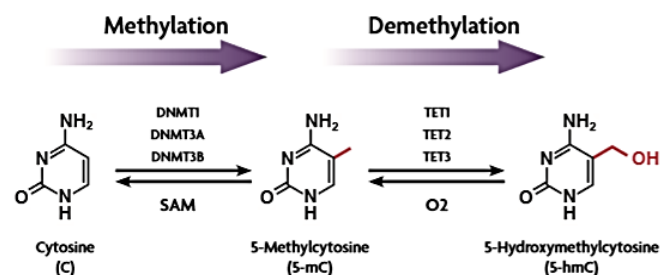


Figure 1 – Regulation of DNA methylation/demethylation. Cytosine conversion in methylated cytosine, through DNMTs, and demethylation to 5-hydroxymethylcytosine by TET enzymes.  
From Hong-Wei Y., *J of Pharma Exp Ther*, 2015.

Another important mechanism of epigenetic regulation involves PTMs of histones. Histone proteins are key component of chromatin, which fundamental unit is the nucleosome. In eukaryotes, it consists of 147 base pairs of DNA wrapped around a histone octamer, the histone core, comprised of two copies for

each H2A, H2B, H3, and H4, while H1 acts as linker protein (Fig. 2).

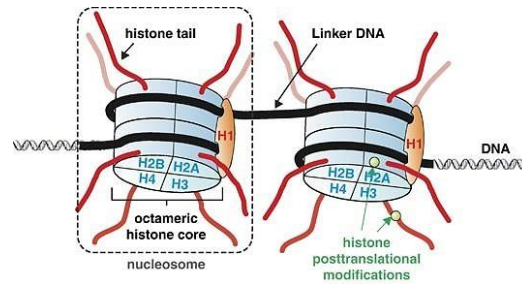


Figure 2 - Schematic representation of the organization and packaging of elements of the nucleosome. From Füllgrabe, J., *Oncogene*, 2011.

Histones have got a specific structural and functional organization due to their role in the dynamic regulation of gene transcription, by controlling accessibility of nuclear transcription factors and RNA polymerase to regulatory DNA elements. Different amino acids of histone amino-terminal tails are subject to PTMs, including methylation, acetylation, phosphorylation, ubiquitylation, and sumoylation, even though several others have been reported (Kouzarides, 2007) (Fig. 3).

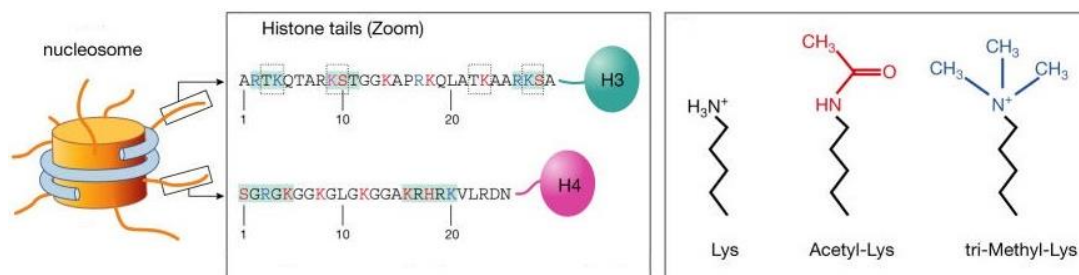


Figure 3 - Post-translational modifications on histone tails; in red are shown amino acids interested by acetylation, while in blue the ones potentially affected by methylation. Lys: lysine. From Bottomley, M. J., *EMBO Rep*, 2004.

These covalent modifications can shape chromatin conformation in different ways: as a results of certain events, such as acetylation of lysine residues responsible for breaking down the positive charge of lysines, the chromatin structure is released facilitating the transcription; conversely, if the affinity between histones and DNA is enhanced, chromatin is condensed in form of heterochromatin, resulting in the inactivation of transcription, as observed for histone sumoylation (Shiio, 2004).

Acetylation and deacetylation are the most abundant and studied histone modifications, controlled by epigenetic writers, known as histone acetyltransferases (HATs) which lay the acetyl group, and erasers, called histone deacetylases (HDACs) which remove marks. The acetylation reaction consists in the transfer of an acetyl ( $\text{CH}_3\text{CO}-$ ) group from the acetyl-CoA to the  $\epsilon$ -amino group of the histone lysine. HATs can act on histone and non-histone protein and work through the HAT domains, who mediate acetylation, which are then recognized by bromodomains (“readers” of the mark) for the activation of

the signal. The acetylating enzymes comprise different families and are associated with cofactors that, making complexes, can direct both gene-specific and genome-wide acetylation (Bottomley, 2004). Some coactivator molecules, such as the CREB-binding protein (CBP) and its homologue p300, act as molecular switches that control gene transcription activation and both have intrinsic HAT activity (Chan, 2001). So, the structure of chromatin can be regulated within a cascade of intracellular signaling, involving cAMP, Ca<sup>2+</sup>, and ERK (Yuan, 2001). In contrast, HDACs, which remove the acetyl groups from lysine residues, confer to the latter a positive charge with the concomitant rearrangement of additional lysine PTMs, and the suppression of gene transcription (Seto, 2014). HDACs operate in complexes with corepressors and can act either on acetyl-lysine residues of histones tails or on non-histone proteins, such as the transcription factor p53 (Vaziri, 2001). The 18 HDACs known are classified in four classes, based on the homology with yeast enzyme counterparts (Fig. 4): class I enzymes (HDAC1, HDAC2, HDAC3, and HDAC8); class II HDACs (HDAC4, HDAC5, HDAC6, HDAC7, HDAC9, and HDAC10); class III HDACs (SIRT1, SIRT2, SIRT3, SIRT4, SIRT5, SIRT6, and SIRT7), known as Sirtuins; and class IV (HDAC11) which share only a weak homology with both class I and II HDACs. Class I, II, and IV are known as “classical” HDACs, sharing structural and functional homologies. They belong to the arginase/deacetylase superfamily, containing both the deacetylase and the arginase-like amidino hydrolase activity. The latter activity is explicated through a zinc finger-binding domain, required for the ion-dependent catalysis of the acetamide bond in acetylated lysine. Conversely, class III HDACs exert a NAD<sup>+</sup>-dependent mechanism of deacetylation through the NAD/FAD-binding domain, producing nicotinamide and the 2'-O-acetyl-ADP-ribose metabolite (Seto, 2014). Many of these HDAC substrates regulate proteins involved in different processes, such as cell-cell adhesion, cell division, and apoptosis. In particular, HDAC-1,-2, and -3 repress genes involved cell cycle regulation (Gui, 2004); HDAC8 regulates cell proliferation (Vannini, 2004); HDAC-4, -5, -7, and -9 recruit repressors on specific genomic regions, inhibiting gene transcription (Di Giorgio, 2016); HDAC6 controls cell migration, protein folding, mis-folded proteins degradation, cellular stress, immune synapse formation, and oncogenic tumorigenesis (Valenzuela-Fernández, 2008; Matthias, 2008; Lee, 2008). Given that histone PTMs modulates chromatin structure and gene expression, it is not surprising that abnormal events of acetylation are associated with multiple diseases, including cancer, interstitial fibrosis, autoimmune and inflammatory diseases, and metabolic disorders (Tang, 2013).

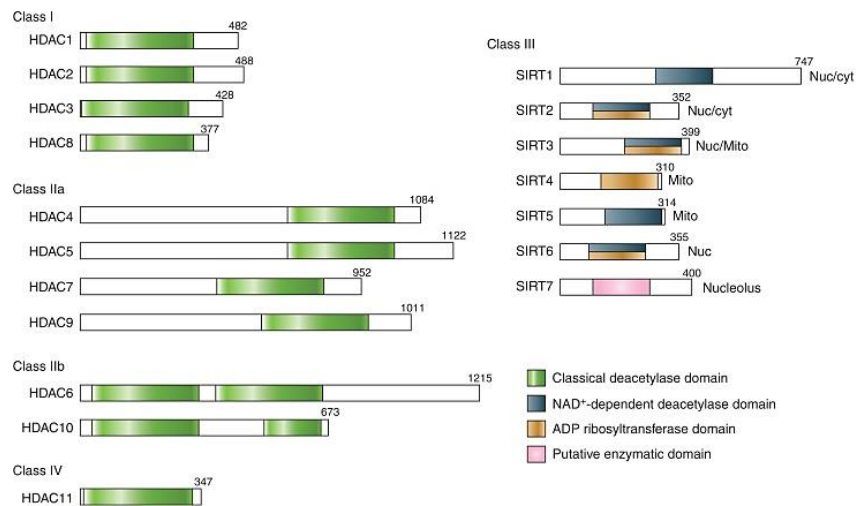


Figure 4 – Representation of different classes of HDACs. Enzymatic domains are shown in colours. From Seto, E., *Cold Spring Harb Perspect Biol*, 2014.

Besides acetylation, methylation of histone tails is one of the major epigenetic PTMs, interesting arginine and, more commonly, lysine (K) residues. The effect of histone methylation depends on histone isoforms and lysine position at the level of N-terminal residue, as well as on the extent of methylation. Methylation of histone lysines is catalysed by lysine methyltransferase (KMT) and removed by lysine demethylase (KDM) enzymes. KDMs play a role both in repression (H3K4 demethylation) and activation (H3K9 demethylation) of transcription, and it has been reported their involvement in mental disorder development as well as cancer (Tahiliani, 2007; Kaniskan, 2018). Canonical lysine methylation sites are found on histone 3 at lysine 4 (H3K4), 9 (H3K9), 27 (H3K27), 36 (H3K36), or 79 (H3K79), and on histone H4 at lysine 20 (H4K20), regulating chromatin structure (Cao, 2015); also, other non-canonical sites have been described, but are much less characterized. Methylated sites on histones are recognized by chromodomains of proteins associated with chromatin remodelling, acting as readers of this specific mark. In this context, two of the most studied chromatin-modifying complexes include the evolutionary-conserved components of the Polycomb and Trithorax groups, operating as antagonists in the regulation of the development. Both groups are recruited directly on DNA motifs, through the recognition of Polycomb/Trithorax response elements (PRE/TRE), which, based on the recruited component, maintain a repressed/active transcriptional state, driving the epigenetic inheritance (Schuettengruber, 2017). Repression of gene expression is mediated by a Polycomb multiprotein system that include the Polycomb-Repressive Complex 1 (PRC1) and 2 (PRC2), and targets H3K27 and H3K9 methylation. The enhancer of zeste homolog (EZH) proteins, notably EZH1 and EZH2, are components of the catalytic subunit of the PRC2 machinery, mediating an independent silencing of gene expression through the H3K27me<sub>3</sub> mark (Tan, 2014). In comparison to EZH2, EZH1 holds a low histone methyltransferase activity and its knockdown does not result in the global reduction of H3K27me<sub>2/3</sub> levels (Margueron,

2008). The PRC2 machinery involve, overall, five subunits (EZH1/2, EED, SUZ12, RbAp46/48, AEBP2) which predominantly exert the methyltransferase activity through the C-terminal SET domain of EZH2, followed by a cascade of downstream events (Fig. 5). The complex is stabilised by non-catalytic subunits, which are also crucial for triggering the enzymatic function of EZH2 (Blackledge, 2015). Pathologic activation of the transcriptional repressor EZH2 is one of the most studied features observed in human cancers, and plays a key role in cell growth and differentiation (Bracken, 2003; Bryant, 2007; Qi, 2013), survival (Varambally, 2002), tumor invasion (Bracken, 2003; Bryant, 2007), and metastasis (Varambally, 2002; Mahmoud, 2016). In contrast to Polycomb multiprotein system, the Trithorax group proteins target H3K4 methylation, maintaining an active state of the gene expression.

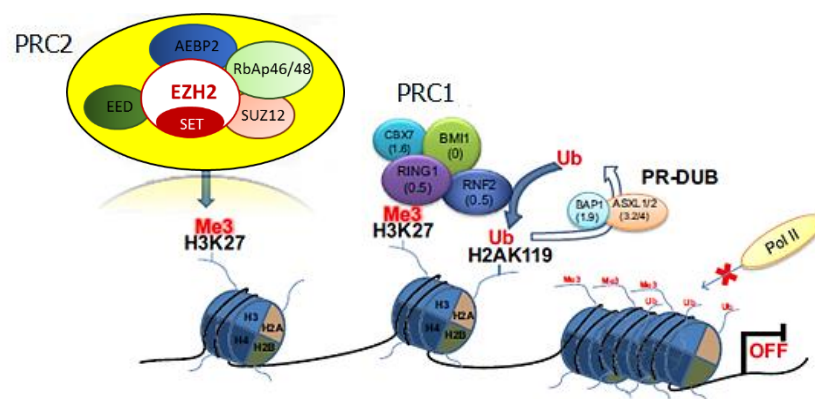


Figure 5 - The PRC2 complex mediates, through the SET domain of EZH2, the tri-methylation of lysine 27 on H3 histones (H3K27me3); after that PRC1, mediating the mono-ubiquitination of lysine 119 on histone H2A (H2AK119ub) is recruited, additional epigenetic enzymes are retrieved, compacting the chromatin structure. Edited from Marchese, I., *Chromatin Remodelling*, 2012.

Overall, despite DNA methylation and histone PTMs are executed by different cellular machinery (all generally classified as writers, erasers, and readers), both are dynamically linked and act synergistically to regulate transcription. Therefore, it is now widely recognized that a significant interplay exists among these epigenetic modulation events. Histone modifications have been shown to induce DNA methylation, a process especially observed during the early development, regulating also the stability of DNMT enzymes (Cedar, 2009; Esteve, 2009). Once established, methylated CpGs are recognized by methyl-CpG-binding proteins, such as MeCP2, which form a complex with histone deacetylase and histone methyltransferases, acting as transcription co-repressive complexes (Feng, 2001; Cedar, 2009). Additionally, to explicate the local histone code, epigenetic rearrangements might be required: for example, if PRC2 is commissioned to methylate H3K27 but this lysine residue is acetylated, HDACs are recruited, making the amino-group of lysine side chain available for the PRC2-mediated methylation (Tan, 2014).

### 1.1.2. The role of epigenetics in cancer initiation and progression

The epigenetic machinery is well known to be implicated in various physiological and pathological events, among the latter neurological disorders (Egger, 2004), asthma (Adcock, 2005), diabetes (Jones, 2007), autoimmunity (Javierre, 2010), and cancer (Jones, 2007). Since genetics alone does not provide an adequate explanation for the complexity of cancer, a comprehensive understanding of the role of epigenetics in cancer might unveil key mechanisms underlying its development and progression. In most cases, besides genetic alterations, the fine control of epigenetic mechanisms is lost; indeed, malignant cells harbour aberrations in DNA methylation and histone modifications, deregulation of non-coding RNAs (*e.g.*, microRNA, long non-coding RNA), as well as alterations of numerous regulatory factors (Fig. 6). Genome sequencing revealed mutations in chromatin proteins in almost 50% of human cancers (You, 2012; Shen, 2013), and disruption of chromatin structure can induce inappropriate gene expression and genomic instability, resulting in the malignant transformation.

Being epigenetics modifications recognized as the key modulator of plasticity, their reversible nature makes them good therapeutic targets to potentially revert cancer-relevant processes by using specific inhibitors.

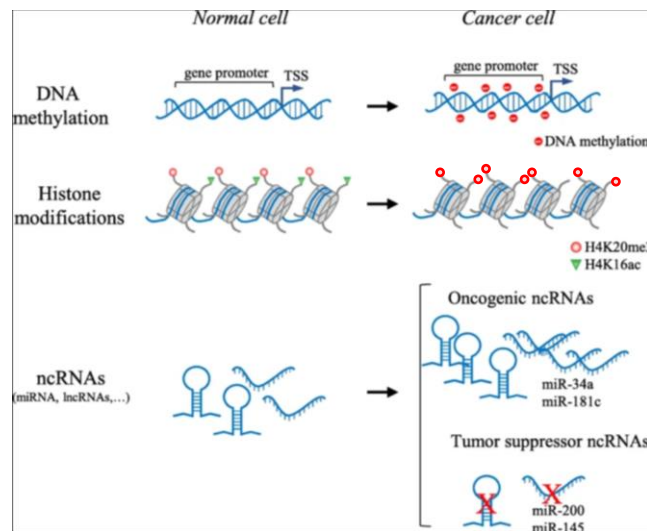


Figure 6 – Main epigenetic abnormalities in cancer. TSS: transcription start site; ncRNA: non-coding RNA; miRNA: microRNA; lncRNA: long non-coding RNA. From Roberti, A., *Clinical Epigenetics*, 2019.

### 1.1.2.1. DNA methylation in cancer and DNMT inhibitors

A well characterized contribution of epigenetics to tumorigenesis concern DNA methylation disruption events, among which predominantly genome-wide DNA hypomethylation and focal hypermethylation, especially interesting CpG islands of tumor-suppressor gene (TSG) promoters (Esteller, 2008; Fernandez, 2012). One of the initial epigenetic abnormalities recognized to occur in tumors is the loss of DNA methylation, mostly affecting repeated DNA sequences, which constitute approximately half of the human genome. It has possibly evolved as a mechanism of defence against foreign DNA elements, including retrotransposons and viral pathogens (Richards, 2009). Different implications of hypomethylation in promoting tumorigenesis have been identified:

1) Chromosomal instability (CIN): a feature of most human cancers, particularly the solid ones. It is a type of genome instability, which ranges from single nucleotide changes to large-scale cytogenetic aberrations, able to alter different regulatory pathways, such as cell cycle control and DNA damages repair. Mutations in CIN genes increase the rate at which entire parts of chromosomes, or large parts of them, are lost or gained during cell division, or result in simple rather than complex chromosomal rearrangements. CIN is a cause of an imbalance in chromosome number (aneuploidy) and an enhanced rate of loss of heterozygosity, which is an important mechanism of inactivation of TSGs, such as for genes coding for p53, p21, or p19<sup>Arf</sup> (Lengauer, 1998). Nowadays, it is evident that more than 70% of common solid neoplasms are aneuploid and, in many instances, the onset of heterogeneous aneuploidy correlates with poor prognosis and aggressiveness of different tumors (Cimini, 2008; McGranahan, 2012);

2) Reactivation of transposable elements: hypomethylation of DNA in malignant cells can reactivate intragenomic DNA, such as the LINE (long interspersed nuclear element) and SINE (short interspersed nuclear element) sequences, as well as LTR (long terminal repeat) retrotransposons. These elements are normally hypermethylated and transcriptionally silenced in somatic cells, but they become demethylated to various degrees in cancer cells (Hoffmann, 2005). Higher levels of hypomethylation in LINE-1 was found in a wide number of tumors, compared to matched normal tissues, such as for urothelial carcinoma (Jurgens, 1996), hepatocellular carcinoma (Takai, 2000), melanoma (Sigalotti, 2011), and prostate cancer (Fiano, 2017). These demethylated transposons can be transcribed or translocated to other genomic regions, thereby disrupting the genome;

3) Loss of imprinting (LOI): it is a common epigenetic alteration observed in human cancers, involving loss of parental origin-specific expression of imprinted genes caused by defects of methylation, either in terms of activation of the normally silenced allele or silencing of the expressed one. For example, LOI of the insulin-like growth factor-2 (IGF-2), through the aberrant methylation of the maternal silent copy, represents a significant risk factor for colorectal

carcinoma (Feinberg, 2002); 4) Global hypomethylation: it's largely secondary to hypomethylation of repeated DNA sequences, even though heterogeneous hypomethylation within gene-coding regions has been reported (Kaneda, 2004). The latter mainly leads to the enhancement of expression of proto-oncogenes and activation of cell proliferation. Hypomethylation of wide regions of the genome seems to be due, almost in part, to a reduction/deletion in DNMT1 enzyme, as well as mutations in TET genes (Gaudet, 2003; Zhang, 2020). From precancerous lesions to full-blown malignant tumors, the hypomethylation status of genomic DNA seems to be more prominent, being related to tumor progression (Hoffmann, 2005). A possible mechanism is that global hypomethylation also results in the hypomethylation and activation of cell motility and invasion genes, methylated in non-metastatic cells (Szyf, 2005). Therefore, DNA hypomethylation levels could be used as a biomarker of tumor aggressiveness (Fraga, 2004). However, Yamada *et al.* registered a dual function of global hypomethylation, able to sustain either tumor induction or inhibition, based on tumor site and stage (Yamada, 2005).

Hypomethylation has no proven relationship with aberrant hypermethylation in inducing cancer, since these processes are independent, targeting different programs at different stages of tumorigenesis (Ehrlich, 2002). The inactivation of TSGs through the hypermethylation of CpG island within their promoter region is a key element in cancer development. Esteller *et al.* hypothesize that the underlie mechanism involves DNMTs, which fail to recognize DNA repeat regions or intronic sequences to be methylated in a normal cell, resulting in the methylation of CpG islands that are normally not recognized by DNMTs (Esteller, 2002). It was discovered at the level of the RB human gene promoter, determining susceptibility to hereditary retinoblastoma; nowadays, it is considered a hallmark of cancer because it is found in every kind of human neoplasms, being responsible for the inactivation of genes dragged into cell cycle regulation, DNA repair, metabolism, cell-cell adhesion, apoptosis, angiogenesis, and invasion (Yáñez, 2015). Several known TSGs are silenced via promoter methylation in different tumors, such as RB, p16INK4a, BRCA-1, VHL, E-cadherin, and MLH1 (Baylin, 2001). Both hypomethylation and hypermethylation processes are implicated in cancer metastasis development (Kong, 2015).

Since DNA methylation events are reversible, it is possible to reactivate TSGs, reprogramming the genome of tumor cells, inhibiting tumor proliferation and inducing cell death using inhibitors of DNMTs (DNMTi), also known as DNA hypomethylating agents (DHAs) (Gopisetty, 2006) (Table 1). DHAs are classified in two families: nucleoside and non-nucleoside analogues. Non-nucleoside inhibitors have low toxicity but exhibit limited hypomethylating activities. Nucleoside inhibitors, such as azacitidine (AZA) and decitabine (DAC), are, instead, characterized by the presence of a nitrogen atom in lieu of carbon 5-position of the pyrimidinic ring, linked to ribose/deoxyribose. After cellular uptake, they are metabolized

by different kinases for the incorporation into DNA (or mainly RNA for AZA) within the S phase of cell cycle. Both undergo the same reaction of normal cytosines leading to two major effects: i) a DNA damage response of apoptosis or, as documented for DAC, senescence (Navada, 2014); ii) the recognition by DNMT proteins which, once having bonded the modified cytidine, are complexed to the structure in an irreversible manner (Santi, 1984). As a result, DNMTs are physically depleted and, with concurrent cell divisions, demethylated DNA is accumulated (Fig. 7).

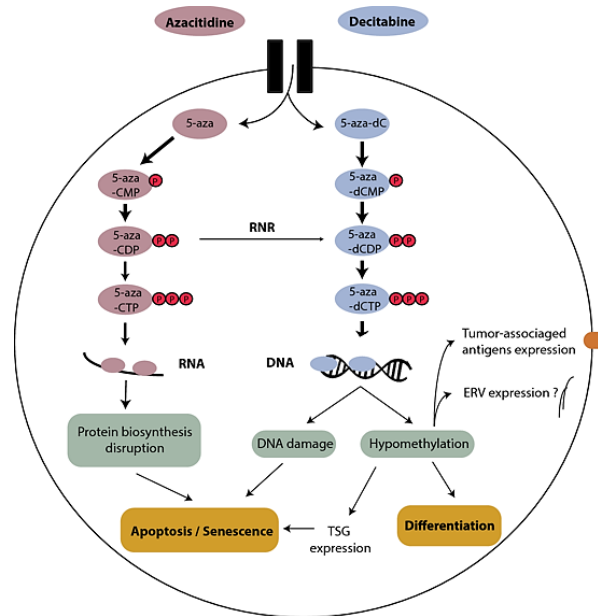


Figure 7 - Steps for the incorporation of azacitidine (5-aza) and decitabine (5-aza-dC) into DNA/RNA during cell cycle and main effects are reported. From Duchmann, M., *Progress in Hematology*, 2019.

Both AZA and DAC received the Food and Drug Administration (FDA) endorsement for the treatment of myelodysplastic syndrome (MDS) and acute myeloid leukaemia (AML). Although AZA and DAC show basically similar mechanisms of action, they have been reported to exert distinct effects, showing different efficacy in clinical trials (Diesch, 2016). However, the latter have short half-life in the blood, due to rapid inactivation by cytidine deaminase (CDA). In order to prevent this, the second-generation DHA guadecitabine has been developed, consisting of a dinucleotide of DAC linked to deoxyguanosine, through a phosphodiester bond. The great advantage of this compound is that, thanks to its configuration, it is resistant to degradation by CDA, increasing *in vivo* exposure of DAC and demonstrating to be safe and well tolerated (Coral, 2013; Roboz, 2016; Jueliger, 2016). Guadecitabine is currently being evaluated in about 40 clinical trials worldwide, between whom phase III trials concerning untreated/previously treated patients with AML, MDS, and chronic myelomonocytic leukemia, as well as phase II studies for the treatment of solid tumors, including ovarian carcinoma, small/non-small cell

lung cancer (SCLC/NSCLC), melanoma, renal cell and hepatocellular carcinoma. Fazio *et al.* demonstrated that treatment of human melanoma cell lines with guadecitabine *in vitro* up-regulated/induced the expression of Melanoma Antigen Gene (MAGE) proteins of Cancer Testis Antigens (CTA) family (Fazio, 2018). The latter are antigens of the family of tumor-associated antigens, unexpressed or expressed at very low levels in normal tissues, except for placenta and testis, and able to positively influence immunogenicity of cancer cells and the immune recognition by cytotoxic T-lymphocytes (CTLs). Also, a strong up-regulation of the constitutive expression of HLA class I antigens and of the costimulatory molecule Intercellular Adhesion Molecule-1 (ICAM-1) was observed with both guadecitabine and DAC in melanoma and hematologic tumor cell lines *in vitro* (Fazio, 2018). These data have been extensively confirmed *in vitro* and *in vivo* over the years, highlighting the strong action of DHAs on augmenting immune responses with the up-regulation of innate and adaptive immunity-related molecules in tumors of different histotype (Covre, 2015; Jones, 2016; Nahas, 2019; Luker, 2020). Several studies also reported the DHA-mediated modulation of the expression of the Natural Killer Group 2D Ligands (NKG2DLs), whose bond with the immunoreceptor represent an activating and a costimulatory signal to boost natural killer-(NK)/T cell-mediated killing. The major histocompatibility complex class I chain-related A and B (MIC-A, -B), and the UL16 binding protein family (ULBP1-6) proteins are the stress-induced ligands, that are normally not expressed by healthy adult tissues but frequently found in tumor cells. However, tumor cells develop strategies to down-regulate NKG2DLs expression and avoid immune recognition, such as promoter hypermethylation. Baragaño Raneros *et al.* reported that AZA and DAC were able to induce demethylation and re-expression of NKG2DLs on the surface of AML cells, restoring the recognition of tumor cells by the immune system (Baragaño Raneros, 2015). The capability of DHA to induce/up-regulate NKG2DLs were also confirmed in different studies, as for glioma and melanoma cell lines, making them attractive targets for DHA-based strategies for solid tumors (Zhang, 2016; Fazio, 2018).

#### 1.1.2.2. Histone acetylation and inhibition of HDACs in cancer

Histone acetylation has been shown to be frequently altered in many cancers, contributing to the epigenetic reprogramming. For example, loss of acetylation at lysine 16, together with the H4K20me3 repressive mark, has been reported to be a common epigenetic modification in human cancers, as well as low levels of H3K18ac observed in pancreatic, breast, prostate, and lung cancers, associated with poor prognosis (Fraga, 2005; Li, 2016). Also, increased expression of HDAC transcriptional repressors were reported in solid and hematologic malignancies: HDAC1 in prostate (Abbas, 2008) and gastric cancer

(Yu, 2019), HDAC-1 and -3 in ovarian cancer (Hayashi, 2010), HDAC-2 and -3 in colorectal carcinoma (Guan, 2000), HDAC6 and SIRT1 in AML (Bradbury, 2005), and HDAC8 in BRAF-mutated melanoma (Wilmott, 2015). In the majority of cases, high levels of HDACs are linked to advanced cancer and poor prognosis of patients, as for HDAC7 in pancreatic cancer (Ouaissi, 2014) or HDAC-1, -2, and -3 in gastric cancer (Sudo, 2011); some exceptions are reported, *e.g.*, HDAC-3 and -8 in metastatic melanoma, whose overexpression is associated with improved survival (Wilmott, 2015). Underlying molecular mechanisms are not always well defined, but they can imply repression of TSGs (especially cell cycle regulators), down-regulation of microRNAs acting as tumor-suppressors, or alteration of oncogenic pathways (Li, 2016). HDAC inhibitors (HDACi), as a result of the inhibition of the zinc-containing enzymes, cause an accumulation of hyperacetylated histones, correlated with a relaxed chromatin conformation and transcription factors attraction, and enhance the expression of genes involved in various biological processes, including differentiation and cell death (Fig. 8). Indeed, HDACi are able to induce the down-regulation of anti-apoptotic genes, to activate the JAK/STAT signaling pathway, and the up-regulation of multiple pro-apoptotic proteins (*e.g.*, Bim), such as the cyclin-dependent kinase inhibitor p21, which, together with the induction of oxidative DNA damage, contribute to cell cycle arrest (Grant, 2012).

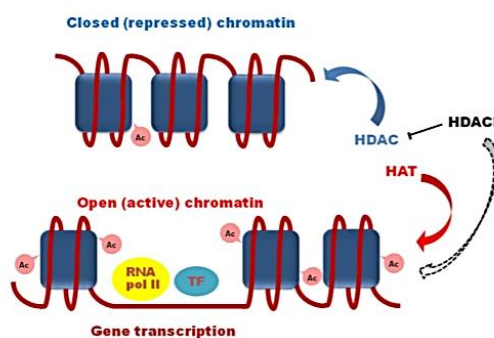


Figure 8 – Representation of HDAC inhibitors (HDACi) mechanism of action. HDAC: histone deacetylase; HAT: histone acetyltransferase; Ac: acetylation; TF: transcription factor. From Pasyukova, E.G., *Mech Ageing Dev*, 2017.

HDACi may act on different subclasses of HDACs, may have different biologic activity, acting at different concentration scales, based on the characteristics of the chemical compound. HDACi include a large range of drugs, which can be classified based on their chemical structure in: hydroxamic acids, benzamides, short chain fatty acids, and macrocycles, even though hybrid compounds are emerging. The majority of hydroxamic acids are classical HDACi, blocking all HDACs but not the NAD<sup>+</sup>-dependent class III enzymes, and work at very low concentrations, inducing differentiation and apoptosis of malignant cells (Richon, 2006). One of the earliest known hydroxamic acids is the natural compound vorinostat, also known as suberoylanilide hydroxamic acid or SAHA (Table 1), which has been the first

HDACi approved by FDA for the treatment, as single agent, of cutaneous T cell lymphoma (CTCL). Short chain fatty acids category includes only three compounds which inhibit class I and II HDACs, that tend to act at millimolar concentrations and are, in fact, less potent than hydroxamic acids, with a non-negligible toxicity. Valproic acid (VPA) (Table 1), approved for epilepsy and other neuropsychiatric disorders, belongs to the fatty acids-based inhibitors exerting its activities, among whom apoptosis, CTA induction, stimulation of T-cell recognition, induction of NKG2DLs and NK-mediated cytotoxicity, in a variety of tumors (Armeanu, 2005; Yamanegi, 2010; Makarevic, 2019). Due to the high concentrations required to achieve antitumor activity, many clinical trials are evaluating low-dose VPA efficacy within combinatorial approaches (Abaza, 2014; Suraweera, 2018). The most potent benzamide is the synthetic oral compound entinostat, a well-tolerated class I and IV HDAC inhibitor active at nanomolar concentrations. It induces inhibition of cell proliferation, terminal differentiation and apoptosis of different tumors, such as breast and non-small cell lung cancer with promising preclinical and clinical data (Ruiz, 2015; Connolly, 2017). Finally, macrocycles are the most potent HDACi, with pronounced selectivity for class I enzymes, whose component romidepsin has been approved by FDA for the treatment of CTCL in 2009. Different research groups have focalised their study on the properties of this class of HDACi, demonstrating their selectivity for HDAC-1,2, and -3, with significant anti-proliferative and immune-stimulating activities (Rajak, 2013).

Epigenetic drugs and their combinations have demonstrated to modulate the sensitivity of tumor cells to anticancer therapy. By far, the most relevant evidence is associated with the combination HDACi *plus* DHA, adding to the capability of inducing chromatin relaxation and apoptosis the restoration of TSGs (Grant, 2012). Numerous studies have supported this hypothesis. For example, the combination of AZA and entinostat in human lung adenocarcinoma cells induced a marked re-expression of pro-apoptotic genes, *e.g.*, p16 and p21 cell cycle regulators, and reprogrammed the expression profile of different other pathways, including genes regulating DNA damage and tissue remodelling (Belinsky, 2011). Also, Tellez *et al.* showed that the combination of entinostat with guadecitabine induced a consistent reduction of the tumor burden in lung cancer mouse model, compared to single treatments, as well as the up-regulation/induction in the expression of p21, Bik, and more than 18 CTA in microarray studies (Tellez, 2014). Many questions, however, need to be resolved about the underlying mechanisms of action of drugs combinations. Nonetheless, many HDACi, such as SAHA, belinostat, VPA, panobinostat, and entinostat, are currently in clinical trials in combination with chemotherapeutic, radiation, and immunotherapeutic strategies, as well as with hormonal therapy, and inhibitors of topoisomerase, proteasome and tyrosin kinases (Suraweera, 2018). Indeed, Amnekar *et al.* demonstrated that the low-dose pre-treatment with HDACi (*i.e.*, VPA and vorinostat) was able to sensitize gastric cancer cells to chemotherapeutic agents, increasing the amount of DNA-bound drug, enhancing also histone acetylation

and cell cycle arrest (Amnekar, 2020). Also, a phase II clinical trial for the treatment of NSCLC combining carboplatin and paclitaxel with vorinostat showed higher response rate, progression-free survival, and overall survival, compared to carboplatin and paclitaxel alone (ClinicalTrial.gov identifier: NCT01413750); however, a lower dose of vorinostat with carboplatin or paclitaxel is being evaluated in advanced solid tumor, in order to reduce toxicity (ClinicalTrial.gov identifier: NCT01281176). Finally, an interesting study has been recently published by Adeshakin *et al.* regarding the immunomodulatory properties of VPA. The study started from the observation, made by Xie *et al.*, that VPA was able to attenuates immunosuppressive function of myeloid-derived suppressor cells (MDSC) either *in vitro* or *in vivo*, and demonstrated synergistic antitumor efficacy when combined with blockade therapy of the immune checkpoint molecule PD-L1 (Xie, 2018). This study demonstrated that VPA, inhibited MDSCs immunosuppressive functions through the down-regulation of IL10, IL6, and ARG1, and the up-regulation of inducible nitric oxide synthase (iNOS) and IL12 (Adeshakin, 2019).

### 1.1.2.3. Targeting the lysine methyltransferase EZH2

Several studies have highlighted the role of the transcriptional repressor EZH2 in cancer development and progression, reporting its hyperactivation in multiple tumors including, firstly, prostate cancer, but also melanoma, gastric, renal cell and breast carcinoma (Varambally, 2002; Gan, 2018). Besides its activity on histone methylation, EZH2 is also able to methylate non-histone proteins, as observed for cancer-relevant regulators of cell signaling and migration, such as STAT3, ROR $\alpha$ , and talin (Gunawan, 2015; Rodriguez-Paredes, 2019). In addition, when EZH2 is phosphorylated in a PRC2-independent manner, it can also act as co-activator for transcription factors that promote tumor development and growth, such as  $\beta$ -catenin and ER $\alpha$  in breast cancer (Shi, 2007), the androgen receptor-associated complex in prostate cancer (Xu, 2013), and other genes of the Wnt/ $\beta$ -catenin pathway in cervical cancer, such as cyclin D and c-myc (Chen, 2016). However, either overexpression or loss-of-function mutations have been detected in the EZH2 gene in AML and MDS, suggesting its ambiguous role as both oncogene and TSG (Gan, 2018). Being EZH2 involved in various pathways of cancer regulation, from cell cycle, epithelial-to-mesenchymal transition (EMT), tumor immunity to drug resistance, it has become an interesting molecule to target using the different available/under investigation small molecules. Two major inhibitors have been reported (Tan, 2014): indirect inhibitors, such as DZNep, that interfere with the metabolism of SAM methyl donor thus inhibiting methylation reactions, and SAM-competitive inhibitors of EZH2, such as GSK126 (GSK2816126A) and EPZ-6438 (Tazemetostat); the latter has been approved by FDA on January 2020 for the treatment of adults and young patients (aged 16 years or over)

with metastatic or locally advanced epithelioid sarcoma ineligible for surgical resection, and on June 2020 in adults with relapsed/refractory follicular lymphoma bearing EZH2 mutations who have no alternative treatment options (Table 1).

Bracken *et al.* demonstrated, for the first time, that EZH2, highly expressed in primary human tumors, was restricted to growing cells and it is required for cell proliferation, acting as a downstream of the RB-E2F pathway (Bracken, 2003). In this regard, its role in cell proliferation has been extensively confirmed in different tumors, such as melanoma, breast and colorectal cancer (Zingg, 2015; Mahara, 2016; Yao, 2016). Indeed, Yao *et al.* demonstrated that in colorectal cancer cell lines the inhibition of EZH2, through DZNep or gene silencing, induced cell cycle arrest, inhibiting G1/S transition, and autophagy (Yao, 2016).

The overexpression of EZH2 has been also associated with aggressiveness and poor prognosis of many tumors, also related to the critical phenomenon of EMT (Tan, 2014). The latter refers to a highly plastic and reversible biological process in which non-motile, polarized epithelial cells undergo a series of biochemical alterations, becoming motile, non-polarized mesenchymal cells with high invasive potential. This process comprises a spectrum of intermediate states that involve alterations of several cell-cell adhesion molecules, such as adherens junctions, induced by EMT-activating transcription factors (*e.g.*, Slug, Snail, Twist, and Zeb), but also modifications of cell-extracellular matrix (ECM) connections; in particular a switch from epithelial markers, such as E-cadherin or occludin, and mesenchymal markers, just like N-cadherin or vimentin, is reported, causing cells to lose anchor and to migrate, favouring the metastatic process (Lachat, 2019). Several epigenetic factors have been reported to be involved in the induction of EMT. For example, the E-cadherin-coding gene has been found to be one of the most frequently hypermethylated gene in malignant pleural mesothelioma (MPM) specimens (McLoughlin, 2017); also, HDAC-1 and -2 enzymes have been implicated in the E-cadherin promoter repression *via* the Zeb-1 transcriptional repressor (Aghdassi, 2012). More prominently, EZH2 has been strongly evidenced as a mediator of EMT through different mechanisms, such as the down-regulation of epithelial markers through the up-regulation of the transcription repressors Slug and Snail, and the repression of tissue inhibitor of metalloproteinases (TIMPs) with the concomitant invasion *via* metalloproteinases (MMPs)-mediated degradation of ECM (Cao, 2008; Yi, 2017). Recently, Stazi *et al.* showed that the inhibition of EZH2 in primary glioblastoma culture by two newly synthesized EH2i, not only induced cell cycle arrest and reduced inflammation, but also reverted EMT, up-regulating E-cadherin and down-regulating N-cadherin, dampening the aggressive phenotype (Stazi, 2019). Also, it was demonstrated that the inhibition of EZH2 by GSK126 could hinder cell migration and angiogenesis *in vitro* and *in vivo*, involving a VEGFA-mediated mechanism (Chen, 2016). Aberrant expression of

EZH2 has been found to have a critical immune role, modulating T cells differentiation, NK activity, and T regulatory (Treg) cells functions, but also regulating notable immune cells within the tumor microenvironment (TME), such as dendritic cells and macrophages (Gan, 2018). Indeed, Wang *et al.* demonstrated that EZH2 was critical for tumor-infiltrating Treg immunosuppressive functions, and its pharmacologic inhibition not merely reprogrammed their activity, but also led to enhanced CD8<sup>+</sup>T cell response within the tumor, without autoimmune toxicity (Wang, 2018). Besides, it was found that EZH2-mediated H3K27me3 repressed the expression of Th1-type chemokines CXCL9 and CXCL10, key intermediaries of effector T cells trafficking within the TME (Nagarsheth, 2016). The same results had been obtained also by Peng *et al.* that also proved how combinatorial treatment with DHA and EZH2i in a mouse ovarian cancer model could restore CXCL9 and CXCL10 production by tumor cells, strongly reducing tumor growth and improving efficacy of immunotherapeutic agents. Also, a negative association between tumor EZH2 and DNMT1 expression levels and outcome of patients have been observed, highlighting the synergistic repressive activity of histone and DNA methylation events (Peng, 2015). Overall, the combination of EZH2 and DNMT inhibitors resulted in inducing consistent anti-neoplastic activity in different tumor histotypes, in terms of re-expression of several TSGs, inhibition of growth, induction of senescence and apoptosis, providing promising evidence for future ground-breaking explorations (Nascimento, 2016; Momparler, 2017).

Table 1 – Investigated epigenetic drugs and targets.

<b>Epigenetic drug class</b>	<b>Drug</b>	<b>Target</b>	<b>Developmental Stage</b>
DNMT inhibitor	Guadecitabine	DNMTs	Phase III
HDAC inhibitor	Valproic acid (VPA)	HDAC class I and II	Approved
	SAHA (Vorinostat)	HDAC class I, IIa, IIb, IV	Approved
EZH2 inhibitor	EPZ-6438 (Tazemetostat)	EZH2	Approved

## 1.2. Malignant Mesothelioma biology

### 1.2.1. Risk factors and pathogenesis

Malignant mesothelioma is a neoplasm arising from mesothelial cells, cells of mesodermal origin, components of pleural and peritoneal cavities, of pericardium and vaginal tunic. The major interested site is the chest, with a percentage of MPM counting 70-80% of total cases (Delgermaa, 2011). Mesothelioma is a relatively low-frequency malignancy, causing the 4% of overall cancer mortality worldwide. However, it is highly aggressive (with a 5-year survival rate of about 5%) and highly resistant to therapies, resulting fatal within 24 months from the diagnosis (Fels Elliott, 2020; Gray, 2020). Its incidence began to increase from the second half of the XX<sup>th</sup> century, especially in industrialized countries, being closely related to the use of asbestos which is responsible for more than 80% of total cases of mesothelioma (Delgermaa, 2011; Micolucci, 2016); despite bans, the incidence is still growing. All types of asbestos have been associated with mesothelioma onset, having all being classified by the International Agency for Research on Cancer (IARC) as human carcinogens. Environmental exposure to either long or short fibers of erionite, a fibrous zeolite constituting volcanic rocks of rural areas, such as the Cappadocian region of Turkey, is likewise an important risk factor for mesothelioma (Baris, 1988). Other collectively recognized predisposing factors are high-dose ionising radiation (especially with the old radioactive contrast agent Thorotrast), simian virus 40 (SV40) infection, chest injuries, as well as genetic aberrations (Comin, 1997; Carbone, 2000; Micolucci, 2016). SV40, a DNA virus, appeared to be co-carcinogenic in humans after asbestos exposure, contributing to early-phase mesothelial cells transformation, impairing key cell-cycle regulators (Carbone, 2020). Nevertheless, the infection alone is not sufficient to cause human malignancy (Kroczyńska, 2006). For the development of the disease, a long and variable latency period after cancerogenic fibers exposure (13-50 years or longer) is observed (Delgermaa, 2011). Since asbestos is responsible as proof of evidence of both benign and malignant cell transformation, ranging from asbestosis and pleural fibrosis to malignant tumors, studying lung responses toward it results pertinent to explore mesothelioma pathogenesis. Specific mechanisms induced by the inhalation of fibers are still poorly understood; anyway, they implicate direct mechanical injury, inflammation, oxidative stress, and DNA and chromosomal alterations. After the deposition in the airways, whose mechanism and site depend on the type of fiber, cytolytic and non-cytolytic injuries occur. The primary event is chronic inflammation, set up by alveolar macrophages. Long fibres, compared to the shortest, are difficultly phagocytized and hardly removed through the lymphatic system (Boulanger, 2014). The incomplete phagocytosis leads macrophages to produce reactive oxygen species (ROS) or reactive nitrogen species (RNS), promoting oxidative stress and interacting with cellular

components (Solbes, 2018). Moreover, protracted fibers persistence also causes the release of cytokines, such as interleukin-1 $\beta$ , transforming growth factor- $\beta$  (TGF- $\beta$ ), and tumour necrosis factor- $\alpha$  (TNF- $\alpha$ ) by alveolar macrophages, lung and pleural cells as well as high mobility group box 1 (HMGB1) protein by necrotic cells, leading to alterations of cellular signaling pathways and exacerbating the process (Carbone, 2012). Oxidative DNA damage, if not effectively resolved, is strongly mutagenic, triggering mutations, deletions, and genomic instability (Sage, 2018). In particular, TNF- $\alpha$  has been described to activate the nuclear factor- $\kappa$ B (NF- $\kappa$ B), a transcription factor regulating many genes involved in both cell proliferation and inflammatory pathways, such as c-myc, leading to the propagation of genetic aberrations and favouring malignant clones' generation (Janssen, 1995; Carbone, 2012).

Mesothelioma can hardly be identified and distinguished from cancer metastasis (*e.g.*, from lung, breast, ovarian, renal cell and colon carcinoma) and the diagnosis requires a multidisciplinary approach able to combine cytohistological aspects with clinico-radiological data. Indeed, the practical guidelines for the pathologic diagnosis of mesothelioma, formulated by the International Mesothelioma Interest Group, list a series of criteria to be considered, ranging from morphology to molecular markers, taking into account the context of the differential diagnosis (Husain, 2018). Overall, mesothelioma can be classified, from the histopathological point of view, into three main types: epithelioid, sarcomatoid and biphasic/mixed, between whom about 70-85% of all cases are represented by the epithelioid subtype, while only 10% are sarcomatoid. The most common epithelioid mesothelioma is characterized by clusters of polygonal cells with eosinophilic cytoplasm and a prominent nucleolus, in a context of fibrous stroma. Sarcomatoid type produces spindle-shape cells organized into bundles, with nuclear atypia and a various degree of mitosis, in an heterogenous stroma. The biphasic variant involves the combination of both previously described patterns. Interestingly, the histological subtypes strongly influence patients' survival, thus defining a crucial prognostic factor (Ali, 2017). Indeed, the best outcome has been observed for the epithelioid variant, with a median overall survival (OS) of 20 months. Conversely, the sarcomatoid phenotype portends a particularly dismal prognosis, being the median OS of about 13 months. Finally, the biphasic subtype shows intermediate OS, depending on the prevalent histological component of the tumor (Yap, 2017). However, lack of subtype-specific markers hinders and delays the diagnosis. Clinical features involve non-specific signs and depend on the tumor site. The most common MPM generally exhibits debilitating symptoms, such as dyspnea, almost caused by pleural effusion, chest pain, fatigue, and weight loss. The early diagnosis is difficult but of pivotal importance, along with a proper surveillance programme of workers who, in the present or past, have been exposed to asbestos or other risk factors, in order to early recognise and control the pathology.

### 1.2.2. The genetic and epigenetic landscape of mesothelioma

A small proportion of cases of mesothelioma have been linked to germline mutations of the gene coding for the BRCA1-Associated Protein 1 (BAP1), leading to the rare “BAP1 cancer predisposition syndrome”, associated with MPM but also with uveal and cutaneous melanoma, clear-cell renal cell carcinoma, breast and other cancers (Carbone, 2013). Acquired somatic mutations of this gene have been also reported in almost 60% of patients with mesothelioma (Nasu, 2015). BAP1 is a nuclear deubiquitinating protein which contributes to double-strand DNA repair and gene expression control. Loss of BAP1 is one of the most frequent genetic features observed in mesothelioma, promoting genomic instability and altering gene transcriptional regulation (Sage, 2018). Other genes frequently mutated in mesothelioma are the neurofibromatosis type 2 gene (NF2), TP53, CDKN2A, and CDKN2B (Sage, 2018). The NF2 is a TSG and a membrane protein associated to cytoskeleton, which inhibit different oncogenic pathways, such as mTOR and Hippo; it was found altered in about 40% of mesotheliomas and loss-of-function mutations led to uncontrolled cell growth (Thurneysen, 2009). Some mutations, such as PIK3CA, STK11, and TP53, have been associated to the time to disease progression of MPM patients (Welch, 2017). Moreover, analysis across The Cancer Genome Atlas (TCGA) revealed that mesothelioma has a DNA damage repair footprint, significantly correlated to progression-free survival and OS (Knijnenburg, 2018). Besides single-gene mutations, different mutational signatures have been identified in mesothelioma. Indeed, Bueno et al. studied 216 human MPM and, interestingly, this signature was not significantly different between patients exposed or not exposed to asbestos, highlighting overall alterations in histone methylation, RNA elicase, Hippo, mTOR and TP53 signaling pathways (Bueno, 2016).

Although genetic aberrations of mesothelioma have been relatively well characterized, the epigenetic landscape of the disease still needs deeper investigations. Based on the analysis of asbestos-exposed MPM cell lines, the overexpression of DNMTs, such as DNMT1, DNMT3A, and DNMT3B have been identified (McLoughlin, 2017). Also, a significant correlation between asbestos exposure and DNA methylation at the gene loci of the metal-binding proteins MT1A and MT2A, involved in the regulation of transcription, has been described in MPM (Shivapurkar, 2004). Similarly, different epigenetic modifier enzymes were found overexpressed in MPM, for example the PRC2 components EZH2 and SUZ12, and the lysine demethylase KDM6A (McLoughlin, 2017; Cregan, 2017). The latter is a JmjC domain-containing protein that catalyzes the demethylation of di-/tri-methylated H3K27, playing an important role in inflammation and tumor progression (Liang, 2019). Besides, EZH2 activation appears to be a key pathogenetic mechanism involved in mesothelioma onset

dependent to BAP1, whose loss can induce either EZH2 over-expression or hypermethylation of PRC2 target genes (Welch, 2017). This is attributable to the interaction between PRC2 and BAP1, which opposes the suppressor function of the complex, acting as polycomb deubiquitinase which remove H2AK119ub mark (Fig. 5); the loss of the tumor suppressor BAP1, then, results in H3K27me3 accumulation (Yamagishi, 2017). EZH2 over-expression has been also demonstrated to significantly correlate with a poor survival of mesothelioma patients (McLoughlin, 2017). In addition, concomitant BAP1 loss and high EZH2 expression is of diagnostic utility, improving accurate malignant mesothelioma differentiation from benign proliferations (Shinozaki-Ushiku, 2017). The BAP1 status in mesothelioma has also become of therapeutic utility, being its loss able to sensitize mesothelioma cells to EZH2 pharmacologic inhibition, opening the path to novel epigenetic-based approach for BAP1-mutant tumors (LaFave, 2015). Indeed, a phase II clinical trial with the EZH2 inhibitor EPZ-6438 is ongoing for the treatment of adult subjects with BAP1-deficient relapsed/refractory malignant mesothelioma (ClinicalTrial.gov identifier: NCT02860286). Sacco *et al.* also showed the BAP1 regulated HDAC enzymes activity, altering sensitivity of mesothelioma cancer cells to HDAC inhibitors (Sacco, 2015). Multiple studies demonstrated the effectiveness of HDACi-based epigenetic combinations in malignant mesothelioma. Anticancer effects of the combination of the HDACi SAHA or VPA *plus* the DNMTi DAC, compared to single-drug treatments, have been investigated in human MPM cells and in the corresponding murine model. Indeed, Leclercq *et al.* showed that the combination of DAC synergised with VPA/SAHA to induce cell death and CTA expression *in vitro*; also, DAC *plus* VPA led to a remarkable inhibition of tumor growth and promoted lymphocyte infiltration within the tumor *in vivo* (Leclercq, 2011). CTA up-regulation was also detected in MPM cell lines treated with guadecitabine, both at mRNA and at protein levels, correlated with the hypomethylation of MAGE-A1 and NY-ESO-1 CTA promoters; moreover, guadecitabine up-regulated HLA class I antigens and the immunostimulatory protein ICAM-1, resulting in an improved recognition of mesothelioma cells by CTLs, and highlighting DHAs utility to potentiate immunotherapeutic-based strategies (Coral, 2013). Finally, a relatively recent study of Bansaid *et al.* showed the immune check-point molecule PD-L1 was induced by the combination of DAC and different HDACi in MPM cell lines, suggesting that the epigenetic regulation of CTA and PD-L1 expression could be exploited using these epigenetic drugs combinations with anti-PD-L1 mAbs in malignant mesothelioma therapy (Bansaid, 2018).

### 1.2.3. Epithelial-to-Mesenchymal Transition in mesothelioma

As already hinted, EMT is a crucial plastic event through which epithelial cells gain a mesenchymal phenotype, remodulating the expression of critical cell-cell adhesion molecules, cell stiffness and polarity, acquiring ECM degradation capability and invasive potential. This multi-step process can occur either in physiological conditions, for example during development and organogenesis, or in wound healing, tumor development, and metastasis formation. During cancer progression, tumor cells might lose epithelial markers and acquire fibroblast-like morphology and characteristics, with the consequent leak of intercellular adhesion, facilitating migration (Cannito, 2010). Normally, the process ends with a mesenchymal-to-epithelial transition (MET) event, thanks to which metastatic cells from the primary tumor, once arrived at the distant homing site, become metastatic lesions leading to a secondary tumor growth (Thiery, 2009).

Common EMT markers include members of adherens and tight junctions, cytokeratins, cytoskeletal protein, and EMT-activating transcription factors. The most important epithelial marker in the context of MPM is the member of adherens junctions E-cadherin (encoded by the CDH1 gene), a calcium-dependent cell-cell adhesion protein, whose immunohistochemical expression has been correlated with MPM survival (Fassina, 2012). Different studies confirmed that the hypermethylation of CDH1 gene promoter occurred with a high incidence in MPM patients' samples, with the consequent loss of its tumor suppressor role (Fischer, 2006). Interestingly, Fassina *et al.* showed that mesothelioma phenotypic subtypes corresponded to specific profiles of expression of EMT markers, investigated both by immunostaining and quantitative Real-Time PCR analyses. Indeed, epithelioid mesotheliomas were associated with the expression of epithelial marker proteins, such as E-cadherin, cytokeratin 5/6, and  $\beta$ -catenin; the sarcomatoid variant owned mesenchymal markers as vimentin, N-cadherin, S100A4, MMP-2 and -9,  $\alpha$ -SMA, Zeb-1 and -2; finally, biphasic histotypes expressed  $\beta$ -catenin, N-cadherin, MMP-2 and -9,  $\alpha$ -SMA, Zeb-2, but weak expression of vimentin, S100A4, and Zeb-1 (Fassina, 2012). The EMT-related features reflected the trans-differentiation steps of the tumor, resulting helpful in malignant mesothelioma histological subtyping (Fassina, 2012).

Given the evidence that a strong and continuous exposure to asbestos was found to induce chronic inflammation and that the HMGB1-mediated inflammation was associated with increased levels of EMT signaling pathways, the study of EMT in the malignant mesothelioma has become fundamental (Qi, 2013). Different factors are able to induce EMT in mesothelioma, among whom the aberrant expression of hepatocyte growth factor (HGF), the fibroblast growth factor-2 (FGF-2), TNF- $\alpha$ , periostin, mesothelin, and TGF- $\beta$  (Qi, 2013; Chen, 2014; Farrell, 2014; Moustakas, 2012; Schramm, 2010; He,

2017). Mesothelin is a membrane protein expressed by almost all mesotheliomas, but also by pancreatic cancer, lung cancer and other solid tumors. Although it seems not to be essential for normal tissues beyond cell adhesion function, its detailed physio-pathological functions have been not clearly defined (Bera, 2000; Morello, 2016). Preclinical studies showed its involvement in cancer cell proliferation, drug-dependent apoptosis and chemosensitivity of different tumor histotypes (Chang, 2009; Bharadwaj, 2011). Mesothelin overexpression is correlated with tumor aggressiveness and reduced OS of patients with mesothelioma, lung adenocarcinoma, and many other solid tumors (Kachala, 2014; Morello, 2016; He, 2017). He *et al.* not only confirmed mesothelin overexpression in mesothelioma, but also demonstrated that the knockdown of its protein-coding gene was able to revert the malignant morphology, passing from spindle-like shape to epithelial-like cells, and to decrease the migratory and invasive capabilities of mesothelioma cell lines. This was translated into the up-regulation of epithelial markers, *e.g.*, E-cadherin and caveolin-2, and the down-regulation of the EMT-activating transcription factors Slug, Snail, and Twist (He, 2017).

Another mediator of EMT, which plays a prominent role in promoting this process, is TGF- $\beta$ . It has been demonstrated that TGF- $\beta$  was able to down-regulate the epithelial marker E-cadherin, to decrease cell-cell contacts, and to up-regulate the mesenchymal marker  $\alpha$ -SMA in human mesothelial cells; moreover, its secretion is closely related to asbestos exposure and it seems to drive EMT acting on different downstream effectors, such as Snail, Twist, and Zeb-1 (Turini, 2019).

*In vitro* studies showed that MMPs, in particular the well-known EMT inducers MMP-2 and -9, were able to proteolytically cleave TGF- $\beta$ , providing a clue on its triggering mechanism (Yu, 2000). Moreover, asbestos exposure, as well as treatment with TGF- $\beta$  itself, seem to induce MMP-2 secretion in mesothelial cells compared to untreated cells, inducing strong changes in the microenvironment and exacerbating the invasive process (Turini, 2019). MMPs are a family of zinc-dependent matrix endopeptidases able to modulate cell signaling pathways and to degrade components of the ECM, including the basement membrane; its overexpression correlates with ECM remodelling, tumor cell invasion, and metastasis (Ying, 2019). MMP-2 and -9, also called gelatinase A and B respectively, are two similar type IV collagenases, both released as soluble secreted enzymes. They are overexpressed in MPM specimens, and MMP-2 resulted also to be an independent prognostic factor, contributing to the staging system (Edwards, 2003; Orlichenko, 2008). Tumor-associated MMPs can cleave multiple intracellular and extracellular targets, stimulating tumor progression and contributing to EMT, but specific mechanisms involved in mesothelioma carcinogenesis remain unclear. Immunohistochemical analysis of MMPs and their tissue inhibitor on MPM samples revealed that MMP-1 and MMP-2 staining were detectable in 100 and 13% of patients, respectively; besides, MMP-1 was overexpressed in contrast

to the lower expression of the tissue MMP inhibitor TIMP-1, suggesting a role of MMP-1 in degrading the stroma (Hirano, 2002). Another protease which is emerging to have a critical role in MPM is ADAM-10 (A Disintegrin And Metalloprotease), demonstrated by S pult *et al.* to be expressed at high levels in MPM, compared to normal pleural samples. The genetic silencing of ADAM-10 in MPM cell lines resulted in the decrease of the soluble N-cadherin, that itself stimulated cell migration (S pult, 2019).

Intriguingly, the metastasis-associated gene 1 (MTA1), up-regulated in many advanced solid tumors correlating with the carcinogenic and metastatic processes, was found to be also overexpressed in MPM specimens respect to corresponding adjacent tissues, demonstrating a negative correlation with E-cadherin expression, thus enhancing invasion and migration of MPM cell lines *in vitro* (Xu, 2015).

Since several EMT markers are often activated or silenced through epigenetic mechanisms, included DNA methylation, histone modifications, or microRNA deregulation, targeting specific epigenetic marks in MPM can act as a bridge to restore epithelial adhesion proteins at the expense of mesenchymal markers. Only few studies targeting the epigenome have been conducted in order to revert EMT. For example, the EZH2i GSK126 was shown to induce a dose-dependent increase of E-cadherin in a mesothelial metastasis of lung cancer from pleural effusion (LaFave, 2015). Also, the potentiality of targeting microRNA in mesothelioma cell lines has coming out studying miR-205, normally dysregulated in different mesothelioma subtypes, which re-induction consistently down-regulated Zeb-1 and -2, and up-regulated E-cadherin, thus interfering with cell motility and invasiveness (Fassina, 2012).

However, less is known about the reversion of EMT through epigenetic compounds in MPM specific subtypes. On these bases, the epigenetic reprogramming of EMT markers could be of great interest in the context of mesothelioma, especially with regard to the most aggressive histological subtype, in order to modify the MPM tumor phenotype and improve patients' outcomes.

#### 1.2.4. Standard treatments and novel immunotherapeutic strategies

Mesothelioma is an orphan tumor, known to be aggressive and highly resistant to conventional therapies. Standard therapeutic options for patients affected by MPM are surgery, often coupled with chemotherapy and/or radiotherapy for resectable tumours, and chemotherapy or radiotherapy for unresectable ones (Boussios, 2018; Nicolini, 2020). Unfortunately, only a small portion of patients are surgical candidates, being contra-indicated in patients with low performance status or advanced disease (De Gooijer, 2018). Extrapleural pneumonectomy (EPP) and pleurectomy/decortication (P/D) are the main surgical resection

types for MPM. EPP is an en-bloc resection of the tumour-affected parietal and visceral pleura, including the whole ipsilateral lung, pericardium and diaphragm (Baas, 2015). Conversely, P/D consists uniquely in the complete removal of parietal and visceral pleura, sparing the lungs. According to the national comprehensive cancer network (NCCN) 2018 guidelines for MPM, P/D resection might be safer, in terms of morbidity and mortality, compared to EPP. However, to define the best surgical approach, NCCN guidelines suggest evaluating several factors, including tumour histology and extension. Until now, the FDA and EMA approved therapy for MPM involves the combination of cisplatin and pemetrexed chemotherapy, that represents the standard of care (SoC) (Hinz, 2019). Due to tolerability problems shown in elderly patients, cisplatin is often substituted by carboplatin (Baas, 2015). The SoC is non-curative and, currently, no second-line treatment is established for MPM once treatment fails. (Gray, 2020). In the case of a long progression-free survival deriving from the first-line treatment, a re-challenge with pemetrexed can be considered to extend the response to therapy (Sherpereel, 2018). Due to the absence of a further-line SoC, enrolling patients into clinical trials is encouraged. Another recent FDA-approved system for MPM treatment is the NovoTFF™-100L system, which use alternating electric fields at different intensity and frequency to hamper mitosis in cancer cells; this approach has been evaluated in the phase II STELLAR trial (ClinicalTrial.gov identifier: NCT02397928) for the treatment of patients with unresectable MPM in the setting of the SoC, reaching median OS of 21.2 and 12.1 months, for epithelial and non-epithelial MPM, respectively (Ceresoli, 2019). However, there is a concern about the lack of sufficient controls.

Nowadays, several immunotherapeutic approaches are under investigation to improve MPM patients' outcomes. Immunotherapy relies on different strategies to reactivate the host' immune system response against tumor cells. The inhibition of immune checkpoints with monoclonal antibodies (mAbs) is one of the major strategies of immunotherapy. The mAbs targets are commonly immune check-point proteins that, in physiological conditions, are predominantly expressed on lymphocytes to prevent an excessive immune response. The immune check-points most frequently targeted by immunotherapy with immune check-point inhibitors (ICI) are the cytotoxic T-lymphocyte associated antigen (CTLA)-4, the programmed cell death protein (PD)-1, or the programmed death-ligand 1 (PD-L1) co-inhibitory receptors (Fig. 9) (Pardoll, 2012).

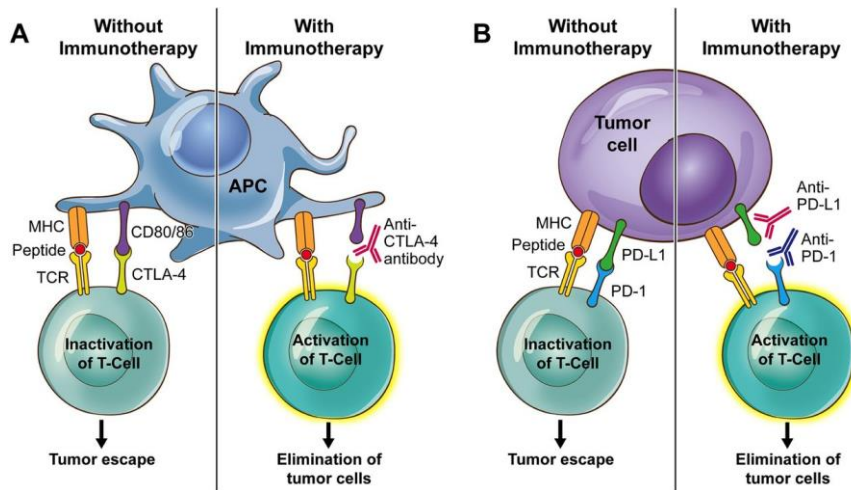


Figure 9 – Inactivation of CTLA-4 and PD-1 signaling pathways. (A) CTLA-4 blocking by a specific mAbs prevents the binding of the protein with its receptor (CD80/86), allowing the activation and proliferation of T-cell clones; (B) the inactivation of the signaling pathway involving PD-1/PD-L1, with mAbs specific for one of these two proteins, reactivates the previously quiescent T cells, prompting their anti-tumor functions. From Soularue, E., *BMJ*, 2018.

The therapeutic efficacy of CTLA-4 blockade by the mAb tremelimumab has been the first to be investigated as a second-line treatment of patients with chemotherapy-resistant advanced MPM, that showed a promising clinical activity and resulted in long-lasting disease control and OS (ClinicalTrial.gov identifiers: NCT01649024, NCT01655888) (Calabrò, 2013; Calabrò, 2015). However, the activity of tremelimumab was not confirmed by the placebo-controlled phase IIb DETERMINE study (ClinicalTrial.gov identifier: NCT01843374), that enrolled patients with unresectable pleural or peritoneal malignant mesothelioma (Maio, 2017). Besides, the use of mAbs targeting the PD-1/PD-L1 axis showed evident anti-tumour activities, being finally approved for the treatment of different tumours in the clinical setting (Balar, 2017). Several trials investigating the use of anti-PD-1/PD-L1 immunotherapeutic mAbs in MPM are ongoing, showing promising and encouraging results either as single agent or in combination with other mAbs (Grey, 2020). As shown in a preliminary report of the phase Ib KEYNOTE-028 trial (ClinicalTrial.gov identifier: NCT02054806), PD-L1-positive MPM patients treated with the anti-PD-1 mAb pembrolizumab reached disease control, with a median OS of 18 months (Alley, 2017). The clinical efficacy of the immunotherapeutic combination approach in MPM patients was firstly proved in the phase II NIBIT-MESO-1 study (ClinicalTrial.gov identifier: NCT02588131), investigating safety and efficacy of the combination of tremelimumab with the anti-PD-L1 mAb Durvalumab, as first-/second-line therapy; the combination had a good safety profile with few manageable toxicities, registering a median OS of 16.6 months (Calabrò, 2018). These results were then confirmed by two other combinatorial studies: the phase II MAPS-2 trial (ClinicalTrial.gov identifier: NCT02716272), comparing the anti-CTLA-4 ipilimumab and the anti-PD-1 nivolumab *versus* nivolumab alone, and observing a median OS of 11.9 or 15.9 months for the single therapy or the combination, respectively (Scherpereel, 2019); the single-arm phase II INITIATE study

(ClinicalTrial.gov identifier: NCT03048474), investigating the combination of ipilimumab *plus* nivolumab in MPM patients. The latter is still ongoing to reach the final endpoint; however, preliminary results are promising (Disselhorst, 2019).

These results support further investigations of ICI therapy in MPM. Besides, considering the established role played by epigenetics in MPM initiation and progression, the investigation of the epigenetic-based immunotherapies seems to have a huge potential (Sage, 2018; Vandermeers, 2013). First-in-human evidence of this previously unexplored strategy has been provided by the phase Ib NIBIT-M4 trial (ClinicalTrial.gov identifier: NCT02608437), where patients with unresectable melanoma were treated in a sequential schedule with the DHA guadecitabine followed by ipilimumab. The combination demonstrated to be safe and tolerable and analysis of the tumor-immune contexture demonstrated the up-regulation of immune-related molecules, such as HLA class I, and an increase in CD8<sup>+</sup>T cells (Di Giacomo, 2019). It has been recently opened, with promising expectations, the phase II NIBIT-ML1 study (ClinicalTrials.gov identifier: NCT04250246) where the therapeutic efficacy of nivolumab *plus* ipilimumab and guadecitabine or nivolumab *plus* ipilimumab will be assessed in melanoma and NSCLC patients resistant to anti-PD-1/PD-L1 therapies. It was also well established that HDACi are able to enhance the antitumor immune response to PD-1/PD-L1 mAbs, being able to up-regulate the expression of PD-L1, antigen presentation genes, and to decrease immune suppressive cell types (Woods, 2015; Briere, 2018). On these bases, few studies are evaluating this combinatorial strategy, for example the phase I/II trial of pembrolizumab *plus* vorinostat in NSCLC (ClinicalTrials.gov identifier: NCT02638090), or the phase Ib/II study of pembrolizumab *plus* entinostat in NSCLC, with expansion cohorts in NSCLC, melanoma, and colorectal cancer (ClinicalTrials.gov identifier: NCT02437136). These data could be precious to plan epigenetic-combined immunotherapy for MPM, considering the antitumor activities of different epigenetic compounds observed in preclinical models of MPM showing, for example, the re-expression of CTA, the up-regulation of PD-L1, and an enhanced immune response, especially when HDACi are combined with DHA (Bensaid, 2018). Immunomodulatory activities of epigenetic drugs are not limited to DHA or HDACi, indeed also methyltransferase inhibitors have been observed to have a key role in the MPM-immune system crosstalk. As recently shown by Hamaidia *et al.*, the inhibition of EZH2 reduced cytotoxic effects of macrophages towards MPM cell lines through the up-regulation of PD-1 on macrophage surface; thus, the concomitant inhibition of EZH2 and PD-1 could restore immunoediting activity of macrophages (Hamaidia, 2019). This data could justify the design of clinical trials combining anti-PD-1 mAbs and EZH2i, and in general ICI and epi-drugs, to explore MPM innovative epigenetic-based immunotherapy for this hard-to-treat tumor.

## 2. Aim of the thesis

Cancer immunotherapy include multiple treatment approaches to induce tumor recognition by the immune system, re-activating T-cell effector functions and boosting co-stimulatory molecules activity, in order to eliminate cancer cells. Growing evidence are showing the efficacy of immunotherapy in MPM. However, during MPM progression, epigenetic modifications can negatively regulate the tumor-immune crosstalk and contribute to an immunosuppressive microenvironment, influencing the efficacy of immunotherapy. Nevertheless, epigenetic changes could be reprogrammed by epigenetic drugs. Moreover, little is known about the effects of epigenetic drugs on the modulation of transcriptional features of MPM histological subtypes, that own critical prognostic significance.

On these bases, the aim of this project was to extensively characterize the effect of the second-generation DHA guadecitabine, known to have strong immunomodulatory activity in different types of cancer, on gene expression profiles of 10 MPM cell lines belonging to the three main histotypes. To further elucidate the biologic functions of genes representing the expression signature of treated vs untreated cells, differentially expressed genes (DEGs) were linked to the “Ingenuity Pathway analysis” for global analysis of their function. Furthermore, molecular and cytofluorimetric analyses have been conducted to explore the potential cooperation between the DHA and other classes of epigenetic drugs, such as HDACi and EZH2i, in regulating the transcription of key genes mainly involved in immune recognition and migration of 5 MPM cell lines (two sarcomatoid, one biphasic, and two epithelioid). In detail, cell lines were treated with guadecitabine followed by the HDACi VPA and SAHA, or the EZH2i EPZ-6438 and changes in the expression of immune-related molecules (including CTA, immune checkpoints, NKG2DLs) and EMT-related cadherins were investigated. These experiments could provide the scientific rationale for new combinatorial treatment strategies of DHA-based immunotherapies and other classes of epigenetic drugs, with the aim to improve the effectiveness of cancer immunotherapy in MPM.

### 3. Materials and methods

#### 3.1. Cell lines

Ten MPM cell lines were selected in order to represent the three main histotypes, based on the expression of EMT markers, as previously described (Fassina, 2012): the epithelioid MMCA and MesCM98, the biphasic MMB, MPP89, Mes-1 and Mes-2, and the sarcomatoid MESMM98, MesOC99, SiMes-1 and SiMes-4. All cell lines, except for SiMes-1 and SiMes-4, originated from pleural effusion of patients affected by MPM and established as previously described (Mutti, 1998; Orengo, 1999; Cacciotti, 2001). SiMes-1 and SiMes-4 were established by our group from pleural effusions of MPM patients deal with in the University Hospital of Siena, under approval by the Committee on Human Research. The adherent cell lines were grown in HAM's F-12 medium (Biochrom, Berlin, Germany) supplemented with 10% heat-inactivated fetal bovine serum (Biochrom, Berlin, Germany), 2 mM L-glutamine, and 100 µg/µL of penicillin/streptomycin (Biochrom, Berlin, Germany). Cells were incubated at 37°C with 5% CO<sub>2</sub>, splitting them when a confluency of about 80-90% was reached.

#### 3.2. Total RNA isolation

Total RNA was extracted by TRIzol reagent (Invitrogen, CA, USA), which allows nucleoprotein complexes dissociation. Cells were pelleted by centrifugation at 491 x g for 5 min and then lysed by adding 1 ml TRIzol per 2x10<sup>6</sup> cells in a 1,5 mL Eppendorf. After an incubation of 10 min at room temperature (RT), 200 µL of chloroform per ml of TRIzol were added and tubes were vigorously shaken for about 15 seconds, then incubated for 3 min at RT and centrifuged at 15871 x g for 15 min at 4°C. After centrifugation, a tri-phase mixture was obtained and the RNAs-contained in the upper aqueous phase was transferred to a new tube and precipitated by the addition of 600 µL of isopropanol (Carlo Erba Reagenti, Milan, Italy). Tubes were gently inverted 8-10 times, incubated at RT for 10 min and centrifuged at 15871 x g for 10 min at 4°C. The supernatant was discarded, and the RNA pellet was washed with 1 mL 75% ethanol and centrifuged again at 15871 x g for 5 min at 4°C. Supernatants were removed and pellets were let dry at RT for about 20 min and ultimately resuspended with 15-50 µL RNase-free water (Invitrogen, CA, USA) according to their dimension. RNA concentration and quality assessment were determined using the NanoDrop™ One spectrophotometer (Thermo Fisher Scientific, Wilmington, USA). Ratios of A260/A280 ≥ 1.9 and A260/A230 ≥ 1.8 identified good quality of RNA extraction.

### 3.3. Multiplexed gene expression analysis

Total RNA extracted from 10 MPM cell lines untreated or treated with Guadecitabine was analyzed with the nCounter® SPRINT Profiler (NanoString Technologies, Seattle, WA). The SPRINT profiler from NanoString exploits the molecular barcoding technology to digitally and simultaneously count up to 800 target molecules, belonging to multiple pathways, from a very low quantity of the input RNA and a minimal hands-on-time. Individual targets own a target-specific probe pair (called CodeSet), consisting in a color-coded Reporter probe and a biotinylated Capture probe, both complementary to the sequence of the target of interest. The Reporter probes have six positions, each of which can be composed of the combination of four colours that identify a specific target; in this way, a wide diversity of probes may be mixed in a single tube maintaining the specificity of the signal. The PanCancer IO 360™ gene expression panel was used to evaluate the number of 770 mRNA targets involved in the crucial interplay between immune system, tumor, and tumor microenvironment, starting from a recommended RNA sample input quantity of 25 to 100 ng. After having create a master mix by adding 70 µL of the hybridization buffer to the Reporter CodeSet tube, the hybridization tubes were labelled and 8 µL Master Mix were added; up to 5 µL RNA were aliquoted to each tube and, lastly, 2 µL Capture CodeSet were incorporated. The overnight hybridization process was set up at 65°C (about 16 hours recommended), using Applied Biosystems™ Veriti 96-Well Thermal Cycler (Thermo Fisher Scientific, Hercules, CA, USA). After the process was over, 30 µL obtained as reaction product were loaded onto the cartridge and transferred into the nCounter® SPRINT instrument, which, first of all, performed the two-step washing of excess probes and non-target cellular transcripts using a magnetic beads-based system. After that, the specific target-probe complexes were immobilized on the cartridge thanks to the biotin moiety on the 3' end of the Capture probe and aligned for data collection. The molecular barcode lecture occurred through an epifluorescence scanner that individually counted them during data collection. Collected data as average counts were analysed by the nSolver 4.0 software from Nanostring Technologies. Background noise was removed subtracting to raw data the negative control counts. Data were then normalized to those housekeeping genes that have a coefficient of variation (%CV) lower than 30. Lastly, advanced analysis was carried out to estimate the differential expression of RNA targets between Guadecitabine-treated cells *versus* untreated control cells.

### 3.4. Cell proliferation assay

Proliferation assays were performed using the WST-1 Cell Proliferation assay from Roche (Roche Molecular Biochemicals, Mannheim, Germany). It consists of a simple colorimetric method to obtain the relative proliferation rate of cultured cell lines, based on the conversion of tetrazolium salt WST-1 ((4-[3-(4-Iodophenyl)-2-(4-nitro-phenyl)-2H-5-tetrazolio]-1,3-benzene sulfonate) by viable cells to formazan. Assays based on tetrazolium salts have become the most widely used tools in cell biology for measuring the metabolic activity of cells, in so far as their reduction is dependent on oxidoreductase enzymes activity, in particular the mitochondrial succinate dehydrogenase (SDH). Cells were then incubated for 1 hour in a humidified atmosphere (37°C, 5% CO<sub>2</sub>), and the absorbance was determined with the Benchmark™ Plus microplate reader (Bio-Rad, Hercules, CA) at 450 nm, subtracting wavelength at 600 nm.

Cells (5x10<sup>3</sup> cells/well) were incubated in a humidified atmosphere for 24 hours before the single-setting or combined treatment with epigenetic drugs. Guadecitabine was used at the previously approved dose of 1 μM, concentration standardized by our laboratory, shown to exert immunomodulatory effects on cancer cells without reaching too high cytotoxic activity (Coral, 2012). For the other epigenetic compounds 3 concentrations have been tested, based on scientific literature: VPA was diluted to 0.25, 0.5, and 1 mM; SAHA was prepared to reach concentrations of 0.625, 1.25, and 2.5 μM; EPZ-6438 concentrations to be tested were 0.5, 1, and 5 μM. For the combinatorial approach, the schedule of treatment is described below (Fig. 10). Each experiment was carried out in triplicate and repeated 3 times. The relative proliferation rate was calculated as the percentage of cells in the medium-treated *versus* medium-untreated cells and reported as percentage of cell growth inhibition.

### 3.5. Compounds preparation and schedules of treatment

Guadecitabine was supplied by MedChemExpress LLC (Monmouth Junction, NJ, USA) as lyophilized powder with a molecular weight of 579.39. It was reconstituted with an appropriate volume of dimethyl sulfoxide (DMSO) to reach the mother solution concentration of 4.38 mM. For the following experiments, aliquots of mother solution of the drug were diluted with water for injection, to achieve the working concentration of 1 mM, filtered using centrifuge tube filters, and furtherly diluted 1:1000 in the cell culture medium to reach the final concentration of 1 μM. VPA sodium salt was purchased by Sigma Aldrich Corporation (St. Luis, MI, USA) as lyophilized powder with a molecular weight of 166.19. The amount of 50 mg was resuspended in 1 mL of water for injection to obtain a stock solution of 300 mM, filtered and then diluted in the cell culture medium to reach the final concentration of 1 mM. SAHA

(molecular weight: 264.3) was supplied by Cayman Chemical (Ann Arbor, MI, USA) as crystalline solid, dissolved in DMSO to obtain a 20 mg/mL solution, and then diluted to the concentration of 1.25  $\mu$ M in water for injection. The EZH2i EPZ-6438 (molecular weight: 572.74) were supplied as lyophilized powder by Selleck Chemicals (Houston, TX, USA), reconstituted with DMSO to create stock solutions of 5 mM, and then diluted to the final concentration of 1  $\mu$ M with the culture medium.

Guadecitabine was administered the day after the seeding (day 0); for the single treatment, cells were treated with 1  $\mu$ M guadecitabine every 12 hours for 2 days (day 1, day 2), and harvested 96 hours later (day 6). The two HDACi and the EZH2i were administered to cell culture media in one pulse and cell were left on drug exposure for 72 hours.

For the combinatorial treatment, guadecitabine was administered first through the 4 pulses just described, followed by the single-pulse administration of the other three epigenetic compounds (day 3), and harvested 72 hours later (day 6) (Fig. 10). Each experiment was carried out in triplicate and repeated 3 times. Untreated cells were used as control.

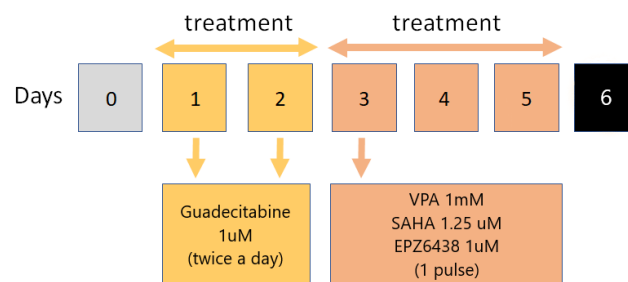


Figure 10 – Schedule of treatment.

### 3.6. Flow cytometry analysis and antibodies

The surface expression of key antigens of interest has been evaluated by the BD FACSCanto™ II Cell Analyzer cytometer (BD Biosciences, Franklin Lakes, NJ, USA). An amount of  $2 \times 10^5$  cells for tube (unstained and stained cells) has been resuspended into 50  $\mu$ L of wash solution, containing 1X PBS (DPBS, Gibco, CA, USA), 2 mM Ethylene Diamine Tetra acetic Acid (EDTA, Sigma-Aldrich, Missouri, USA) and 0.5% Bovine Serum Albumin (BSA, Calbiochem, Milan, Italy), and incubated for 10 min on ice, in order to saturate non-specific sites. For direct immunofluorescence staining, cells were incubated for 30 min in the dark at +4°C with antibodies mixture, directly conjugated to fluorochromes:  $\alpha$ -ICAM-1 clone 84H10, phycoerythrin (PE)-labeled, from Beckman Coulter (Miami, FL, USA);  $\alpha$ -HLA class I clone W6/32, labelled with AlexaFluor 488®, from Biolegend (San Diego, CA, USA). Subsequently, a two-step washing has been conducted to remove the unbound antibody and, finally, samples have been

resuspended in 200  $\mu$ L 1X PBS and read on the flow cytometer. Data analysis has been conducted with the Kaluza analysis software (Beckman Coulter, CA, USA). Results were expressed as percentage (%) of positive cells and as mean fluorescence intensity (MFI) values, of which the latter derives from the subtraction of MFI of the unstained cells from the MFI of stained cells.

### 3.7. DNase I treatment of RNA samples and reverse transcription

In order to remove contamination from genomic DNA within RNA samples, total RNA, extracted with the phenol/chloroform method, was digested with the DNase I enzyme (Roche Diagnostics GmbH, Mannheim, Germany). 2  $\mu$ g RNA for each sample underwent the enzymatic digestion in a total volume of 16  $\mu$ L RNase-free water containing 2  $\mu$ L reaction buffer (200 mM Tris-HCl pH 8, 500 mM KCl, 20 mM MgCl<sub>2</sub>) and 2  $\mu$ L DNase I RNase-free endonuclease 10 U/ $\mu$ L (Roche, Basel, Switzerland). After a 30 min incubation at RT, DNase I was definitively inactivated by adding 2  $\mu$ L EDTA 25 mM at 65°C for 10 min.

After that, 0.545  $\mu$ g digested RNA underwent the reverse transcription with hexamer primers, by adding to 6  $\mu$ L of sample 1  $\mu$ L Random Primer 500  $\mu$ g/mL (Promega, Madison, WI, U.S.A.), and 4  $\mu$ L dNTPs mixture 10 mM (dATP, dGTP, dCTP, dTTP 2.5 mM each, Takara Bio, Kusatsu, Japan) for each sample. Following the incubation at 65°C for 5 min, 9  $\mu$ L of a second mix was added, containing 4  $\mu$ L First Strand Buffer 5X (250 mM Tris-HCl pH 8.3, 375 mM KCl, 15 mM MgCl<sub>2</sub>, Invitrogen, CA, USA), 2  $\mu$ L Dithiothreitol 0.1 mM (DTT, Invitrogen, CA, USA), 2  $\mu$ L RNase inhibitor 40 U/ $\mu$ L (Invitrogen, CA, USA), and 1  $\mu$ L Murine Leukaemia Virus Reverse Transcriptase 10000 U/mL (M-MLV RT, Invitrogen, CA, USA). Samples were then incubated 10 min at 25°C, 50 min at 37°C, and 15 min at 70°C. 80  $\mu$ L RNase-free water were finally added to each cDNA sample to reach the final volume of 100  $\mu$ L with a concentration of 5.45 ng/ $\mu$ L.

### 3.8. Real-time polymerase chain reaction (RT-PCR)

Quantitative RT-PCR was performed on 10.9 ng cDNA in a final volume of 20  $\mu$ L, containing SYBR Green Master Mix (Applied Biosystem, CA, USA) and specific primers (Table 2) for the detection of target genes and the  $\beta$ -actin reference gene, at 95°C for 10 min, followed by 45 cycles at 95°C for 15 s and at 60°C for 1 min, and dissociation performed at 95°C for 15 s, 60°C for 1 min and 95°C for 15 s. Absolute quantifications were carried out using calibration curves, based on known scalar dose

concentrations of recombinant plasmid DNA containing the corresponding gene to amplify. The copy number of genes was determined extrapolating values from the calibration curves, and then copy number of genes were normalized to the number of  $\beta$ -actin copies. Gene expression was considered: i) positive if numbers of target genes/ $\beta$ -actin molecules were  $\geq 1E-04$ ; ii) upregulated or down-regulated if its positive expression was increased or decreased ( $FC \geq 1.5$  or  $FC \leq 0.5$ ), respectively. QuantStudio™ 5 Real-Time PCR System (Applied Biosystems™, CA, USA) and its analyses software were used to conduct the quantitative RT-PCR analyses.

Table 2 – Primer's sequences of genes of interest.

	<b>Forward sequence</b>	<b>Reverse sequence</b>
$\beta$ -ACTIN	5'-CGAGCGGGCTACAGCTT-3'	5'-CCTTAATGTCACGCACGATT-3'
PD-L1	5'-GGCATCCAAGATACAACTCAA-3'	5'-CAGAAGTTCCAATGCTGGATTA-3'
NY-ESO-1	5'-TGCTTGAGTTCTACCTCGCCA-3'	5'-TATGTTGCCGGACACAGTGAA-3'
MAGE-A1	5'-GCCAAGCACCTCTGTATCCTG-3'	5'-GGAGCAGAAAACCAACCAAATC-3'
MAGE-A3	5'-TGTCGTCGGAAATTGGCAGTAT-3'	5'-CAAAGACCAGCTGCAAGGAACT-3'
MICA	5'-CCTTGCCATGAACGTCAGG-3'	5'-CCTCTGAGGCCTCGCTGCG-3'
MICB	5'-AGGAGAGGAGCAGAGGTTAC-3'	5'-TGGCATAGCAGCAGAAACATA-3'
ULBP2	5'-CTCTGGGTCCTTAATGGCAG-3'	5'-GGGATGACGGTGATGTCATA-3'
CDH1	5'-AGAGACTGGGTTATTCCTCC-3'	5'-GGATTTGATCTGAACCAGGT-3'
CDH2	5'-CCTTTCAAACACAGCCACGG-3'	5'-TGTTTGGGTCGGTCTGGATG-3'

### 3.9. Statistical analysis

Results were analyzed by descriptive statistics to determine mean, mean Fold Change (mFC) and percentage ranges of modulated pathways. DEGs of MPM guadecitabine-treated cell lines, with respect to the untreated ones, considered were selected if genes showed a  $FC \geq 1.5$  or  $\leq -1.5$  ( $\log_2$  ratio  $\geq 0.58$  or  $\leq -0.58$ ) and used for Ingenuity Pathway Analysis (IPA) to investigate modulated canonical pathways and upstream regulators. Modulation, activation, and inhibition scores of canonical pathways and upstream regulators were calculated counting the number of tumor cell lines for which a specific pathway was modulated ( $Z$ -score  $\geq 2$  or  $Z$ -score  $\leq -2$ ), activated ( $Z$ -score  $\geq 2$ ), or inhibited ( $Z$ -score  $\leq -2$ ), by guadecitabine compared to baseline. The percentages of activation or inhibition were calculated as the ratio between the activation or inhibition, respectively, and the modulation score. Cytofluorimetric and molecular analyses results were analysed through the one-way Anova test, carried out by GraphPad Prism 7.05 (GraphPad Software Inc., San Diego, CA, USA). A p-value  $< 0.05$  was considered statistically significant.

## 4. Results

### 4.1. nCounter gene expression panel analysis

The gene expression profile of 10 MPM cell lines untreated or treated with guadecitabine was evaluated using the NanoString PanCancer IO 360 gene expression panel on the nCounter SPRINT Profiler (Table S1). Results demonstrated that, among 770 investigated genes, a mean of 337.7 (range: 250-422) genes were differentially ( $FC \geq 1.5$ ;  $FC \leq -1.5$ ) expressed in treated versus untreated cells. Mean of 54.5% (range: 7.9%-86.7%) and 45.5% (range: 13.3%-92.1%) of differentially expressed genes were up-regulated ( $FC \geq 1.5$ ) and downregulated ( $FC \leq -1.5$ ), respectively. Of the 241 canonical pathways that were significantly modulated according to ingenuity pathway analysis (IPA) ( $Z\text{-score} \geq 2$  or  $Z\text{-score} \leq -2$ ) in treated versus untreated cells, in at least 1 cell line, the most frequently activated ( $Z\text{-score} \geq 2$ ) was the one involved in the crosstalk between dendritic cells and natural killer cells, with a frequency of activation of 50%, observed in 5 out of 10 cell lines, followed by others involved in the immune system response to infections and inflammation (30%) (Fig. 11).

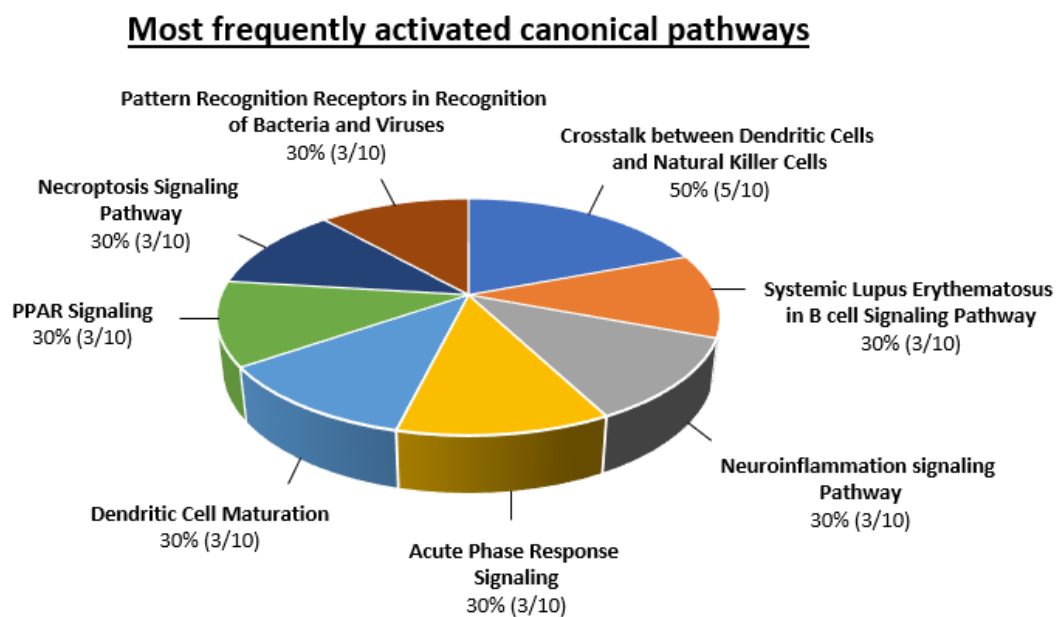


Fig. 11 – The pie chart shows the most frequently activated canonical pathways resulted from the investigation of the gene expression profile of 10 MPM cell lines untreated or treated with guadecitabine and submitted to the NanoString nCounter profiler; the single-cell analysis ( $\log_2$  ratio of treated vs untreated cells) were elaborated through IPA software, filtered by  $Z\text{-score} \geq 2$ , and cumulated based on the frequency of modulation and activation. The frequency of activation is shown as percentage, followed by the number of cells exhibiting the modulation out of the 10 investigated cell lines in brackets.

We also investigated the predicted upstream regulators responsible for changes in the expression profiles observed after guadecitabine treatment. Among the most frequently modulated upstream regulators, the most frequently activated ones are those related to the interferon (IFN)- $\gamma$  signaling pathway. In detail, the most frequently activated upstream regulators were IFNL1, STAT1, IRF3 and TNFSF14, activated in 6 out of 10 MPM cell lines (60%), as well as TNF, IFN- $\gamma$ , IFN- $\alpha$ , IFNA2, IFNB1, PRL and EIF2AK2, activated in the 50% of all investigated cell lines (Fig. 12).

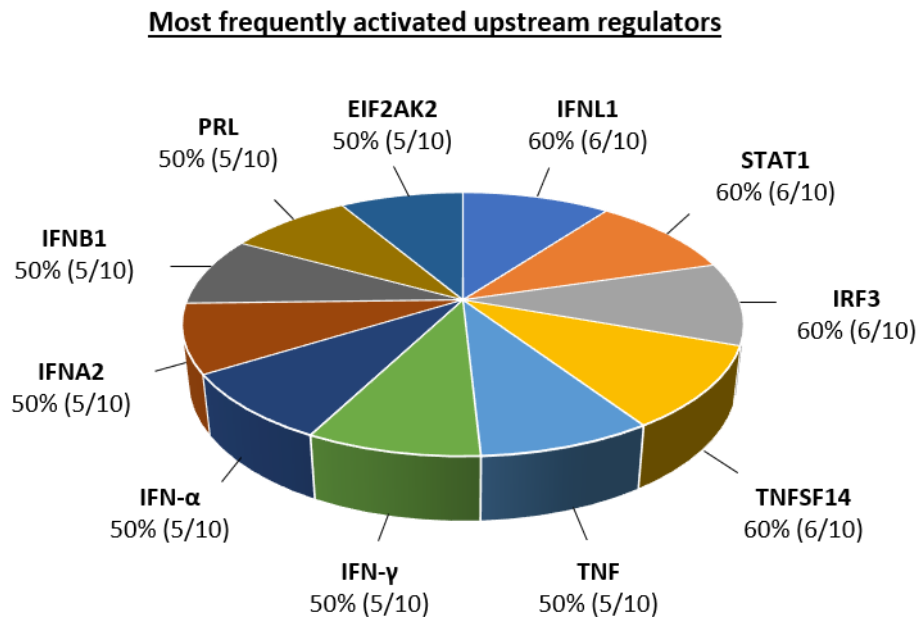


Fig. 12 – The pie chart shows the most frequently activated upstream regulators resulted from the investigation of the gene expression profile of 10 MPM cell lines untreated or treated with guadecitabine and submitted to the NanoString nCounter profiler; the single-cell upstream regulators analysis ( $\log_2$  ratio of treated vs untreated cells) were elaborated through IPA software, filtered by  $Z\text{-score} \geq 2$  and  $p < 0.05$ , and cumulated based on the frequency of modulation and activation. The frequency of activation is shown as percentage, followed by the number of cells exhibiting the modulation out of 10 investigated cell lines in brackets.

Considering that the activated pathways affected mainly the immune system regulation, we deepened the investigation of the most frequently modulated gene families owning immune-related functions, such as CTA, IFN-responsive and HLA-related genes, chemokines, and cytokines (Table S1). The results showed a strong up-regulation ( $FC \geq 1.5$ ) in the expression of almost all investigated CTA. Notably genes coding for the MAGE protein family members, such as MAGE-B2 and MAGE-A4, and CTAG1B, coding for the highly immunogenic NY-ESO-1 antigen, were upregulated in the 90% of cell lines analysed with a mFC of 13.09, 13.07, and 13.16, respectively. Besides, other immune-cell regulators, belonging to the TNF superfamily, showed an up-regulation: TNF increased in 80% of cell lines with a mFC of 5.67; TNFRSF10C, ligand of the TNF-related apoptosis inducing ligand TRAIL, was up-regulated in the 70% of cell lines, with a mFC of 5.27; and CD70, regulators of T-cell functions, had a

mFC of up-regulation of 5.69, resulting increased in 7 out of 10 cell lines after treatment with guadecitabine.

We also focused our attention on HLA antigens and HLA-related genes. It is noteworthy the increased expression of 2 among the major ligands of the NKG2D receptor, MICB and ULBP2, with a mFC of up-regulation of 2 and 2.69 each; also, CD74, belonging to the Major Histocompatibility Complex Class II, increased in the 70% of treated cell lines *versus* control, with a mFC of 3.52. A down-regulation ( $FC \leq -1.5$ ) of HLA-DPA1 and -DPB1, expressed on antigen-presenting cells (APC) where they function by presenting extracellular antigens to CD4<sup>+</sup> T cells, was observed in 30% and 40% of cells with a mFC of -2.02 and -1.89, respectively.

As highlighted in the upstream regulators analysis, IFN and IFN-responsive genes resulted highly regulated in guadecitabine-treated MPM cell lines, with particular refer to IFI27, MX1, IFITM1, ISG15, and IFI6.

Heterogeneous results have been obtained from the study of mRNA coding for cytokines and receptors: from the one hand, up-regulated values have been recorded for IL2RG, IL6R, and IL24, enhanced in 60% of all cell lines for both IL2RG and IL6R, and 70% for IL24; on the other hand, IL18R1 and IL17A showed a down-regulation with a mFC of -2.58 and -1.97. Among chemokines and receptors, the highest positive modulation concerned the chemotactic factors CCL20, CX3CL1 and CXCL14, and the receptor CXCR4, with a mFC of 10.45, 4.03, 3.28, and 5.13, respectively.

Interesting results came out from the analysis of mRNA coding for adhesion molecules: we detected a high up-regulation of molecules required for leukocyte transendothelial migration, such as PECAM1 (mFC = 4.86), EPCAM (mFC = 3.18), and VCAM1 (mFC = 4.74), sided by the down-regulation of CDH11, an oncogenic cadherin which promotes metastasis, in the 70% of the cell lines, and of the mesenchymal stem cells marker NCAM1, which was down-regulated with a mFC of -1.80. Moreover, we reported the upregulation of the inflammatory mediators F2RL1 (mFC = 3.55) and NOD2 (mFC = 2.07). A strong increase in the TLR system component TLR4 was observed, which displayed a mFC of 6.56, coupled by the down-regulation of TICAM1, a NF- $\kappa$ B and IFN-regulatory factor (IRF) activation regulator, observed in 40% of cell lines. Finally, an up-regulation of the immune checkpoint molecule CTLA-4 was observed in 60% of the cell lines with a mFC of 4.81, of LAG3 in 50% of cell lines with a mFC of 1.78, of PD-L1 in 40% of cell lines with a mFC of 1.86, of TIGIT in 30% of cell lines with a mFC of 1.50, and of the co-stimulatory molecule CD40 in 50% of cell lines with a mFC of 3.64.

In addition, we performed a histological type-specific investigation, in order to explore more in detail molecular changes induced by guadecitabine in each MPM subtype (Fig. 13). As already described, we observed a strong up-regulation of CTA with very low differences among the three histotypes, with the strongest up-regulation in the biphasic MMB cell line, and a tendency toward the down-regulation of

MAGE-A3/A6 gene in the epithelioid subtype (Fig. 13A). Members of different gene classes, such as TNF-regulating genes, chemokines, and HLA-related molecules, were particularly up-regulated in the sarcomatoid phenotype compared to the others (Fig. 13B, 13C, 13D). In particular, TNFRSF1B, involved in the recruitment of anti-apoptotic proteins, CD70, or ULBP2, resulted to be highly regulated in sarcomatoid cells (mFC = 4.83, 10.66, or 3.69), rather than biphasic (mFC = 3.33, 2.63 or 2.58) and epithelioid (mFC = -2.95, 1.90, or 0.93) tumor cell types. Other genes, such as TNFRSF18, involved in interactions between activated T-lymphocytes and endothelial cells and in the regulation of T-cell receptor-mediated cell death, exhibited an inverse correlation between the up-regulation and the aggressiveness of the histotype, ranging from sarcomatoid (mFC = -2.65) to biphasic (mFC = -0.02) and epithelioid phenotype (mFC = 4.36). The mixed nature of biphasic cell lines was clearly visible studying the cytokines gene family, for which we obtained heterogeneous results (Fig. 13E). Interestingly, the expression of IFN and IFN-responsive genes resulted evidently enhanced in the sarcomatoid phenotype after guadecitabine treatment (Fig. 13F). It is worthwhile that, among all the adhesion molecules analyzed (Fig. 13G), epithelial markers, such as CDH1, resulted up-regulated mainly in sarcomatoid MPM cell lines; in fact, this phenotype showed a mFC of up-regulation of the CDH1-specific mRNA of 7.56, *versus* -0.59 and -0.79 observed in the biphasic and epithelioid cell lines, respectively. Overall a more heterogeneous expression among the three different histotypes was observed for genes belonging to inflammatory genes (Fig. 13H), positive/negative co-stimulatory molecules (Fig. 13I), and TLR system (Fig. 13J).

A	SARCOMATOID cells					BIPHASIC cells					EPITHELIOID cells		
	MesMM98	MesOC99	SiMes1	SiMes4	mFC	MMB	Mes1	Mes2	MPP89	mFC	MMCA	MesCM98	mFC
MAGEC1	5.61 <sup>a</sup>	10.11	0.03	-0.18	<b>3.89<sup>b</sup></b>	6.67 <sup>a</sup>	-0.36	-0.49	-0.23	<b>1.40<sup>b</sup></b>	9.39 <sup>a</sup>	6.10	<b>7.75<sup>b</sup></b>
MAGEA12	2.72	6.88	0.03	8.28	<b>4.47</b>	9.67	2.59	10.97	-1.53	<b>5.42</b>	12.31	2.51	<b>7.41</b>
MAGEA3/A6	0.72	3.85	3.98	11.84	<b>5.10</b>	16.76	8.09	16.81	-2.12	<b>9.89</b>	-2.64	0.18	<b>-1.23</b>
MAGEA1	1.94	0.80	12.83	15.21	<b>7.69</b>	17.46	0.88	6.96	-1.66	<b>5.91</b>	8.43	10.55	<b>9.49</b>
MAGEC2	0.88	<b>17.38</b>	0.03	<b>17.53</b>	<b>8.95</b>	16.22	<b>12.88</b>	10.97	-9.85	<b>7.55</b>	16.58	18.10	<b>17.34</b>
CTAG1B	<b>22.86</b>	13.68	0.03	6.36	<b>10.73</b>	<b>20.30</b>	8.74	12.52	<b>15.08</b>	<b>14.16</b>	16.09	15.93	<b>16.01</b>
MAGEB2	8.17	<b>18.70</b>	11.30	6.65	<b>11.20</b>	18.44	14.51	16.63	-0.57	<b>12.25</b>	16.58	<b>20.53</b>	<b>18.56</b>
MAGEA4	<b>19.73</b>	16.32	10.11	<b>14.84</b>	<b>15.25</b>	15.93	9.57	13.34	-0.23	<b>9.65</b>	15.62	15.41	<b>15.52</b>
CEP55	0.00	-0.10	0.83	2.02	<b>0.69</b>	2.09	-2.15	3.47	-1.84	<b>0.39</b>	10.91	2.77	<b>6.84</b>

B	SARCOMATOID cells					BIPHASIC cells					EPITHELIOID cells		
	MesMM98	MesOC99	SiMes1	SiMes4	mFC	MMB	Mes1	Mes2	MPP89	mFC	MMCA	MesCM98	mFC
TNFRSF18	-7.58 <sup>a</sup>	-5.22	2.38	-0.18	<b>-2.65<sup>b</sup></b>	2.09 <sup>a</sup>	-0.59	-1.34	-0.23	<b>-0.02<sup>b</sup></b>	0.34 <sup>a</sup>	8.38	<b>4.36<sup>b</sup></b>
TNFRSF8	-8.66	0.03	0.03	-0.18	<b>-2.20</b>	-0.16	-0.36	-0.49	-0.23	<b>-0.31</b>	-0.72	-0.28	<b>-0.50</b>
TNFRSF11B	-8.48	2.25	10.11	2.22	<b>1.53</b>	-0.16	2.46	-5.46	-0.85	<b>-1.00</b>	-0.57	2.25	<b>0.84</b>
TRAF1	1.47	1.32	-1.01	4.55	<b>1.58</b>	3.21	1.14	-4.47	0.26	<b>0.03</b>	8.69	5.77	<b>7.23</b>
TNFRSF4	-6.59	5.92	7.22	-0.18	<b>1.59</b>	5.28	3.91	-0.49	1.06	<b>2.44</b>	-9.16	5.43	<b>-1.86</b>
TNFSF13	0.26	3.96	0.03	3.75	<b>2.00</b>	-0.16	-0.36	-0.49	-0.23	<b>-0.31</b>	-5.48	6.26	<b>0.39</b>
TNFAIP3	4.34	2.41	1.89	1.27	<b>2.48</b>	3.75	-1.84	1.01	-1.76	<b>0.29</b>	-3.39	2.61	<b>-0.39</b>
TNFRSF1B	2.64	3.16	6.18	7.29	<b>4.82</b>	10.58	-0.62	3.13	0.23	<b>3.33</b>	-0.72	-5.17	<b>-2.95</b>
TNF	8.97	2.43	14.97	-0.75	<b>6.41</b>	10.42	5.35	4.22	-0.23	<b>4.94</b>	8.12	3.21	<b>5.66</b>
TNFRSF10C	7.42	8.74	4.91	6.93	<b>7.00</b>	9.31	3.65	-2.07	-3.72	<b>1.79</b>	0.54	16.94	<b>8.74</b>
TNFSF10	2.25	8.41	6.28	12.39	<b>7.33</b>	-0.16	6.83	-0.49	-0.10	<b>1.52</b>	2.43	4.40	<b>3.41</b>
CD70	6.75	4.97	15.10	15.80	<b>10.66</b>	-0.23	7.53	3.36	-0.13	<b>2.63</b>	-4.29	8.09	<b>1.90</b>
TNFRSF9	-1.19	6.75	0.59	-1.45	<b>1.18</b>	0.59	-3.47	-1.66	-5.25	<b>-2.44</b>	0.34	16.01	<b>8.17</b>
TNFRSF1A	-2.02	-1.76	0.47	-1.40	<b>-1.18</b>	-0.05	-2.74	-1.91	-1.63	<b>-1.58</b>	-1.11	-1.06	<b>-1.09</b>
TNFRSF11A	1.22	-0.85	-0.72	0.05	<b>-0.08</b>	8.82	-3.93	8.92	-1.29	<b>3.13</b>	0.05	0.05	<b>0.05</b>
TNFSF4	-1.55	3.00	-3.28	5.61	<b>0.94</b>	11.79	7.29	3.96	-3.03	<b>5.00</b>	3.41	-3.98	<b>-0.28</b>
TNFRSF10D	3.85	1.22	0.03	0.52	<b>1.40</b>	15.21	2.69	12.80	-2.02	<b>7.17</b>	-1.37	-0.39	<b>-0.88</b>

C	SARCOMATOID cells					BIPHASIC cells					EPITHELIOID cells		
	MesMM98	MesOC99	SiMes1	SiMes4	mFC	MMB	Mes1	Mes2	MPP89	mFC	MMCA	MesCM98	mFC
CCL19	0.26 <sup>a</sup>	0.03	0.03	-8.33	<b>-2.00<sup>b</sup></b>	-3.44 <sup>a</sup>	-0.36	-0.49	-0.23	<b>-1.13<sup>b</sup></b>	-0.72 <sup>a</sup>	4.58	<b>1.93<sup>b</sup></b>
CMKLR1	-7.11	0.03	0.03	-0.18	<b>-1.81</b>	-0.16	-0.36	-0.49	0.00	<b>-0.25</b>	-0.72	-0.28	<b>-0.50</b>
CXCL2	3.21	2.84	1.22	-0.93	<b>1.58</b>	16.71	1.11	-0.72	-2.72	<b>3.59</b>	-1.03	3.36	<b>1.16</b>
CCL2	0.28	1.16	3.78	1.22	<b>1.61</b>	1.32	-1.76	-2.33	-2.41	<b>-1.29</b>	3.41	-0.28	<b>1.56</b>
CXCL3	2.90	3.21	0.88	1.84	<b>2.20</b>	6.65	0.54	-1.97	-3.39	<b>0.46</b>	0.00	4.89	<b>2.44</b>
CXCL5	0.26	0.03	10.11	-0.18	<b>2.55</b>	-0.16	-0.36	-0.49	-4.42	<b>-1.36</b>	-0.72	-0.28	<b>-0.50</b>
CXCL6	0.26	0.03	11.38	-0.18	<b>2.87</b>	-0.16	3.91	4.89	-1.68	<b>1.74</b>	4.27	1.37	<b>2.82</b>
CXCL16	5.35	1.09	4.09	1.81	<b>3.08</b>	0.65	-1.81	1.42	-2.12	<b>-0.47</b>	-2.59	1.29	<b>-0.65</b>
CX3CL1	5.33	4.29	3.49	-0.18	<b>3.23</b>	10.78	-0.36	8.95	3.96	<b>5.83</b>	2.20	12.80	<b>7.50</b>
CXCL1	8.64	6.98	1.63	-0.98	<b>4.07</b>	9.41	-1.14	-2.02	-2.35	<b>0.98</b>	-0.65	1.47	<b>0.41</b>
CXCL8	7.34	8.09	0.70	0.23	<b>4.09</b>	12.70	-0.36	0.85	-1.60	<b>2.90</b>	0.34	1.66	<b>1.00</b>
CXCL14	2.61	-1.01	9.21	7.53	<b>4.58</b>	4.01	0.21	7.01	-0.23	<b>2.75</b>	3.91	-0.44	<b>1.73</b>
CXCL11	5.12	2.09	1.66	10.27	<b>4.78</b>	6.03	-1.06	-9.36	-2.51	<b>-1.73</b>	13.11	-1.89	<b>5.61</b>
CCL5	8.84	0.21	4.63	7.89	<b>5.39</b>	7.73	-1.47	-0.96	-0.62	<b>1.17</b>	-0.72	8.72	<b>4.00</b>
CXCR4	10.37	1.63	11.72	8.64	<b>8.09</b>	4.24	-1.66	2.38	3.96	<b>2.23</b>	-0.72	-0.28	<b>-0.50</b>
CCL20	18.41	14.07	5.33	11.87	<b>12.42</b>	10.37	8.43	10.68	1.11	<b>7.65</b>	0.98	23.22	<b>12.10</b>
CXCL13	0.26	0.03	0.03	-0.18	<b>0.03</b>	-3.44	-0.36	-0.49	-0.23	<b>-1.13</b>	3.41	-0.28	<b>1.56</b>
CCL22	0.26	0.03	5.09	-0.18	<b>1.30</b>	-0.16	-0.36	-0.49	-0.23	<b>-0.31</b>	7.47	10.01	<b>8.74</b>

D

	MesMM98	MesOC99	SiMes1	SiMes4	mFC	MMB	Mes1	Mes2	MPP89	mFC	MMCA	MesCM98	mFC
HLA-DPA1	-12.72 <sup>a</sup>	0.03	0.03	-0.18	-3.21 <sup>b</sup>	-0.16 <sup>a</sup>	-0.36	-0.49	-2.04	-0.76 <sup>b</sup>	-0.72 <sup>a</sup>	-3.59	-2.16 <sup>b</sup>
HLA-DRA	0.26	0.03	0.03	-6.67	-1.59	-0.16	-0.36	-0.49	-0.23	-0.31	4.34	-5.20	-0.43
CTSS	1.42	1.09	2.53	1.91	1.74	-0.28	-2.82	0.67	-1.22	-0.91	-6.47	-3.03	-4.75
TAP1	3.75	3.52	1.11	1.19	2.39	1.06	-3.28	-1.09	-1.81	-1.28	-0.08	1.19	0.56
MICB	4.60	2.87	0.98	1.81	2.57	2.12	-1.47	5.17	-0.78	1.26	3.03	1.66	2.34
HERC6	4.34	3.80	0.75	2.38	2.82	0.52	-1.27	3.41	-4.29	-0.41	-2.74	0.75	-1.00
HLA-DMB	12.16	0.03	0.03	-0.18	3.01	-0.16	-0.36	-0.49	-0.23	-0.31	5.09	0.41	2.75
ULBP2	4.27	4.89	2.09	3.52	3.69	3.83	2.43	4.97	-0.91	2.58	1.19	0.67	0.93
CD74	11.07	2.74	2.07	-0.28	3.90	4.34	4.91	3.91	6.98	5.04	0.36	-0.91	-0.27
FCGRT	-1.09	-2.97	0.59	-0.47	-0.98	-1.22	-4.22	-2.33	-2.04	-2.45	-0.72	8.72	4.00
HLA-DPB1	1.16	-6.03	0.03	-0.18	-1.25	-0.16	-0.36	-4.32	-1.60	-1.61	-7.14	-0.28	-3.71
TAPBP	-1.47	-0.72	0.39	-1.66	-0.87	0.00	-2.38	-1.78	-2.15	-1.58	-2.07	-0.70	-1.38
HLA-DMA	-1.63	-3.57	1.32	0.78	-0.78	2.38	-1.14	-1.66	-5.84	-1.56	1.42	-1.22	0.10
HLA-DOB	-3.23	0.03	0.03	-0.18	-0.84	-0.16	-0.36	-0.49	-0.23	-0.31	5.09	4.58	4.84

E

	MesMM98	MesOC99	SiMes1	SiMes4	mFC	MMB	Mes1	Mes2	MPP89	mFC	MMCA	MesCM98	mFC
IL10	-6.59 <sup>a</sup>	-4.19	0.03	-0.18	-2.73 <sup>b</sup>	-0.16 <sup>a</sup>	-4.78	-0.49	-0.23	-1.42 <sup>b</sup>	-0.72 <sup>a</sup>	4.58	1.93 <sup>b</sup>
IL18R1	-5.53	-0.59	-1.37	-2.66	-2.54	-4.14	-2.04	-3.54	-2.95	-3.17	-3.44	0.52	-1.46
IL4	0.26	-2.74	0.03	-5.25	-1.93	-0.16	-0.36	-4.32	-0.23	-1.27	-0.72	-0.28	-0.50
STAT1	4.19	0.72	0.85	1.01	1.69	0.34	-1.55	0.31	-2.51	-0.85	-0.80	3.00	1.10
IL6	4.71	2.87	0.36	-1.09	1.71	-2.53	6.18	2.30	-3.23	0.68	0.67	10.47	5.57
STAT4	4.03	-0.03	3.16	-0.18	1.75	3.93	-0.36	9.44	-4.97	2.01	2.30	0.52	1.41
IL34	-6.67	1.84	2.15	10.03	1.84	0.57	-4.16	-2.38	-7.03	-3.25	0.34	3.83	2.08
CSF3	0.26	0.03	8.17	-0.18	2.07	-0.16	-0.36	-0.49	-2.43	-0.86	-0.72	-0.28	-0.50
IL2RB	8.59	0.03	0.03	-0.18	2.11	-0.16	-0.36	11.28	-2.12	2.16	-0.72	4.99	2.13
IL22RA1	3.67	-1.66	8.95	-0.18	2.70	5.92	-2.69	2.72	-1.89	1.02	1.11	6.36	3.74
IL12RB2	6.13	7.73	0.03	-0.18	3.43	-0.16	-0.36	7.99	-0.23	1.81	-0.72	-0.28	-0.50
IL24	0.47	7.73	0.52	8.95	4.42	3.85	-5.79	7.06	0.41	1.38	10.47	9.28	9.88
CSF1R	0.10	1.66	5.95	10.68	4.60	-1.42	-3.44	8.92	5.38	2.36	3.91	3.83	3.87
IL6R	8.38	4.47	5.95	0.03	4.71	7.34	-1.19	8.82	-0.23	3.69	4.55	8.82	6.69
IL11	4.89	7.22	1.06	6.00	4.79	5.17	-3.18	4.06	-1.50	1.14	-2.09	2.69	0.30
CSF2	3.34	11.38	0.62	8.64	5.99	-0.16	-3.44	0.98	4.29	0.42	-0.16	3.23	1.54
SPP1	4.78	14.61	0.03	7.27	6.67	-0.16	-0.36	-0.49	-0.83	-0.46	-0.72	-0.28	-0.50
IL2RG	11.51	15.05	0.03	12.13	9.68	3.05	7.71	14.84	-0.23	6.34	-0.72	9.00	4.14
IL17A	0.26	-1.89	0.03	-4.14	-1.44	-6.47	-0.36	-8.15	-0.23	-3.80	-0.72	1.97	0.62
CSF1	-1.50	-0.98	1.50	-1.94	-0.73	-2.38	-2.22	-6.03	-1.73	-3.09	7.11	1.16	4.14
LIF	0.16	-0.67	-0.93	-1.37	-0.70	0.26	-1.78	-2.84	-2.48	-1.71	-3.31	0.18	-1.56
IL7R	-3.91	2.82	3.41	2.69	1.25	4.29	2.48	2.66	-1.50	1.98	-0.72	13.11	6.19
JAK1	-1.81	-0.80	0.44	-0.93	-0.78	-0.03	-1.97	-0.16	-2.07	-1.05	-2.28	-1.03	-1.66
IL15	-0.18	1.19	3.59	0.78	1.34	5.09	1.06	-1.32	-2.77	0.52	0.52	2.59	1.55
IL1A	4.73	2.64	-0.93	-0.52	1.48	1.63	0.88	4.86	-3.00	1.09	0.47	3.34	1.90
IL32	-0.75	4.16	-0.41	-0.96	0.51	2.43	0.21	0.28	-2.46	0.12	-1.63	6.00	2.19
IL2RA	0.26	0.03	0.03	-0.18	0.03	6.67	-0.36	-0.49	-0.23	1.40	-0.72	7.63	3.45
JAK3	0.26	0.03	2.38	-0.18	0.62	-0.16	-0.36	3.98	-0.21	0.81	8.69	-0.28	4.20
IL10RA	0.26	-0.36	0.03	-2.53	-0.65	-0.16	-0.36	-3.91	-0.23	-1.16	-0.72	9.28	4.28
IL1R2	9.91	-6.03	0.03	-0.49	0.85	-0.16	9.31	-9.70	2.56	0.50	0.80	8.92	4.86

F

	MesMM98	MesOC99	SiMes1	SiMes4	mFC
IFI35	3.75 <sup>a</sup>	2.56	0.16	1.78	2.06 <sup>b</sup>
IFIH1	3.85	3.00	1.40	0.83	2.27
OAS3	7.89	3.54	0.62	1.68	3.43
OAS1	4.84	5.66	0.59	3.34	3.61
IFI27	8.12	3.98	1.66	0.78	3.63
IFIT3	5.15	4.27	1.40	4.42	3.81
IFI6	7.55	6.36	0.05	1.63	3.90
IFITM1	6.54	5.30	1.29	4.66	4.45
ISG15	9.93	5.51	0.67	5.64	5.44
OAS2	4.91	7.03	0.78	12.39	6.28
MX1	17.35	4.42	0.75	3.36	6.47
IFNG	-1.53	3.96	0.03	-0.18	0.57
IFNAR1	-0.26	-1.29	0.36	-0.05	-0.31
IFITM2	-2.69	-0.83	0.41	1.58	-0.38

MMB	Mes1	Mes2	MPP89	mFC
-0.41 <sup>a</sup>	-2.72	0.83	-3.13	-1.36 <sup>b</sup>
1.01	-1.40	1.42	-2.97	-0.48
2.46	-1.58	1.94	-2.33	0.12
-0.16	-1.11	0.08	-3.00	-1.05
11.22	5.74	0.10	-1.53	3.89
1.47	-2.59	-0.49	-2.56	-1.04
2.28	-1.22	2.46	-1.89	0.41
7.71	2.41	2.38	-1.27	2.81
4.63	-0.78	1.27	-1.78	0.83
-0.16	-1.99	-0.98	-2.72	-1.46
2.25	-2.59	0.47	-4.16	-1.01
-0.16	-7.22	-0.49	-0.23	-2.02
0.49	-3.26	-1.03	-3.18	-1.75
4.42	-1.73	0.96	-1.66	0.50

MMCA	MesCM98	mFC
-0.96 <sup>a</sup>	0.91	-0.03 <sup>b</sup>
-1.55	2.35	0.40
-2.09	1.45	-0.32
-2.97	2.69	-0.14
-0.34	0.13	-0.10
-2.53	-0.59	-1.56
0.85	1.99	1.42
-0.59	-0.98	-0.79
-2.72	0.57	-1.07
-0.65	0.26	-0.19
1.53	4.03	2.78
0.34	-0.28	0.03
-2.77	-0.03	-1.40
-3.28	-0.52	-1.90

G

	MesMM98	MesOC99	SiMes1	SiMes4	mFC
ITGAX	-1.94 <sup>a</sup>	4.27	-8.64	-2.77	-2.27 <sup>b</sup>
NCAM1	-4.58	-2.82	0.03	-0.59	-1.99
CDH11	-3.23	-2.04	0.13	-1.66	-1.70
CDH2	-1.66	-2.72	-0.67	-1.22	-1.56
ICAM1	1.78	4.01	0.80	0.18	1.69
NECTIN1	2.02	1.89	2.79	2.15	2.21
ITGA1	-2.69	6.62	1.45	5.66	2.76
ICAM2	12.31	0.03	0.03	-0.18	3.05
ITGA4	7.68	3.18	3.98	-0.18	3.67
VCAM1	-5.97	11.02	12.47	2.22	4.93
THY1	-1.73	-2.53	5.09	19.32	5.04
EPCAM	5.22	5.97	8.59	0.62	5.10
CDH1	7.27	8.77	4.42	9.78	7.56
PECAM1	12.31	3.70	6.65	14.15	9.20
CD47	-0.08	0.23	1.29	0.18	0.41
CDH5	-4.40	0.03	0.03	3.57	-0.19
ITGB8	-0.91	-1.14	6.23	0.10	1.07
ITGB2	2.07	0.88	0.23	-0.70	0.62
ITGB3	-3.49	-3.96	4.29	0.62	-0.63
ITGA6	-0.80	0.72	-1.09	3.44	0.57
ITGAM	0.26	0.03	0.03	-4.14	-0.96
SIGLEC1	-3.23	7.73	0.03	-4.14	0.10

MMB	Mes1	Mes2	MPP89	mFC
-0.85 <sup>a</sup>	3.72	-1.09	-0.59	0.30 <sup>b</sup>
-2.53	-2.04	-0.49	-3.98	-2.26
0.13	-2.17	-2.38	-2.15	-1.64
-0.91	-1.01	-0.44	-2.46	-1.20
1.84	0.44	-0.28	-1.91	0.02
1.66	-2.48	1.91	-1.19	-0.03
-0.16	-0.36	8.82	-1.24	1.77
-0.16	-0.36	-0.49	-0.23	-0.31
10.37	3.70	8.92	-1.40	5.40
7.27	9.05	12.62	-2.51	6.61
10.50	-2.64	3.08	2.56	3.38
11.64	-7.34	15.70	-10.40	2.40
0.62	-1.78	-1.22	0.00	-0.59
-0.16	-0.36	-0.49	1.66	0.16
-0.03	-5.22	0.13	-1.11	-1.56
2.09	4.86	-0.49	-0.23	1.56
2.20	-0.18	5.64	-1.11	1.64
11.61	4.91	0.54	-1.40	3.92
3.36	-3.03	0.62	-0.85	0.03
2.51	-1.68	4.29	-2.09	0.76
-3.44	6.83	-3.91	-0.23	-0.19
1.09	-0.54	-4.32	-0.23	-1.00

MMCA	MesCM98	mFC
-5.48 <sup>a</sup>	-0.28	-2.88 <sup>b</sup>
-0.72	-0.28	-0.50
-2.59	-0.83	-1.71
-0.72	3.52	1.40
4.71	4.37	4.54
-0.85	-1.50	-1.18
6.70	1.76	4.23
-6.21	4.63	-0.79
-0.72	5.43	2.35
-0.72	1.97	0.62
-4.29	3.52	-0.39
-0.57	2.33	0.88
-3.18	1.60	-0.79
2.20	9.00	5.60
-0.65	-1.22	-0.93
-3.00	7.06	2.03
-2.46	2.64	0.09
5.09	3.39	4.24
-1.34	-4.97	-3.16
-2.95	-1.94	-2.44
-0.72	4.58	1.93
5.09	-0.28	2.41

H

	MesMM98	MesOC99	SiMes1	SiMes4	mFC
PTGS2	0.91 <sup>a</sup>	-0.49	8.92	1.14	2.62 <sup>b</sup>
F2RL1	15.39	2.74	1.89	10.68	7.67
ADORA2A	0.28	-4.78	1.66	1.11	-0.43
APOE	-6.44	5.41	0.03	3.75	0.69
NOD2	7.11	-7.27	5.95	-0.18	1.40

MMB	Mes1	Mes2	MPP89	mFC
6.57 <sup>a</sup>	-0.34	-0.10	-2.17	0.99 <sup>b</sup>
4.29	-0.36	5.64	-3.05	1.63
1.76	-3.13	-3.21	-5.38	-2.49
9.88	0.49	6.59	-1.68	3.82
5.28	-2.53	-0.52	-0.49	0.43

MMCA	MesCM98	mFC
-5.35 <sup>a</sup>	-1.24	-3.30 <sup>b</sup>
-2.30	0.54	-0.88
-1.37	2.79	0.71
-0.72	-0.28	-0.50
8.69	4.66	6.67



#### 4.2. Cytofluorimetric analysis of HLA class I antigens and ICAM-1 surface expression on MPM cell lines treated with combined epigenetic drugs

To explore the immunomodulatory activity of different classes of epigenetic drugs such as HDACi and EZH2i, on mesothelioma cell lines, and the potential cooperation among them and guadecitabine, cytofluorimetric analyses have been conducted to investigate the expression of key genes mainly involved in immune recognition.

The immunomodulatory activity of selected doses of the HDACi VPA and SAHA, of the EZH2i EPZ-6438, and of guadecitabine used alone or as guadecitabine-based combinations, was evaluated on 5 MPM cell lines, studying the modulation of the constitutive expression levels of HLA class I antigens and of the costimulatory molecule ICAM-1, by flow cytometry. Results showed that treatments with guadecitabine or VPA as single agents induced an up-regulation ( $FC \geq 1.5$ ) of the expression of HLA antigens in 2/5 MPM cell lines, with a total mean value of mean fluorescence intensity (MFI)  $\pm$  standard deviation (SD) of  $176.80 \pm 112.26$  and of  $155.48 \pm 102.51$ , respectively, *vs*  $128.31 \pm 104.98$  of untreated cells; SAHA and EPZ-6438 were able to up-regulate the expression of aforementioned antigens only in MMB cell line. Besides, combined treatments with both HDACi up-regulated HLA class I antigens in 3/5 cell lines, with a total mean MFI  $\pm$  SD of  $215.85 \pm 112.68$  for guadecitabine *plus* VPA, and of  $203.94 \pm 102.80$  for guadecitabine *plus* SAHA ( $p < 0.05$ ); the combination of guadecitabine and EPZ-6438 induced the strongest significant ( $p = 0.001$ ) difference compared to the control, strengthening the effect of either single drugs in 4/5 MPM cell lines, and reaching a total mean value of MFI  $\pm$  SD of  $223.33 \pm 94.37$  (Fig. 14A). No differences in the percentage of HLA class I antigens positive cells were observed after any treatment, in all investigated MPM cell lines (Fig. 14B). Moreover, guadecitabine alone up-regulated ICAM-1 expression in 4/5 MPM cell lines with a total mean value of MFI  $\pm$  SD of  $15.03 \pm 14.03$  compared to  $8.42 \pm 12.29$  of untreated cells (Fig. 14C). HDACi in the single-use setting did not induce any increased expression of ICAM-1, except for MesMM98 cell line in which the expression was upregulated with a FC of 2.34 by SAHA, compared to the control. At the same way, MesMM98 cell line showed up-regulated expression of ICAM-1 induced by EPZ-6438 treatment. Except for the latter results, overall, treatment with HDACi and with EZH2i alone reduced the constitutive expression of ICAM-1 in investigated mesothelioma cell lines. Concomitant treatments of guadecitabine either with VPA, SAHA or EPZ-6438, resulted in the up-regulation of the molecule expression in 4/5 MPM cell lines, inducing total mean values of MFI  $\pm$  SD of  $18.35 \pm 17.02$ ,  $17.18 \pm 13.77$ , and  $16.38 \pm 12.11$ , respectively compared to untreated MPM cell lines (Fig. 14C). Moreover, no relevant differences in the percentage of ICAM-1-positive cells were detected after guadecitabine-based combinations compared to controls in 2 out of 5 cell lines that constitutively

showed high expression of the surface molecule, while an increase of the percentage of ICAM-1-positive cells after treatment with both guadecitabine and guadecitabine-based combinations were registered in the remaining 3 cell lines (Fig. 14D).

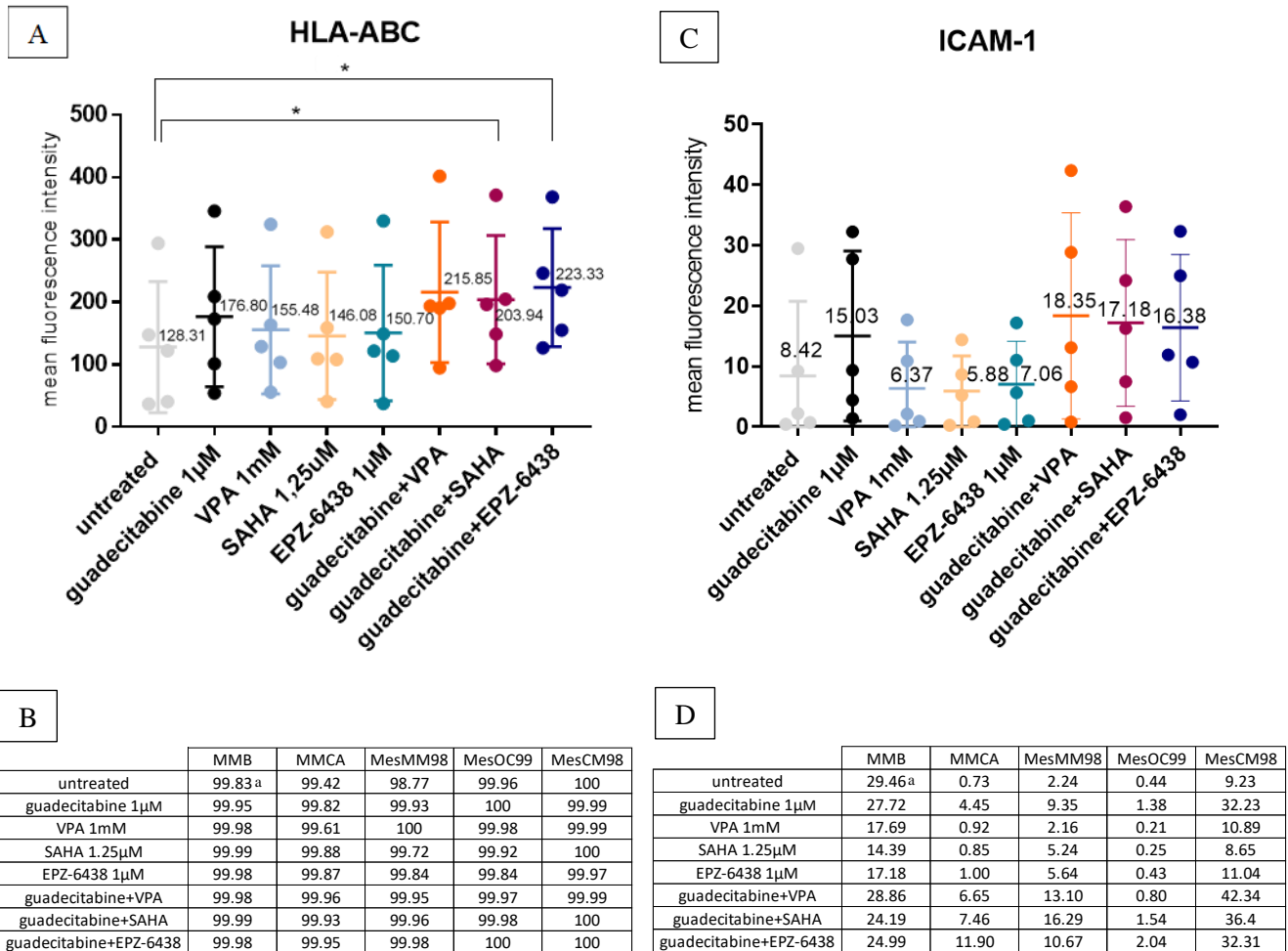


Fig. 14 – MPM cell lines untreated or treated with guadecitabine, VPA, SAHA, EPZ-6438, and guadecitabine-based combinations were incubated with (A) anti-human HLA class I or (C) anti-human ICAM-1 antibody and studied by flow cytometry. Data were analyzed by Kaluza software. *p*-value was calculated by one-way Anova test between values of mean fluorescence intensity of surface molecules expressed on drugs-treated cells compared to untreated cells. Each data point represents an individual cell line. Percentage of positive cells for (B) HLA class I antigens and (D) ICAM-1 for each treatment or untreated cells are reported. \*,  $p < 0.05$ . <sup>a</sup>, values reported correspond to percentage of positive cells.

### 4.3. Molecular analysis of CTA expression in MPM cell lines treated with combined epigenetic drugs

Quantitative Real-time PCR analyses were performed to investigate changes in the expression levels of CTA (i.e., NY-ESO-1, MAGE-A1, and MAGE-A3) induced by the different investigated epigenetic drugs and their combinations, in MPM cell lines. A *de novo* expression of the constitutive negative (gene/ $\beta$ -actin molecules  $< 1E-04$ ) NY-ESO-1 was induced by guadecitabine in 5/5 MPM cell lines with

a mean expression of  $1.10E-02 \pm 1.55E-02$  mRNA molecules (Fig. 15A). Treatment of MPM cells with epigenetic drugs belonging to other classes did not induce the expression of NY-ESO-1 gene, except for MMB cell line after EPZ-6438 treatment. Differently, combined treatments resettled the guadecitabine-prompted induction, reaching mean values of NY-ESO-1-specific mRNA molecules  $\pm$  SD of  $2.37E-02 \pm 2.85E-02$ ,  $1.07E-02 \pm 1.34E-02$ ,  $1.42E-02 \pm 1.94E-02$  for VPA, SAHA, and EPZ-6438, respectively, compared to controls (Fig. 15A). Besides, baseline levels of MAGE-A1 expression were heterogenous being positive for the 2 sarcomatoid cell lines MesMM98 and MesOC99 and negative for the other 3 MPM cell lines. Guadecitabine induced the expression of MAGE-A1 in 2 out of 3 MAGE-A1-negative cells and up-regulated the constitutive expression in the 2 positive sarcomatoid cells. Treatment with VPA and SAHA up-regulated the level of expression only in 2 sarcomatoid cell lines, while EPZ-6438 did not induce any modification. Combined treatments of guadecitabine with the other 2 classes of epigenetic drugs induced/upregulated MAGE-A1 gene expression in 4/5 cell lines, with total mean values of molecules  $\pm$  SD of  $1.16E-02 \pm 9.15E-03$  for VPA,  $5.22E-03 \pm 5.50E-03$  for SAHA, and  $6.26E-03 \pm 6.49E-03$  for EPZ-6438, compared to  $2.12E-03 \pm 3.37E-03$  of untreated cells (Fig. 15B). The third CTA investigated was MAGE-A3, which showed negative baseline levels in only 1 biphasic MPM cell line. Guadecitabine or VPA alone induced the expression of MAGE-A3 in the biphasic MAGE-A3-negative cell line, and up-regulated the expression of the gene in the 2 sarcomatoid cell lines; treatment with SAHA alone up-regulated MAGE-A3 expression in only MesOC99 cell line, and no changes of MAGE-A3 constitutive expression was observed after treatment with EPZ-6438. Compared to the single treatment with guadecitabine, the combination of the DHA with the other 3 epigenetic agents induced higher levels of MAGE-A3 in the negative MMB cell line and confirmed the similarly up-regulated constitutive levels of MAGE-A3 expression in the 2 CTA-positive cell lines. Total mean MAGE-A3 mRNA expression levels  $\pm$  SD were  $2.26E-02 \pm 1.79E-02$  for VPA,  $1.49E-02 \pm 1.34E-02$  for SAHA, and  $1.65E-02 \pm 1.50E-02$  after EPZ-6438 treatment, compared to baseline levels of  $9.30E-03 \pm 1.45E-02$  (Fig. 15C).

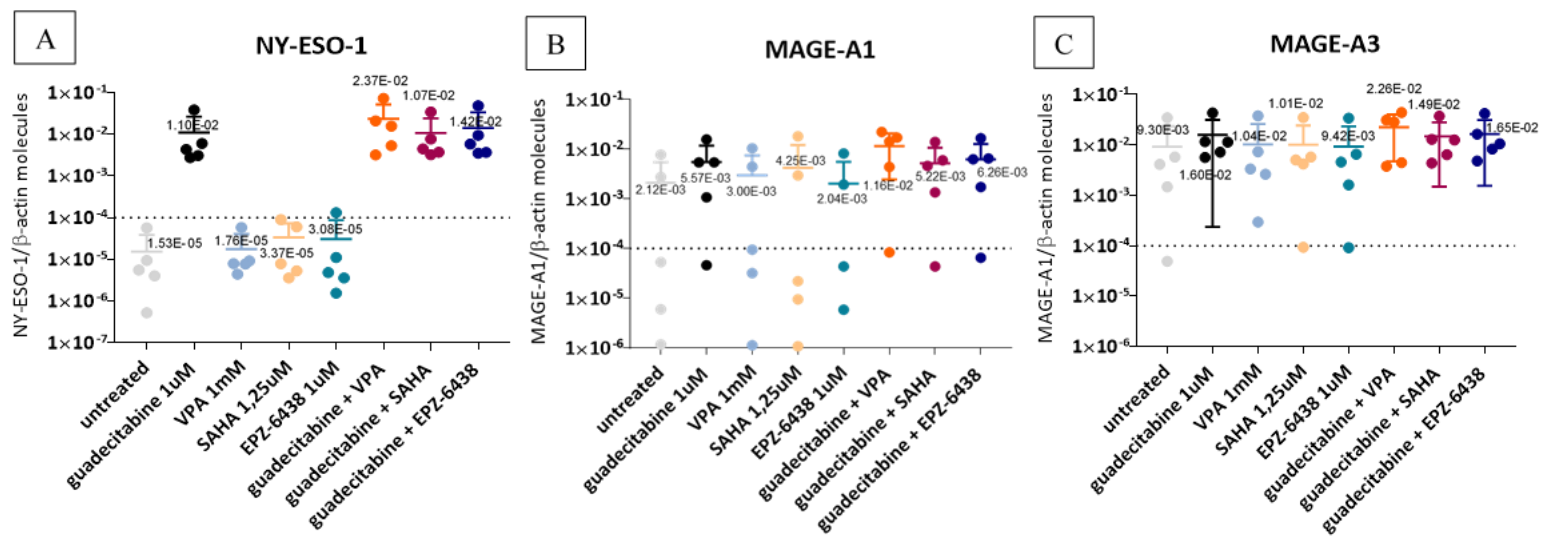


Fig. 15 – Quantitative RT-PCR analysis of CTA expression in MPM cell lines. Total RNA was extracted from MPM cell lines, untreated or treated with guadecitabine, VPA, SAHA, EPZ-6438, and guadecitabine-based combinations. Scatter plots report the number of molecules of (A) NY-ESO-1, (B) MAGE-A1, and (C) MAGE-A3 mRNA, expressed as mean values normalized to the expression of the  $\beta$ -actin gene. *p*-value was calculated by one-way Anova test between values of CTA expression in epigenetic drugs-treated compared to untreated cells. Each data point represents an individual cell line. Dotted line represents gene expression values  $\geq 1E-04$ .

#### 4.4. Molecular analysis of gene expression of PD-L1 expression on MPM cell lines treated with combined epigenetic drugs

All investigated MPM cell lines were constitutively positive for the expression of the immune checkpoint molecule PD-L1. Single treatments with guadecitabine or with VPA up-regulated PD-L1-specific mRNA levels in 3/5 cell lines, with a total mFC of 2.13 and 2.76, respectively, compared to untreated cells (Fig. 16). The HDACi SAHA and the EZH2i EPZ-6438 alone up-regulated the expression level of the gene in only 1/5 investigated MPM cell lines. Diversely, combined treatments increased PD-L1 expression in 5/5 cell lines by guadecitabine *plus* VPA, with a mFC of 6.95, and in 4/5 cell lines after treatments of guadecitabine *plus* SAHA or EPZ-6438, with a total mFC of 2.42 or 2.50, respectively (Fig. 16).

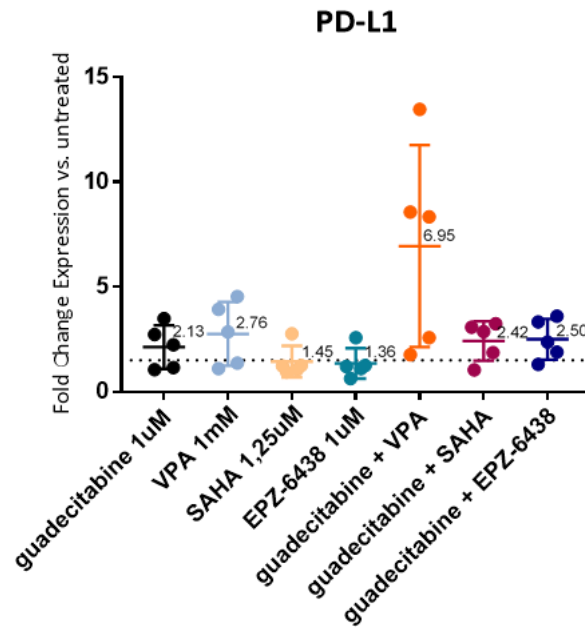


Fig. 16 – Quantitative RT-PCR analysis of PD-L1 expression in MPM cell lines. Total RNA was extracted from MPM cell lines, untreated or treated with guadecitabine, VPA, SAHA, EPZ-6438, and guadecitabine-based combinations. Scatter plots report the FC of PD-L1 expression in treated vs. untreated cell lines. *p-value* was calculated by one-way Anova test between values of PD-L1 expression in epigenetic drugs-treated compared to untreated cells. Each data point represents an individual cell line. Dotted line represents FC expression values  $\geq 1.5$ .

#### 4.5. Molecular analysis of gene expression of NKG2DLs expression on MPM cell lines treated with combined epigenetic drugs

Changes in the expression of the NKG2DLs MICA, MICB, and ULBP2 in 5 MPM cell lines treated with guadecitabine or guadecitabine *plus* VPA, SAHA, or EPZ-6438, compared to untreated cells, have been studied through quantitative real-time PCR. Positive constitutive levels of the investigated NKG2DLs have been recorded in all cell lines analyzed. The expression levels of MICA and MICB mRNA resulted up-regulated in 4/5 MPM cell lines after treatment with guadecitabine. MICA-specific mRNA levels were up-regulated in 2/3 cell lines after HDACi treatments, while MICB levels were up-regulated in 3/5 and in 1/5 cell lines, treated with VPA and SAHA, respectively. Finally, EPZ-6438 up-regulated the mRNA levels of MICB only in 1/5 on MPM cell lines. The combined treatment of guadecitabine *plus* VPA consistently up-regulated MICA and MICB levels showing a total mFC of 3.48 and 6.80, respectively, compared to untreated cells (Fig. 17A-17B). The addition of SAHA to guadecitabine up-regulated MICA and MICB expression in 4/5 and 3/5 MPM cell lines, respectively. Combining EPZ-6438 to guadecitabine up-regulated both MICA and MICB levels in 4/5 cell lines. The strongest results have been obtained in the study of ULBP2 expression levels: single guadecitabine, HDACi and EZH2i treatments resulted in the up-regulation in 4/5, 4/5, 2/5, and 1/5 of

cell lines, showing total mean values of normalized mRNA molecules  $\pm$  SD of  $1.48\text{E-}03 \pm 8.30\text{E-}04$  for guadecitabine,  $1.56\text{E-}03 \pm 9.77\text{E-}04$  for VPA,  $7.58\text{E-}04 \pm 6.05\text{E-}04$  for SAHA, and  $7.84\text{E-}04 \pm 6.37\text{E-}04$  for EPZ-6438, compared to baseline levels of  $6.90\text{E-}04 \pm 5.42\text{E-}04$  (Fig. 17C). The addition of the other 3 epigenetic compounds to guadecitabine induced a consistent up-regulation of ULBP2-specific mRNA levels in 5/5 MPM cell lines, that was significant for guadecitabine plus SAHA or EPZ-6438, and reached mean values  $\pm$  SD of  $4.42\text{E-}03 \pm 2.28\text{E-}03$ , and  $1.59\text{E-}03 \pm 8.82\text{E-}04$  for HDACi-based combinations, and of  $1.85\text{E-}03 \pm 8.51\text{E-}04$  for guadecitabine *plus* EPZ-6438 (Fig. 17C).

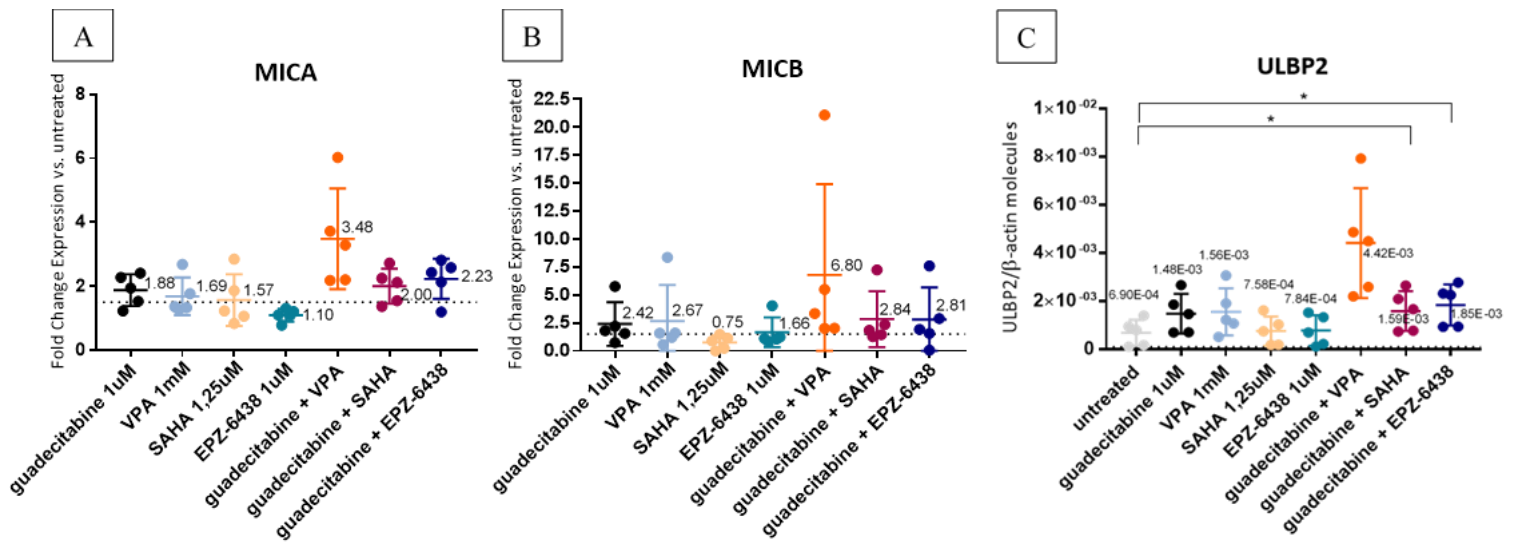


Fig. 17 – Quantitative RT-PCR analysis of NKG2DLs expression in MPM cell lines. Total RNA was extracted from MPM cell lines, untreated or treated with guadecitabine, VPA, SAHA, EPZ-6438, and guadecitabine-based combinations. Scatter plots report the number of molecules of (A) MICA, (B) MICB, and (C) ULBP2 mRNA, expressed as fold change expression of treated *versus* untreated cells (A, B) or mean values normalized to the expression of the  $\beta$ -actin gene (C). *p*-value was calculated by one-way Anova test between values of NKG2DLs expression in epigenetic drugs-treated compared to untreated cells. Each data point represents an individual cell line. \*,  $p < 0.05$ . Dotted line represents gene expression values  $\geq 1\text{E-}04$  or FC expression values  $\geq 1.5$ .

#### 4.7. Molecular analysis of gene expression of EMT-regulating genes on MPM cell lines treated with combined epigenetic drugs

The expression levels of genes coding for adhesion molecules have been investigated by quantitative real-time PCR to study the effect of the DHA guadecitabine and guadecitabine-based combinations on the EMT phenomenon. Results showed that the expression of both cadherin-coding genes were histotypes-specific: i) expression of CDH1 gene, coding for the epithelial cadherin (E-cadherin), was negative in the sarcomatoid cell lines, while both biphasic and epithelial MPM cell lines expressed positive constitutive levels of CDH1-specific mRNA (Fig. 18A). The constitutive negative expression

of CDH1, observed in the sarcomatoid cell lines was induced only by guadecitabine and guadecitabine-based combinations, reaching a mean expression value  $\pm$  SD of  $4.36E-04 \pm 8.16E-04$ ,  $1.73E-03 \pm 1.44E-03$ ,  $4.76E-04 \pm 4.43E-04$  and  $6.68E-04 \pm 5.26E-04$  for guadecitabine, and its combinations with VPA, SAHA, and EPZ-6438, respectively, compared to the control  $4.02E-05 \pm 2.75E-05$  (data not shown). The CDH1-positive cell lines registered the up-regulation only in 1/5 cell lines after the guadecitabine *plus* EPZ-6438 combined treatment, while the other treatments did not induce any significant modulation of the gene expression; ii) besides, the opposite situation has been registered for CDH2 gene, coding for the mesenchymal stem cells and lineage-specific marker N-cadherin. Both sarcomatoid and biphasic cell lines had positive baseline expression levels of CDH2, showing a mean value of normalized molecules of mRNA  $\pm$  SD of  $5.60E-03 \pm 2.05E-03$ , *versus* the epithelioid phenotype that had a negative mean value  $\pm$  SD of  $1.43E-03 \pm 2.91E-07$  (data not shown). Although the expression of CDH2 was upregulated only by SAHA and SAHA *plus* guadecitabine in 1/5 of CDH2-positive cells and in 2/5 and 3/5 cell lines in VPA and VPA *plus* guadecitabine combinations compared to control, respectively, no treatments affected CDH2 expression in the constitutive negative epithelioid cell lines (Fig. 18B). Results obtained in the present study are summarized in figure 19.

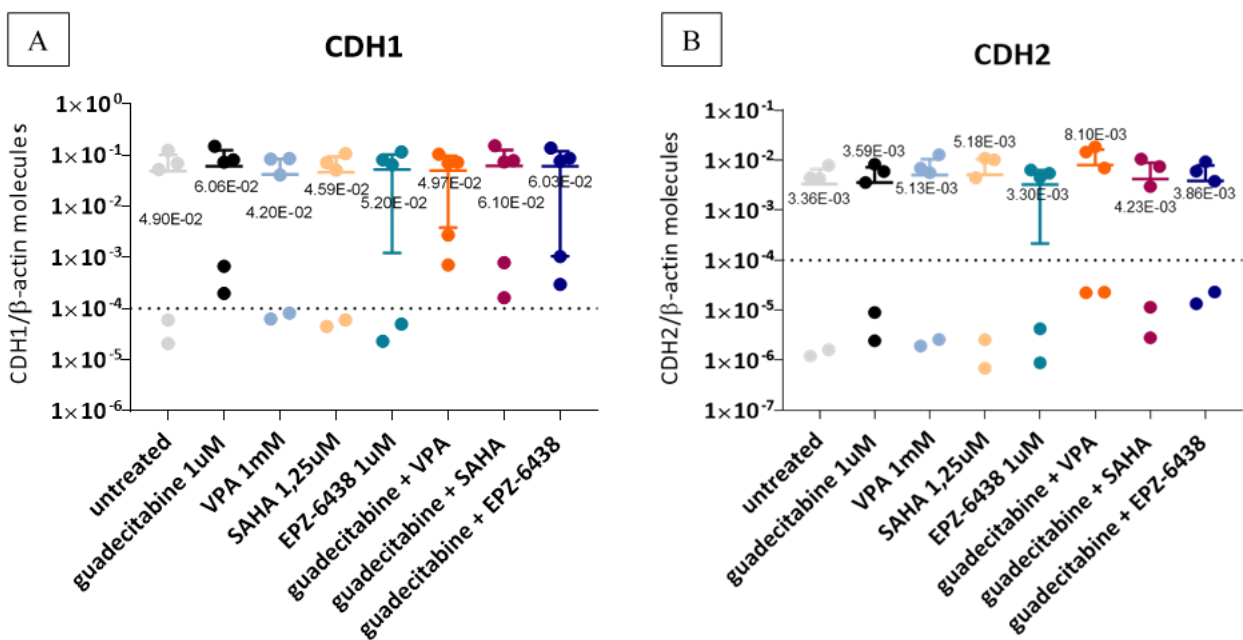
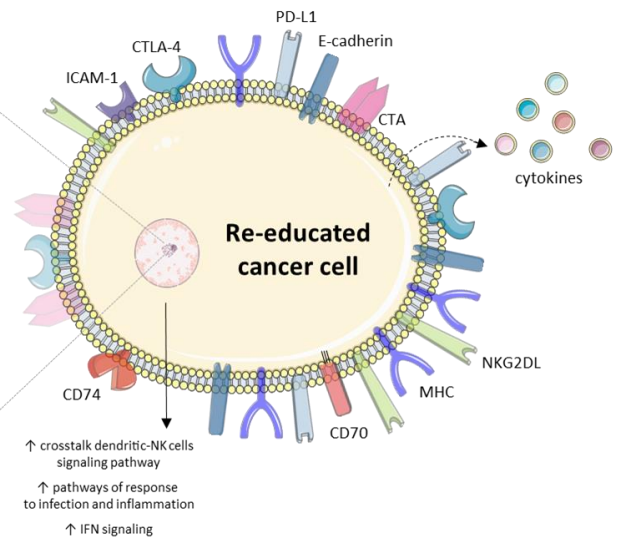


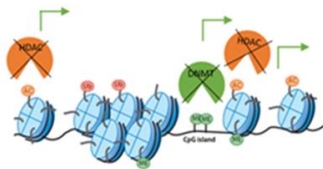
Fig. 18 - Quantitative RT-PCR analysis of the expression of cadherin-coding genes in MPM cell lines. Total RNA was extracted from MPM cell lines, untreated or treated with guadecitabine, VPA, SAHA, EPZ-6438, and guadecitabine-based combinations. Scatter plots report the number of molecules of (A) CDH1 and (B) CDH2 mRNA, expressed as mean values normalized to the expression of the  $\beta$ -actin gene. p-value was calculated by one-way Anova test between values of CDH-specific mRNA expression in epigenetic drugs-treated compared to untreated cells. Each data point represents an individual cell line. Dotted line represents gene expression values  $\geq 1E-04$ .

## Treatment with guadecitabine re-educates malignant pleural mesothelioma cell lines

Gene groups modulated by guadecitabine	Example genes
IFN and IFN-related genes	↑ IFI27, MX1, IFITM1, ISG15, IFI6
TNF superfamily	↑ TNF, TNFRSF10, CD70 ↓ TNFRSF1A
Cancer-Testis Antigens	↑ MAGE-B2/-A1/-A3/-A4, NY-ESO-1
HLA antigens and HLA-related genes	↑ HLA-ABC, CD74, MICB, ULBP2
Cytokines and receptors	↑ IL2RG, IL24 ↓ IL17A, IL10, IL18R1
Chemokines and receptors	↑ CCL20, CX3CL1, CXCL14, CXCR4
Adhesion molecules	↑ ICAM1, PECAM1, EPCAM, VCAM1, CDH1, ITGB2 ↓ CDH2, CDH11, NCAM1
Inflammatory mediators	↑ F2RL1, NOD2, TLR4 ↓ TICAM1
Immune checkpoint and co-stimulatory molecules	↑ CTLA-4, LAG3, PD-L1, TIGIT, CD40

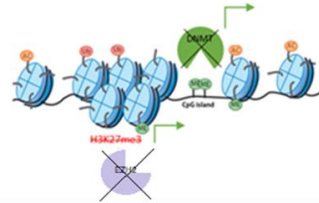


### Combination of guadecitabine with HDACi



- More pronounced up-regulation of HLA class I antigens and ICAM-1
- More pronounced up-regulation of PD-L1
- More pronounced up-regulation of NKG2D ligands MIC-A/-B and ULBP2
- More pronounced up-regulation/induction of CDH1

### Combination of guadecitabine with EZH2i



- More pronounced up-regulation of HLA class I antigens

Fig. 19 – Summarized results obtained in the present study.

## 5. Discussion

Despite the accumulation of novel insights about mesothelioma biology and the considerable number of clinical investigations ongoing, MPM is still an aggressive cancer with dismal prognosis and limited therapeutic options. ICI therapy represents an attracting strategy in the treatment of solid tumors; however, modest results have been obtained in this tumor type by single-agent or combined ICI-targeted immunotherapy, due to multiple mechanisms of resistance (Chu, 2019). Since epigenetic derangements are known to contribute to the pathogenesis of MPM and to its highly immunosuppressive microenvironment (Peng, 2015), it is reasonable to explore the efficacy of epigenetic compounds in MPM, in the attempt to improve tumor immunogenicity, remodeling the tumor phenotype and provide a rationale for epigenetic-based strategies able to enhance efficacy of immunotherapy.

On these bases, in the first instance, we characterized the effect of the second-generation DHA guadecitabine, known to own immunomodulatory activity, on the gene expression fingerprint of 10 MPM cell lines. Through the nCounter® methodology, which helped to fill the gap between genome-wide analysis and quantitative real-time PCR expression profiling, it was possible to comprehensively investigate the expression of a wide number of genes related to tumor, microenvironment and immune response signatures, before and after treatment with guadecitabine. “Ingenuity Pathway analysis” elaborations have been conducted to extrapolate the modulated canonical pathways, revealing, most frequently among all, the activation of the crosstalk between dendritic cells and NK cells signaling pathway in 50% of MPM cell lines. Historical data report how dendritic cells can trigger the NK-mediated innate immunity in HLA class I-negative cells, thus promoting NK cell killing and IFN- $\gamma$  production *in vivo* (Fernandez, 1999). From cytofluorimetric assays, we observed that the tested cell lines were positive for HLA class I antigens and guadecitabine up-regulated their surface expression only in the 2 sarcomatoid cell lines. Consistent with this, the activation of the dendritic-NK cells crosstalk induced by guadecitabine in the 50% of cell lines, was specifically observed in biphasic and sarcomatoid cell lines, supporting the hypothesis that guadecitabine could enhance adaptive and non-adaptive immunity in the most aggressive histological subtypes. Moreover, we found that one of the most frequently activated upstream regulator pathways was the IFN- $\gamma$  signaling one; this is of pivotal importance, given the involvement of IFN- $\gamma$  in host–tumor interactions and in mechanisms of tumor resistance to therapeutic CTLA-4 blockade (Gao, 2016; Castro, 2018). Moreover, guadecitabine exerted its strongest action in inducing IFN-related genes in the sarcomatoid phenotype, in which we observed a higher up-regulation of ISG15 gene and its target proteins, *e.g.*, MX1, required for NK cells proliferation, neutrophils chemotaxis, and IFN- $\gamma$ -inducing cytokines production (Scarno, 2019),

compared to biphasic and epithelioid phenotypes. These data confirmed results about the epigenetic activation of immune response through the IFN pathway signaling, previously obtained in cell lines of different tumor types (Chiappinelli, 2015; Fazio, 2018), supporting the thesis that this epi-drug could increase immune response against MPM tumor cells, potentially also with sarcomatoid features.

Several data supported the involvement of epigenetic drugs in facilitating the immunological target of cancer cells, related to their capability to modulate pivotal antigens regulating the tumor-immune system crosstalk (Sigalotti, 2014). Our data confirmed the immunomodulatory capabilities of guadecitabine, that induced a strong upregulation of CTA, especially CTAG1B (NY-ESO-1) and MAGE family members, able to potentially elicit both humoral and cell-mediated immune responses, in all the 3 main histological subtypes of MPM. Opposite to the well-known activity of CTA, the role of TNF-dependent immune response in cancer progression is still contradictory. Although some members of the superfamily can induce immune response through the release of “danger signals”, other components seem to be pro-tumor agents (Montfort, 2019). Based on our results, guadecitabine up-regulated TNFRSF10A in the 3 histotypes, and TNFRSF1B in sarcomatoid and biphasic cell lines, sustaining cell death signals and apoptosis, but also CD70 in 7 mixed cell lines, which could potentially enhance the generation of cytolytic T cells and contribute to T cell activation. Moreover, a recent study reports the overexpression of the mesenchymal-associated TNFRSF1A to be strongly related to poor prognosis, and its knockdown to inhibit proliferation and migration of tumor cell lines *in vitro* (Yang, 2020); also, it seems to induce the production of IL17 by CD4<sup>+</sup> T cells, recruiting myeloid cells and supporting tumor growth (Charles, 2009). A down-regulation of TNFRSF1A, more pronounced in sarcomatoid and biphasic cell lines was found in MPM cell lines treated with guadecitabine, and this could be a mechanism, induced by guadecitabine, to impair tumor progression and to avoid the recruitment of immunosuppressive cells, that act as a barrier to cancer immunotherapy. This hypothesis is also supported by the down-regulation of the expression of IL17A-specific mRNA observed in the aforementioned phenotypes after guadecitabine treatment.

Noteworthy, in addition to the above-mentioned effects of guadecitabine on adaptive immunity, recent data indicated that it is responsible for the enhancement, on tumor cells, of the expression of NKG2DLs, able to activate the NKG2D receptor on NK cells (Fazio, 2018). In this context, our results are concordant with scientific literature, demonstrating the up-regulation of MICB and ULBP2 in almost all investigated cell lines, highlighting the potential guadecitabine-mediated contribution to tumor cell recognition and killing by the innate immune system.

Also, we reported the expression of the HLA-related molecule and migration inhibitory factor (MIF) ligand CD74, which represents an independent prognostic factor of survival for MPM patients, whatever the histological subtype, being however more expressed in the epithelial type; indeed, its low tumoral

expression was associated with dismal prognosis (Otterstrom, 2014). Some studies also support the CD74 involvement in the prevention of the EMT process in other tumor histotypes (Cufi, 2010; Heinrichs, 2011; Lee, 2013). CD74 molecule resulted up-regulated by guadecitabine only in cell lines of the sarcomatoid and biphasic phenotypes, encouraging the use of DHAs to revert mesenchymal features of MPM. The presence of epithelial or mesenchymal molecules, as well as EMT-regulating markers, reflects the progress of a tumor that underwent EMT, as observed in MPM histological subtypes, switching cell components from epithelioid, to biphasic and sarcomatoid phenotype. This has been confirmed to have prognostic significance, with epithelioid histology associated with the longest survival (Fassina, 2012). The guadecitabine-induced up-regulation of the expression of epithelial markers (*e.g.*, CDH1, EPCAM, PECAM1), observed at higher levels in sarcomatoid cell lines, is an interesting clue to support the action of guadecitabine in reverting the multi-step EMT phenomenon. This was supported also by the down-regulation of mesenchymal origin molecules (*e.g.*, NCAM, CDH2), demonstrated to facilitate the assembly of focal adhesions, migration and invasion (Lehembre, 2008; Lamouille, 2014). In addition, considering that adhesion molecules may have a role in immune system regulation, the up-regulation of molecules such as ICAM1 and ICAM ligands (*e.g.*, ITGB2), observed in 50% of cell lines, might suggest a strongest transmigration of leukocytes within the tumor (Mutti, 1993).

DHAs were demonstrated to sensitize tumors to ICI treatment through the up-regulation of immune checkpoint molecules (Wrangle, 2013; Fazio, 2018). In line with this, guadecitabine induced a strong up-regulation of CTLA-4 in sarcomatoid and biphasic cell lines, as well as of PD-L1 (CD274) in the biphasic phenotype, and of the co-stimulatory molecule CD40 in 50% of cell lines, making these molecules more targetable by immunotherapeutic strategies and supporting the use of epigenetic drugs in combination with immune checkpoint mAbs in the clinical setting.

Considering that the immunomodulatory activity of DHAs has been confirmed in different tumor histotypes, and that few studies have been conducted to investigate the potential of combining DHAs with other classes of epigenetic compounds in MPM (Leclercq, 2011; Bensaid, 2018; Aspeslagh, 2018), we aimed to investigate whether the treatment of MPM cell lines with guadecitabine-based combinations with HDACi or EZH2i could strengthened the DHA-mediated immunomodulatory effects, compared to single agent treatments.

Combining guadecitabine with VPA, SAHA, or EPZ-6438 increased its capability to up-regulate immune and immune-related molecules, such as HLA class I and ICAM-1. Particularly, SAHA and EPZ-6438 *plus* guadecitabine induced a statistically significant up-regulation of the constitutive positive surface expression of HLA class I antigens, compared to untreated cells; moreover, a higher expression of HLA class I antigens was observed after all the 3 guadecitabine-combined treatments

compared to guadecitabine alone.

Among co-stimulatory molecules, the strongest up-regulation of ICAM-1 was observed when guadecitabine was combined with VPA, even though either VPA, SAHA, or EPZ-6438 were able to enhance ICAM-1, both in terms of MFI and percentage of positive cells, compared to the control and guadecitabine-treated cells. CTA molecules expression is highly regulated by guadecitabine, that mainly contributes to the up-regulation of guadecitabine-based combinations enhancement. These results are in line with what observed from previous studies with decitabine and HDACi (Leclercq, 2011).

Moreover, molecular analysis revealed that guadecitabine up-regulated the expression of PD-L1, one of the most controversial predictive biomarkers of response to ICI therapy as well as one of the most important targets of immunotherapeutic mAbs therapy (Lantuejoul, 2017). This is in line with what observed through the nCounter gene expression analysis; furthermore, the combined treatment involving guadecitabine and VPA resulted in the higher up-regulation of the immune checkpoint target, supporting further *in vivo* studies to validate the epi-drugs combination as promising strategy to couple with ICI mAbs.

Studying the expression profile of NKG2DLs, we observed a constitutive positive level of expression of the 3 ligands investigated in all the 5 MPM investigated cell lines and confirmed their guadecitabine-mediated up-regulation; again, the strongest action in increasing the expression of MICA, MICB, and ULBP2 molecules was exerted by guadecitabine *plus* VPA condition, resulting an exciting option to enhance tumor cell recognition by NK and T cells and the consequential NK/T cell-mediated tumor killing.

The study of cadherins expression confirmed previous results about the expression of epithelial or mesenchymal markers in epithelioid or sarcomatoid MPM, respectively, with the biphasic histological subtype owning both molecule classes (Fassina, 2012). On these bases, the induction of E-cadherin expression obtained with guadecitabine and guadecitabine-based combinations, could be of great interest to remodel tumor phenotype to a less aggressive one. In addition, the absent modulation observed for the mesenchymal marker N-cadherin in the constitutive negative epithelial cell lines, strengthened the anti-EMT potential of guadecitabine.

Overall, our study showed that guadecitabine, which immunomodulatory effects have been studied more intensively in the recent years in different tumor histotypes, is a promising enhancer of immunogenicity of MPM tumor cell lines and a potential inducer of increased immune cell recognition of tumor cells, especially in the most aggressive phenotype. Moreover, its combination with other classes of epigenetic compounds strengthened its antitumor activity, able to up-regulate immune co-stimulatory molecules and pivotal targets of immunotherapeutic treatments, such as HLA class I

antigens, ICAM-1, CTA, and PD-L1. The study of epigenetic drugs combinations is of great interest in the context of EMT investigations, given the high influence of EMT-regulating molecules on survival of MPM patients, and our results are among the first evidence of the effects of epigenetic drugs on MPM histological subtypes. Further studies are needed to comprehensively deepen the role of epigenetic machinery actors on the pathogenesis of MPM and its progression. A greater number of cell lines belonging to the 3 histotypes will be treated with the promising combination to conduct both molecular, phenotypic and functional analyses, in order to better characterize either the behaviour of tumor and its interaction with immune cell components. These studies will lay the groundwork for planning further *in vivo* studies to demonstrate the potential of guadecitabine-based epigenetic drugs combinations, taking into account the influence of subtypes of mesothelioma for the selection of immunotherapeutic targets and biomarkers.

## 6. References

- Abaza, M. S., Bahman, A. M., and Al-Attiyah, R. J. Valproic acid, an anti-epileptic drug and a histone deacetylase inhibitor, in combination with proteasome inhibitors exerts antiproliferative, pro-apoptotic and chemosensitizing effects in human colorectal cancer cells: underlying molecular mechanisms. *Int J Mol Med*, 34: 513-532, **2014**.
- Abbas, A. and Gupta, S. The role of histone deacetylases in prostate cancer. *Epigenetics*, 3: 300-309, **2008**.
- Adcock, I. M., Ito, K., and Barnes, P. J. Histone deacetylation: an important mechanism in inflammatory lung diseases. *Copd*, 2: 445-455, **2005**.
- Adeshakin, A. O., Yan, D., Zhang, M., Wang, L., Adeshakin, F. O., Liu, W., and Wan, X. Blockade of myeloid-derived suppressor cell function by valproic acid enhanced anti-PD-L1 tumor immunotherapy. *Biochem Biophys Res Commun*, 522: 604-611, **2019**.
- Aghdassi, A., Sendler, M., Guenther, A., Mayerle, J., Behn, C. O., Heidecke, C. D., Friess, H., Buchler, M., Evert, M., Lerch, M. M., and Weiss, F. U. Recruitment of histone deacetylases HDAC1 and HDAC2 by the transcriptional repressor ZEB1 downregulates E-cadherin expression in pancreatic cancer. *Gut*, 61: 439-448, **2012**.
- Ali, G., Bruno, R., and Fontanini, G. The pathological and molecular diagnosis of malignant pleural mesothelioma: a literature review. *J Thorac Dis*, 10: S276-S284, **2017**.
- Alley, E. W., Lopez, J., Santoro, A., Morosky, A., Saraf, S., Piperdi, B., and van Brummelen, E. Clinical safety and activity of pembrolizumab in patients with malignant pleural mesothelioma (KEYNOTE-028): preliminary results from a non-randomised, open-label, phase 1b trial. *Lancet Oncol*, 18: 623-630, **2017**.
- Amnekar, R. V., Khan, S. A., Rashid, M., Khade, B., Thorat, R., Gera, P., Shrikhande, S. V., Smoot, D. T., Ashktorab, H., and Gupta, S. Histone deacetylase inhibitor pre-treatment enhances the efficacy of DNA-interacting chemotherapeutic drugs in gastric cancer. *World J Gastroenterol*, 26: 598-613, **2020**.
- Armeanu, S., Bitzer, M., Lauer, U. M., Venturelli, S., Pathil, A., Krusch, M., Kaiser, S., Jobst, J., Smirnow, I., Wagner, A., Steinle, A., and Salih, H. R. Natural killer cell-mediated lysis of hepatoma cells via specific induction of NKG2D ligands by the histone deacetylase inhibitor sodium valproate. *Cancer Res*, 65: 6321-6329, **2005**.
- Baas, P., Fennell, D., Kerr, K. M., Van Schil, P. E., Haas, R. L., and Peters, S. Malignant pleural mesothelioma: ESMO Clinical Practice Guidelines for diagnosis, treatment and follow-up. *Ann Oncol*, 26 Suppl 5: v31-39, **2015**.
- Baragano Raneros, A., Martin-Palanco, V., Fernandez, A. F., Rodriguez, R. M., Fraga, M. F., Lopez-Larrea, C., and Suarez-Alvarez, B. Methylation of NKG2D ligands contributes to immune system evasion in acute myeloid leukemia. *Genes Immun*, 16: 71-82, **2015**.
- Baris, Y. I., Bilir, N., Artvinli, M., Sahin, A. A., Kalyoncu, F., and Sebastien, P. An epidemiological study in an Anatolian village environmentally exposed to tremolite asbestos. *Br J Ind Med*, 45: 838-840, **1988**.
- Baylin, S. B., Esteller, M., Rountree, M. R., Bachman, K. E., Schuebel, K., and Herman, J. G. Aberrant patterns of DNA methylation, chromatin formation and gene expression in cancer. *Hum Mol Genet*, 10: 687-692, **2001**.
- Belinsky, S. A., Grimes, M. J., Picchi, M. A., Mitchell, H. D., Stidley, C. A., Tesfaigzi, Y., Channell, M. M., Liu, Y., Casero, R. A., Jr., Baylin, S. B., Reed, M. D., Tellez, C. S., and March, T. H. Combination therapy with vidaza and entinostat suppresses tumor growth and reprograms the epigenome in an orthotopic lung cancer model. *Cancer Res*, 71: 454-462, **2012**.
- Bensaid, D., Blondy, T., Deshayes, S., Dehame, V., Bertrand, P., Gregoire, M., Errami, M., and Blanquart, C. Assessment of new HDAC inhibitors for immunotherapy of malignant pleural mesothelioma. *Clin Epigenetics*, 10: 79, **2018**.
- Bera, T. K. and Pastan, I. Mesothelin is not required for normal mouse development or reproduction. *Mol Cell Biol*, 20: 2902-2906, **2000**.
- Bharadwaj, U., Marin-Muller, C., Li, M., Chen, C., and Yao, Q. Mesothelin confers pancreatic cancer cell resistance to TNF-alpha-induced apoptosis through Akt/PI3K/NF-kappaB activation and IL-6/Mcl-1 overexpression. *Mol Cancer*, 10: 106, **2011**.
- Blackledge, N. P., Rose, N. R., and Klose, R. J. Targeting Polycomb systems to regulate gene expression: modifications to a complex story. *Nat Rev Mol Cell Biol*, 16: 643-649, **2015**.
- Boulanger, G., Andujar, P., Pairon, J. C., Billon-Galland, M. A., Dion, C., Dumortier, P., Brochard, P., Sobaszek, A., Bartsch, P., Paris, C., and Jaurand, M. C. Quantification of short and long asbestos fibers to assess asbestos exposure: a review of fiber size toxicity. *Environ Health*, 13: 59, **2014**.
- Boussios, S., Moschetta, M., Karathanasi, A., Tsiouris, A. K., Kanellos, F. S., Tatsi, K., Katsanos, K. H., and Christodoulou, D. K. Malignant peritoneal mesothelioma: clinical aspects, and therapeutic perspectives. *Ann Gastroenterol*, 31: 659-669, **2018**.
- Bracken, A. P., Pasini, D., Capra, M., Prosperini, E., Colli, E., and Helin, K. EZH2 is downstream of the pRB-E2F pathway, essential for proliferation and amplified in cancer. *Embo J*, 22: 5323-5335, **2003**.
- Bradbury, C. A., Khanim, F. L., Hayden, R., Bunce, C. M., White, D. A., Drayson, M. T., Craddock, C., and Turner, B. M. Histone

deacetylases in acute myeloid leukaemia show a distinctive pattern of expression that changes selectively in response to deacetylase inhibitors. *Leukemia*, 19: 1751-1759, **2005**.

Branco, M. R., Ficz, G., and Reik, W. Uncovering the role of 5-hydroxymethylcytosine in the epigenome. *Nat Rev Genet*, 13: 7-13, **2011**.

Briere, D., Sudhakar, N., Woods, D. M., Hallin, J., Engstrom, L. D., Aranda, R., Chiang, H., Sodre, A. L., Olson, P., Weber, J. S., and Christensen, J. G. The class I/IV HDAC inhibitor mocetinostat increases tumor antigen presentation, decreases immune suppressive cell types and augments checkpoint inhibitor therapy. *Cancer Immunol Immunother*, 67: 381-392, **2018**.

Bryant, R. J., Cross, N. A., Eaton, C. L., Hamdy, F. C., and Cunliffe, V. T. EZH2 promotes proliferation and invasiveness of prostate cancer cells. *Prostate*, 67: 547-556, **2007**.

Bueno, R., Stawiski, E. W., Goldstein, L. D., Durinck, S., De Rienzo, A., Modrusan, Z., Gnad, F., Nguyen, T. T., Jaiswal, B. S., Chirieac, L. R., Sciaranghella, D., Dao, N., Gustafson, C. E., Munir, K. J., Hackney, J. A., Chaudhuri, A., Gupta, R., Guillory, J., Toy, K., Ha, C., Chen, Y. J., Stinson, J., Chaudhuri, S., Zhang, N., Wu, T. D., Sugarbaker, D. J., de Sauvage, F. J., Richards, W. G., and Seshagiri, S. Comprehensive genomic analysis of malignant pleural mesothelioma identifies recurrent mutations, gene fusions and splicing alterations. *Nat Genet*, 48: 407-416, **2016**.

Cacciotti, P., Strizzi, L., Vianale, G., Iaccheri, L., Libener, R., Porta, C., Tognon, M., Gaudino, G., and Mutti, L. The presence of simian-virus 40 sequences in mesothelioma and mesothelial cells is associated with high levels of vascular endothelial growth factor. *Am J Respir Cell Mol Biol*, 26: 189-193, **2002**.

Calabrò, L., Morra, A., Fonsatti, E., Cutaia, O., Amato, G., Giannarelli, D., Di Giacomo, A. M., Danielli, R., Altomonte, M., Mutti, L., and Maio, M. Tremelimumab for patients with chemotherapy-resistant advanced malignant mesothelioma: an open-label, single-arm, phase 2 trial. *Lancet Oncol*, 14: 1104-1111, **2013**.

Calabrò, L., Morra, A., Fonsatti, E., Cutaia, O., Fazio, C., Annesi, D., Lenoci, M., Amato, G., Danielli, R., Altomonte, M., Giannarelli, D., Di Giacomo, A. M., and Maio, M. Efficacy and safety of an intensified schedule of tremelimumab for chemotherapy-resistant malignant mesothelioma: an open-label, single-arm, phase 2 study. *Lancet Respir Med*, 3: 301-309, **2015**.

Calabrò, L., Morra, A., Giannarelli, D., Amato, G., D'Incecco, A., Covre, A., Lewis, A., Rebelatto, M. C., Danielli, R., Altomonte, M., Di Giacomo, A. M., and Maio, M. Tremelimumab combined with durvalumab in patients with mesothelioma (NIBIT-MESO-1): an open-label, non-randomised, phase 2 study. *Lancet Respir Med*, 6: 451-460, **2018**.

Cannito, S., Novo, E., di Bonzo, L. V., Busletta, C., Colombatto, S., and Parola, M. Epithelial-mesenchymal transition: from molecular mechanisms, redox regulation to implications in human health and disease. *Antioxid Redox Signal*, 12: 1383-1430, **2010**.

Cao, Q., Yu, J., Dhanasekaran, S. M., Kim, J. H., Mani, R. S., Tomlins, S. A., Mehra, R., Laxman, B., Cao, X., Yu, J., Kleer, C. G., Varambally, S., and Chinnaiyan, A. M. Repression of E-cadherin by the polycomb group protein EZH2 in cancer. *Oncogene*, 27: 7274-7284, **2008**.

Cao, Y., Li, Y., Zhang, N., Hu, J., Yin, L., Pan, Z., Li, Y., Du, X., Zhang, W., and Li, F. Quantitative DNA hypomethylation of ligand *Jagged1* and receptor *Notch1* signifies occurrence and progression of breast carcinoma. *Am J Cancer Res*, 5: 1621-1634, **2015**.

Carbone, M., Gazdar, A., and Butel, J. S. SV40 and human mesothelioma. *Transl Lung Cancer Res*, 9: S47-S59, **2020**.

Carbone, M., Rizzo, P., and Pass, H. Simian virus 40: the link with human malignant mesothelioma is well established. *Anticancer Res*, 20: 875-877, **2000**.

Carbone, M. and Yang, H. Molecular pathways: targeting mechanisms of asbestos and erionite carcinogenesis in mesothelioma. *Clin Cancer Res*, 18: 598-604, **2012**.

Carbone, M., Yang, H., Pass, H. I., Krausz, T., Testa, J. R., and Gaudino, G. BAP1 and cancer. *Nat Rev Cancer*, 13: 153-159, **2013**.

Castro, F., Cardoso, A. P., Goncalves, R. M., Serre, K., and Oliveira, M. J. Interferon-Gamma at the Crossroads of Tumor Immune Surveillance or Evasion. *Front Immunol*, 9: 847, **2018**.

Cedar, H. and Bergman, Y. Linking DNA methylation and histone modification: patterns and paradigms. *Nat Rev Genet*, 10: 295-304, **2009**.

Ceresoli, G. L., Aerts, J. G., Dziadziuszko, R., Ramlau, R., Cedres, S., van Meerbeeck, J. P., Mencoboni, M., Planchard, D., Chella, A., Crino, L., Krzakowski, M., Russel, J., Maconi, A., Gianoncelli, L., and Grosso, F. Tumour Treating Fields in combination with pemetrexed and cisplatin or carboplatin as first-line treatment for unresectable malignant pleural mesothelioma (STELLAR): a multicentre, single-arm phase 2 trial. *Lancet Oncol*, 20: 1702-1709, **2019**.

Charles, K. A., Kulbe, H., Soper, R., Escorcio-Correia, M., Lawrence, T., Schultheis, A., Chakravarty, P., Thompson, R. G., Kollias, G., Smyth, J. F., Balkwill, F. R., and Hagemann, T. The tumor-promoting actions of TNF-alpha involve TNFR1 and IL-17 in ovarian cancer in mice and humans. *J Clin Invest*, 119: 3011-3023, **2009**.

Chen, J., Chen, G., Yan, Z., Guo, Y., Yu, M., Feng, L., Jiang, Z., Guo, W., and Tian, W. TGF-beta1 and FGF2 stimulate the epithelial-mesenchymal transition of HERS cells through a MEK-dependent mechanism. *J Cell Physiol*, 229: 1647-1659, **2014**.

Chen, Q., Zheng, P. S., and Yang, W. T. EZH2-mediated repression of GSK-3beta and TP53 promotes Wnt/beta-catenin signaling-dependent cell expansion in cervical carcinoma. *Oncotarget*, 7: 36115-36129, **2016**.

Chen, Y. T., Zhu, F., Lin, W. R., Ying, R. B., Yang, Y. P., and Zeng, L. H. The novel EZH2 inhibitor, GSK126, suppresses cell migration and angiogenesis via down-regulating VEGF-A. *Cancer Chemother Pharmacol*, 77: 757-765, **2016**.

Cheng, W. F., Huang, C. Y., Chang, M. C., Hu, Y. H., Chiang, Y. C., Chen, Y. L., Hsieh, C. Y., and Chen, C. A. High mesothelin correlates with chemoresistance and poor survival in epithelial ovarian carcinoma. *Br J Cancer*, 100: 1144-1153, **2009**.

Chiappinelli, K. B., Strissel, P. L., Desrichard, A., Li, H., Henke, C., Akman, B., Hein, A., Rote, N. S., Cope, L. M., Snyder, A., Makarov, V., Budhu, S., Slamon, D. J., Wolchok, J. D., Pardoll, D. M., Beckmann, M. W., Zahnow, C. A., Merghoub, T., Chan, T. A., Baylin, S. B., and Strick, R. Inhibiting DNA Methylation Causes an Interferon Response in Cancer via dsRNA Including Endogenous Retroviruses. *Cell*, 162: 974-986, **2015**.

Chu, G. J., van Zandwijk, N., and Rasko, J. E. J. The Immune Microenvironment in Mesothelioma: Mechanisms of Resistance to Immunotherapy. *Front Oncol*, 9: 1366, **2019**.

Cimini, D. Merotelic kinetochore orientation, aneuploidy, and cancer. *Biochim Biophys Acta*, 1786: 32-40, **2008**.

Comin, C. E., Anichini, C., Boddi, V., Novelli, L., and Dini, S. MIB-1 proliferation index correlates with survival in pleural malignant mesothelioma. *Histopathology*, 36: 26-31, **2000**.

Connolly, R. M., Rudek, M. A., and Piekarz, R. Entinostat: a promising treatment option for patients with advanced breast cancer. *Future Oncol*, 13: 1137-1148, **2017**.

Coral, S., Parisi, G., Nicolay, H. J., Colizzi, F., Danielli, R., Fratta, E., Covre, A., Taverna, P., Sigalotti, L., and Maio, M. Immunomodulatory activity of SGI-110, a 5-aza-2'-deoxycytidine-containing demethylating dinucleotide. *Cancer Immunol Immunother*, 62: 605-614, **2012**.

Coral, S., Parisi, G., Nicolay, H. J., Colizzi, F., Danielli, R., Fratta, E., Covre, A., Taverna, P., Sigalotti, L., and Maio, M. Immunomodulatory activity of SGI-110, a 5-aza-2'-deoxycytidine-containing demethylating dinucleotide. *Cancer Immunol Immunother*, 62: 605-614, **2013**.

Covre, A., Coral, S., Nicolay, H., Parisi, G., Fazio, C., Colizzi, F., Fratta, E., Di Giacomo, A. M., Sigalotti, L., Natali, P. G., and Maio, M. Antitumor activity of epigenetic immunomodulation combined with CTLA-4 blockade in syngeneic mouse models. *Oncoimmunology*, 4: e1019978, **2015**.

Cregan, S., Breslin, M., Roche, G., Wennstedt, S., MacDonagh, L., Albadri, C., Gao, Y., O'Byrne, K. J., Cuffe, S., Finn, S. P., and Gray, S. G. Kdm6a and Kdm6b: Altered expression in malignant pleural mesothelioma. *Int J Oncol*, 50: 1044-1052, **2017**.

Cufi, S., Vazquez-Martin, A., Oliveras-Ferreros, C., Martin-Castillo, B., Joven, J., and Menendez, J. A. Metformin against TGFbeta-induced epithelial-to-mesenchymal transition (EMT): from cancer stem cells to aging-associated fibrosis. *Cell Cycle*, 9: 4461-4468, **2010**.

de Gooijer, C. J., Baas, P., and Burgers, J. A. Current chemotherapy strategies in malignant pleural mesothelioma. *Transl Lung Cancer Res*, 7: 574-583, **2018**.

Delgermaa, V., Takahashi, K., Park, E. K., Le, G. V., Hara, T., and Sorahan, T. Global mesothelioma deaths reported to the World Health Organization between 1994 and 2008. *Bull World Health Organ*, 89: 716-724, 724A-724C, **2011**.

Di Giorgio, E. and Brancolini, C. Regulation of class IIa HDAC activities: it is not only matter of subcellular localization. *Epigenomics*, 8: 251-269, **2016**.

Diesch, J., Zwick, A., Garz, A. K., Palau, A., Buschbeck, M., and Gotze, K. S. A clinical-molecular update on azanucleoside-based therapy for the treatment of hematologic cancers. *Clin Epigenetics*, 8: 71, **2016**.

Disselhorst, M. J., Quispel-Janssen, J., Lalezari, F., Monkhorst, K., de Vries, J. F., van der Noort, V., Harms, E., Burgers, S., and Baas, P. Ipilimumab and nivolumab in the treatment of recurrent malignant pleural mesothelioma (INITIATE): results of a prospective, single-arm, phase 2 trial. *Lancet Respir Med*, 7: 260-270, **2019**.

Edwards, J. G., McLaren, J., Jones, J. L., Waller, D. A., and O'Byrne, K. J. Matrix metalloproteinases 2 and 9 (gelatinases A and B) expression in malignant mesothelioma and benign pleura. *Br J Cancer*, 88: 1553-1559, **2003**.

Egger, G., Liang, G., Aparicio, A., and Jones, P. A. Epigenetics in human disease and prospects for epigenetic therapy. *Nature*, 429: 457-463, **2004**.

Ehrlich, M. DNA methylation in cancer: too much, but also too little. *Oncogene*, 21: 5400-5413, **2002**.

Emran, A. A., Chatterjee, A., Rodger, E. J., Tiffen, J. C., Gallagher, S. J., Eccles, M. R., and Hersey, P. Targeting DNA Methylation and EZH2 Activity to Overcome Melanoma Resistance to Immunotherapy. *Trends Immunol*, 40: 328-344, **2019**.

Esteller, M. CpG island hypermethylation and tumor suppressor genes: a booming present, a brighter future. *Oncogene*, 21: 5427-5440, **2002**.

Esteller, M. Epigenetics in cancer. *N Engl J Med*, 358: 1148-1159, **2008**.

Esteve, P. O., Chin, H. G., Benner, J., Feehery, G. R., Samaranyake, M., Horwitz, G. A., Jacobsen, S. E., and Pradhan, S. Regulation of DNMT1 stability through SET7-mediated lysine methylation in mammalian cells. *Proc Natl Acad Sci U S A*, 106: 5076-5081, **2009**.

Farrell, J., Kelly, C., Rauch, J., Kida, K., Garcia-Munoz, A., Monsefi, N., Turriziani, B., Doherty, C., Mehta, J. P., Matallanas, D., Simpson, J. C., Kolch, W., and von Kriegsheim, A. HGF induces epithelial-to-mesenchymal transition by modulating the mammalian hippo/MST2 and ISG15 pathways. *J Proteome Res*, 13: 2874-2886, **2014**.

Fassina, A., Cappellesso, R., Guzzardo, V., Dalla Via, L., Piccolo, S., Ventura, L., and Fassan, M. Epithelial-mesenchymal transition in malignant mesothelioma. *Mod Pathol*, 25: 86-99, **2012**.

Fazio, C., Covre, A., Cutaia, O., Lofiego, M. F., Tunici, P., Chiarucci, C., Cannito, S., Giacobini, G., Lowder, J. N., Ferraldeschi, R., Taverna, P., Di Giacomo, A. M., Coral, S., and Maio, M. Immunomodulatory Properties of DNA Hypomethylating Agents: Selecting the Optimal Epigenetic Partner for Cancer Immunotherapy. *Front Pharmacol*, 9: 1443, **2018**.

Feinberg, A. P., Cui, H., and Ohlsson, R. DNA methylation and genomic imprinting: insights from cancer into epigenetic mechanisms. *Semin Cancer Biol*, 12: 389-398, **2002**.

Fels Elliott, D. R., Jones, K. D. Diagnosis of Mesothelioma. *Surg Pathol Clin*, 13: 73-89, **2020**.

Feng, Q. and Zhang, Y. The MeCP1 complex represses transcription through preferential binding, remodeling, and deacetylating methylated nucleosomes. *Genes Dev*, 15: 827-832, **2001**.

Fernandez, A. F., Assenov, Y., Martin-Subero, J. I., Balint, B., Siebert, R., Taniguchi, H., Yamamoto, H., Hidalgo, M., Tan, A. C., Galm, O., Ferrer, I., Sanchez-Céspedes, M., Villanueva, A., Carmona, J., Sanchez-Mut, J. V., Berdasco, M., Moreno, V., Capella, G., Monk, D., Ballestar, E., Ropero, S., Martínez, R., Sanchez-Carbayo, M., Prosper, F., Agirre, X., Fraga, M. F., Grana, O., Perez-Jurado, L., Mora, J., Puig, S., Prat, J., Badimon, L., Puca, A. A., Meltzer, S. J., Lengauer, T., Bridgewater, J., Bock, C., and Esteller, M. A DNA methylation fingerprint of 1628 human samples. *Genome Res*, 22: 407-419, **2012**.

Fernandez, N. C., Lozier, A., Flament, C., Ricciardi-Castagnoli, P., Bellet, D., Suter, M., Perricaudet, M., Tursz, T., Maraskovsky, E., and Zitvogel, L. Dendritic cells directly trigger NK cell functions: cross-talk relevant in innate anti-tumor immune responses in vivo. *Nat Med*, 5: 405-411, **1999**.

Fiano, V., Zugna, D., Grasso, C., Trevisan, M., Delsedime, L., Molinaro, L., Gillio-Tos, A., Merletti, F., and Richiardi, L. LINE-1 methylation status in prostate cancer and non-neoplastic tissue adjacent to tumor in association with mortality. *Epigenetics*, 12: 11-18, **2017**.

Fischer, J. R., Ohnmacht, U., Rieger, N., Zemaitis, M., Stoffregen, C., Kostrzewa, M., Buchholz, E., Manegold, C., and Lahm, H. Promoter methylation of RASSF1A, RARBeta and DAPK predict poor prognosis of patients with malignant mesothelioma. *Lung Cancer*, 54: 109-116, **2006**.

Fraga, M. F., Ballestar, E., Villar-Garea, A., Boix-Chornet, M., Espada, J., Schotta, G., Bonaldi, T., Haydon, C., Ropero, S., Petrie, K., Iyer, N. G., Perez-Rosado, A., Calvo, E., Lopez, J. A., Cano, A., Calasanz, M. J., Colomer, D., Piris, M. A., Ahn, N., Imhof, A., Caldas, C., Jenuwein, T., and Esteller, M. Loss of acetylation at Lys16 and trimethylation at Lys20 of histone H4 is a common hallmark of human cancer. *Nat Genet*, 37: 391-400, **2005**.

Fraga, M. F., Herranz, M., Espada, J., Ballestar, E., Paz, M. F., Ropero, S., Erkek, E., Bozdogan, O., Peinado, H., Niveleau, A., Mao, J. H., Balmain, A., Cano, A., and Esteller, M. A mouse skin multistage carcinogenesis model reflects the aberrant DNA methylation patterns of human tumors. *Cancer Res*, 64: 5527-5534, **2004**.

Gan, L., Yang, Y., Li, Q., Feng, Y., Liu, T., and Guo, W. Epigenetic regulation of cancer progression by EZH2: from biological insights to therapeutic potential. *Biomark Res*, 6: 10, **2018**.

Gao, J., Shi, L. Z., Zhao, H., Chen, J., Xiong, L., He, Q., Chen, T., Roszik, J., Bernatchez, C., Woodman, S. E., Chen, P. L., Hwu, P., Allison, J. P., Futreal, A., Wargo, J. A., and Sharma, P. Loss of IFN-gamma Pathway Genes in Tumor Cells as a Mechanism of Resistance to Anti-CTLA-4 Therapy. *Cell*, 167: 397-404 e399, **2016**.

Gaudet, F., Hodgson, J. G., Eden, A., Jackson-Grusby, L., Dausman, J., Gray, J. W., Leonhardt, H., and Jaenisch, R. Induction of tumors in mice by genomic hypomethylation. *Science*, 300: 489-492, **2003**.

Gopisetty, G., Ramachandran, K., and Singal, R. DNA methylation and apoptosis. *Mol Immunol*, 43: 1729-1740, **2006**.

Grant, S. and Dai, Y. Histone deacetylase inhibitors and rational combination therapies. *Adv Cancer Res*, 116: 199-237, **2012**.

Gray, S. G. and Mutti, L. Immunotherapy for mesothelioma: a critical review of current clinical trials and future perspectives. *Transl Lung Cancer Res*, 9: S100-S119, **2020**.

Guan, R. J., Ford, H. L., Fu, Y., Li, Y., Shaw, L. M., and Pardee, A. B. Drg-1 as a differentiation-related, putative metastatic suppressor gene in human colon cancer. *Cancer Res*, 60: 749-755, **2000**.

Gui, C. Y., Ngo, L., Xu, W. S., Richon, V. M., and Marks, P. A. Histone deacetylase (HDAC) inhibitor activation of p21WAF1 involves changes in promoter-associated proteins, including HDAC1. *Proc Natl Acad Sci U S A*, 101: 1241-1246, **2004**.

Gunawan, M., Venkatesan, N., Loh, J. T., Wong, J. F., Berger, H., Neo, W. H., Li, L. Y., La Win, M. K., Yau, Y. H., Guo, T., See, P. C., Yamazaki, S., Chin, K. C., Gingras, A. R., Shochat, S. G., Ng, L. G., Sze, S. K., Ginhoux, F., and Su, I. H. The methyltransferase Ezh2 controls cell adhesion and migration through direct methylation of the extranuclear regulatory protein talin. *Nat Immunol*, 16: 505-516, **2015**.

Hamaidia, M., Gazon, H., Hoyos, C., Hoffmann, G. B., Louis, R., Duysinx, B., and Willems, L. Inhibition of EZH2 methyltransferase

decreases immunoediting of mesothelioma cells by autologous macrophages through a PD-1-dependent mechanism. *JCI Insight*, 4, **2019**.

Hassler, M. R. and Egger, G. Epigenomics of cancer - emerging new concepts. *Biochimie*, 94: 2219-2230, **2012**.

Hayashi, A., Horiuchi, A., Kikuchi, N., Hayashi, T., Fuseya, C., Suzuki, A., Konishi, I., and Shiozawa, T. Type-specific roles of histone deacetylase (HDAC) overexpression in ovarian carcinoma: HDAC1 enhances cell proliferation and HDAC3 stimulates cell migration with downregulation of E-cadherin. *Int J Cancer*, 127: 1332-1346, **2010**.

He, X., Wang, L., Riedel, H., Wang, K., Yang, Y., Dinu, C. Z., and Rojanasakul, Y. Mesothelin promotes epithelial-to-mesenchymal transition and tumorigenicity of human lung cancer and mesothelioma cells. *Mol Cancer*, 16: 63, **2017**.

Heinrichs, D., Knauel, M., Offermanns, C., Berres, M. L., Nellen, A., Leng, L., Schmitz, P., Bucala, R., Trautwein, C., Weber, C., Bernhagen, J., and Wasmuth, H. E. Macrophage migration inhibitory factor (MIF) exerts antifibrotic effects in experimental liver fibrosis via CD74. *Proc Natl Acad Sci U S A*, 108: 17444-17449, **2011**.

Hinz, T. K. and Heasley, L. E. Translating mesothelioma molecular genomics and dependencies into precision oncology-based therapies. *Semin Cancer Biol*, 61: 11-22, **2019**.

Hirano, H., Tsuji, M., Kizaki, T., Sashikata, T., Yoshi, Y., Okada, Y., and Mori, H. Expression of matrix metalloproteinases, tissue inhibitors of metalloproteinase, collagens, and Ki67 antigen in pleural malignant mesothelioma: an immunohistochemical and electron microscopic study. *Med Electron Microsc*, 35: 16-23, **2002**.

Hoffmann, M. J. and Schulz, W. A. Causes and consequences of DNA hypomethylation in human cancer. *Biochem Cell Biol*, 83: 296-321, **2005**.

Husain, A. N., Colby, T. V., Ordonez, N. G., Allen, T. C., Attanoos, R. L., Beasley, M. B., Butnor, K. J., Chirieac, L. R., Churg, A. M., Dacic, S., Galateau-Salle, F., Gibbs, A., Gown, A. M., Krausz, T., Litzky, L. A., Marchevsky, A., Nicholson, A. G., Roggli, V. L., Sharma, A. K., Travis, W. D., Walts, A. E., and Wick, M. R. Guidelines for Pathologic Diagnosis of Malignant Mesothelioma 2017 Update of the Consensus Statement From the International Mesothelioma Interest Group. *Arch Pathol Lab Med*, 142: 89-108, **2018**.

Janssen, Y. M., Barchowsky, A., Treadwell, M., Driscoll, K. E., and Mossman, B. T. Asbestos induces nuclear factor kappa B (NF-kappa B) DNA-binding activity and NF-kappa B-dependent gene expression in tracheal epithelial cells. *Proc Natl Acad Sci U S A*, 92: 8458-8462, **1995**.

Javierre, B. M., Fernandez, A. F., Richter, J., Al-Shahrouf, F., Martin-Subero, J. I., Rodriguez-Ubreva, J., Berdasco, M., Fraga, M. F., O'Hanlon, T. P., Rider, L. G., Jacinto, F. V., Lopez-Longo, F. J., Dopazo, J., Forn, M., Peinado, M. A., Carreno, L., Sawalha, A. H., Harley, J. B., Siebert, R., Esteller, M., Miller, F. W., and Ballestar, E. Changes in the pattern of DNA methylation associate with twin discordance in systemic lupus erythematosus. *Genome Res*, 20: 170-179, **2010**.

Jones, P. A. and Baylin, S. B. The epigenomics of cancer. *Cell*, 128: 683-692, **2007**.

Jones, P. A., Issa, J. P., and Baylin, S. Targeting the cancer epigenome for therapy. *Nat Rev Genet*, 17: 630-641, **2016**.

Jueliger, S., Lyons, J., Cannito, S., Pata, I., Pata, P., Shkolnaya, M., Lo Re, O., Peyrou, M., Villarroya, F., Paziienza, V., Rappa, F., Cappello, F., Azab, M., Taverna, P., and Vinciguerra, M. Efficacy and epigenetic interactions of novel DNA hypomethylating agent guadecitabine (SGI-110) in preclinical models of hepatocellular carcinoma. *Epigenetics*, 11: 709-720, **2016**.

Jurgens, B., Schmitz-Drager, B. J., and Schulz, W. A. Hypomethylation of L1 LINE sequences prevailing in human urothelial carcinoma. *Cancer Res*, 56: 5698-5703, **1996**.

Kachala, S. S., Bograd, A. J., Villena-Vargas, J., Suzuki, K., Servais, E. L., Kadota, K., Chou, J., Sima, C. S., Vertes, E., Rusch, V. W., Travis, W. D., Sadelain, M., and Adusumilli, P. S. Mesothelin overexpression is a marker of tumor aggressiveness and is associated with reduced recurrence-free and overall survival in early-stage lung adenocarcinoma. *Clin Cancer Res*, 20: 1020-1028, **2014**.

Kaneda, A., Tsukamoto, T., Takamura-Enya, T., Watanabe, N., Kaminishi, M., Sugimura, T., Tatematsu, M., and Ushijima, T. Frequent hypomethylation in multiple promoter CpG islands is associated with global hypomethylation, but not with frequent promoter hypermethylation. *Cancer Sci*, 95: 58-64, **2004**.

Kaniskan, H. U., Martini, M. L., and Jin, J. Inhibitors of Protein Methyltransferases and Demethylases. *Chem Rev*, 118: 989-1068, **2018**.

Knijnenburg, T. A., Wang, L., Zimmermann, M. T., Chambwe, N., Gao, G. F., Cherniack, A. D., Fan, H., Shen, H., Way, G. P., Greene, C. S., Liu, Y., Akbani, R., Feng, B., Donehower, L. A., Miller, C., Shen, Y., Karimi, M., Chen, H., Kim, P., Jia, P., Shinbrot, E., Zhang, S., Liu, J., Hu, H., Bailey, M. H., Yau, C., Wolf, D., Zhao, Z., Weinstein, J. N., Li, L., Ding, L., Mills, G. B., Laird, P. W., Wheeler, D. A., Shmulevich, I., Monnat, R. J., Jr., Xiao, Y., and Wang, C. Genomic and Molecular Landscape of DNA Damage Repair Deficiency across The Cancer Genome Atlas. *Cell Rep*, 23: 239-254 e236, **2018**.

Kouzarides, T. Chromatin modifications and their function. *Cell*, 128: 693-705, **2007**.

Kroczyńska, B., Cutrone, R., Bocchetta, M., Yang, H., Elmishad, A. G., Vacek, P., Ramos-Nino, M., Mossman, B. T., Pass, H. I., and Carbone, M. Crocidolite asbestos and SV40 are cocarcinogens in human mesothelial cells and in causing mesothelioma in hamsters. *Proc Natl Acad Sci U S A*, 103: 14128-14133, **2006**.

Lachat, C., Boyer-Guittaut, M., Peixoto, P., and Hervouet, E. Epigenetic Regulation of EMT (Epithelial to Mesenchymal Transition) and Tumor Aggressiveness: A View on Paradoxical Roles of KDM6B and EZH2. *Epigenomes*, 3: 1, **2019**.

LaFave, L. M., Beguelin, W., Koche, R., Teater, M., Spitzer, B., Chramiec, A., Papalexis, E., Keller, M. D., Hricik, T., Konstantinoff, K., Micol, J. B., Durham, B., Knutson, S. K., Campbell, J. E., Blum, G., Shi, X., Doud, E. H., Krivtsov, A. V., Chung, Y. R., Khodos, I., de Stanchina, E., Ouerfelli, O., Adusumilli, P. S., Thomas, P. M., Kelleher, N. L., Luo, M., Keilhack, H., Abdel-Wahab, O., Melnick, A., Armstrong, S. A., and Levine, R. L. Loss of BAP1 function leads to EZH2-dependent transformation. *Nat Med*, 21: 1344-1349, **2015**.

Lamouille, S., Xu, J., and Derynck, R. Molecular mechanisms of epithelial-mesenchymal transition. *Nat Rev Mol Cell Biol*, 15: 178-196, **2014**.

Lantuejoul, S., Le Stang, N., Damiola, F., Scherpereel, A., and Galateau-Salle, F. PD-L1 Testing for Immune Checkpoint Inhibitors in Mesothelioma: For Want of Anything Better? *J Thorac Oncol*, 12: 778-781, **2017**.

Leclercq, S., Gueugnon, F., Boutin, B., Guillot, F., Blanquart, C., Rogel, A., Padiou, M., Pouliquen, D., Fonteneau, J. F., and Gregoire, M. A 5-aza-2'-deoxycytidine/valproate combination induces cytotoxic T-cell response against mesothelioma. *Eur Respir J*, 38: 1105-1116, **2011**.

Lee, J. H., Kim, J. H., Kim, J. S., Chang, J. W., Kim, S. B., Park, J. S., and Lee, S. K. AMP-activated protein kinase inhibits TGF-beta-, angiotensin II-, aldosterone-, high glucose-, and albumin-induced epithelial-mesenchymal transition. *Am J Physiol Renal Physiol*, 304: F686-697, **2013**.

Lee, Y. S., Lim, K. H., Guo, X., Kawaguchi, Y., Gao, Y., Barrientos, T., Ordentlich, P., Wang, X. F., Counter, C. M., and Yao, T. P. The cytoplasmic deacetylase HDAC6 is required for efficient oncogenic tumorigenesis. *Cancer Res*, 68: 7561-7569, **2008**.

Lehembre, F., Yilmaz, M., Wicki, A., Schomber, T., Strittmatter, K., Ziegler, D., Kren, A., Went, P., Derksen, P. W., Berns, A., Jonkers, J., and Christofori, G. NCAM-induced focal adhesion assembly: a functional switch upon loss of E-cadherin. *Embo J*, 27: 2603-2615, **2008**.

Lengauer, C. and Issa, J. P. The role of epigenetics in cancer. DNA Methylation, Imprinting and the Epigenetics of Cancer--an American Association for Cancer Research Special Conference. Las Croabas, Puerto Rico, 12-16 1997 December. *Mol Med Today*, 4: 102-103, **1998**.

Li, E., Bestor, T. H., and Jaenisch, R. Targeted mutation of the DNA methyltransferase gene results in embryonic lethality. *Cell*, 69: 915-926, **1992**.

Li, Y. and Seto, E. HDACs and HDAC Inhibitors in Cancer Development and Therapy. *Cold Spring Harb Perspect Med*, 6, **2016**.

Liang, S., Yao, Q., Wei, D., Liu, M., Geng, F., Wang, Q., and Wang, Y. S. KDM6B promotes ovarian cancer cell migration and invasion by induced transforming growth factor-beta1 expression. *J Cell Biochem*, 120: 493-506, **2019**.

Luker, A. J., Graham, L. J., Smith, T. M., Jr., Camarena, C., Zellner, M. P., Gilmer, J. S., Damle, S. R., Conrad, D. H., Bear, H. D., and Martin, R. K. The DNA methyltransferase inhibitor, guadecitabine, targets tumor-induced myelopoiesis and recovers T cell activity to slow tumor growth in combination with adoptive immunotherapy in a mouse model of breast cancer. *BMC Immunol*, 21: 8, **2020**.

Mahara, S., Lee, P. L., Feng, M., Tergaonkar, V., Chng, W. J., and Yu, Q. HIFI-alpha activation underlies a functional switch in the paradoxical role of Ezh2/PRC2 in breast cancer. *Proc Natl Acad Sci U S A*, 113: E3735-3744, **2016**.

Mahmoud, F., Shields, B., Makhoul, I., Hutchins, L. F., Shalin, S. C., and Tackett, A. J. Role of EZH2 histone methyltransferase in melanoma progression and metastasis. *Cancer Biol Ther*, 17: 579-591, **2016**.

Maio, M., Scherpereel, A., Calabrò, L., Aerts, J., Perez, S. C., Bearz, A., Nackaerts, K., Fennell, D. A., Kowalski, D., Tsao, A. S., Taylor, P., Grosso, F., Antonia, S. J., Nowak, A. K., Taboada, M., Puglisi, M., Stockman, P. K., and Kindler, H. L. Tremelimumab as second-line or third-line treatment in relapsed malignant mesothelioma (DETERMINE): a multicentre, international, randomised, double-blind, placebo-controlled phase 2b trial. *Lancet Oncol*, 18: 1261-1273, **2017**.

Makarevic, J., Rutz, J., Juengel, E., Maxeiner, S., Tsaur, I., Chun, F. K., Bereiter-Hahn, J., and Blaheta, R. A. Influence of the HDAC Inhibitor Valproic Acid on the Growth and Proliferation of Temsirolimus-Resistant Prostate Cancer Cells In Vitro. *Cancers (Basel)*, 11, **2019**.

Margueron, R., Li, G., Sarma, K., Blais, A., Zavadil, J., Woodcock, C. L., Dynlacht, B. D., and Reinberg, D. Ezh1 and Ezh2 maintain repressive chromatin through different mechanisms. *Mol Cell*, 32: 503-518, **2008**.

Matthias, P., Yoshida, M., and Khochbin, S. HDAC6 a new cellular stress surveillance factor. *Cell Cycle*, 7: 7-10, **2008**.

McGranahan, N., Burrell, R. A., Endesfelder, D., Novelli, M. R., and Swanton, C. Cancer chromosomal instability: therapeutic and diagnostic challenges. *EMBO Rep*, 13: 528-538, **2012**.

McLoughlin, K. C., Kaufman, A. S., and Schrump, D. S. Targeting the epigenome in malignant pleural mesothelioma. *Transl Lung Cancer Res*, 6: 350-365, **2017**.

Micolucci, L., Akhtar, M. M., Olivieri, F., Rippon, M. R., and Procopio, A. D. Diagnostic value of microRNAs in asbestos exposure and malignant mesothelioma: systematic review and qualitative meta-analysis. *Oncotarget*, 7: 58606-58637, **2016**.

Momparler, R. L., Cote, S., Momparler, L. F., and Idaghdour, Y. Inhibition of DNA and Histone Methylation by 5-Aza-2'-Deoxycytidine (Decitabine) and 3-Deazaneplanocin-A on Antineoplastic Action and Gene Expression in Myeloid Leukemic Cells. *Front Oncol*, 7: 19, **2017**.

- Montfort, A., Colacios, C., Levade, T., Andrieu-Abadie, N., Meyer, N., and Segui, B. The TNF Paradox in Cancer Progression and Immunotherapy. *Front Immunol*, 10: 1818, **2019**.
- Morello, A., Sadelain, M., and Adusumilli, P. S. Mesothelin-Targeted CARs: Driving T Cells to Solid Tumors. *Cancer Discov*, 6: 133-146, **2016**.
- Morris, M. J. and Monteggia, L. M. Role of DNA methylation and the DNA methyltransferases in learning and memory. *Dialogues Clin Neurosci*, 16: 359-371, **2014**.
- Moustakas, A. and Heldin, C. H. Induction of epithelial-mesenchymal transition by transforming growth factor beta. *Semin Cancer Biol*, 22: 446-454, **2012**.
- Mutti, L., Piacenza, A., Valenti, V., Castagneto, B., and Betta, P. G. Expression of intercellular adhesion molecule-1 (ICAM-1) by reactive mesothelial cells in pleural effusions. *Pathologica*, 85: 725-728, **1993**.
- Mutti, L., Valle, M. T., Balbi, B., Orengo, A. M., Lazzaro, A., Alciato, P., Gatti, E., Betta, P. G., and Pozzi, E. Primary human mesothelioma cells express class II MHC, ICAM-1 and B7-2 and can present recall antigens to autologous blood lymphocytes. *Int J Cancer*, 78: 740-749, **1998**.
- Nagarsheth, N., Peng, D., Kryczek, I., Wu, K., Li, W., Zhao, E., Zhao, L., Wei, S., Frankel, T., Vatan, L., Szeliga, W., Dou, Y., Owens, S., Marquez, V., Tao, K., Huang, E., Wang, G., and Zou, W. PRC2 Epigenetically Silences Th1-Type Chemokines to Suppress Effector T-Cell Trafficking in Colon Cancer. *Cancer Res*, 76: 275-282, **2016**.
- Nahas, M. R., Stroopinsky, D., Rosenblatt, J., Cole, L., Pyzer, A. R., Anastasiadou, E., Sergeeva, A., Ephraim, A., Washington, A., Orr, S., McMasters, M., Weinstock, M., Jain, S., Leaf, R. K., Ghiasuddin, H., Rahimian, M., Liegel, J., Mollidrem, J. J., Slack, F., Kufe, D., and Avigan, D. Hypomethylating agent alters the immune microenvironment in acute myeloid leukaemia (AML) and enhances the immunogenicity of a dendritic cell/AML vaccine. *Br J Haematol*, 185: 679-690, **2019**.
- Nascimientto, A., Côté, S., Jeong, L.S., Jinha, Y., & Momparler R.L. Synergistic antineoplastic action of 5-aza-2'deoxyctidine (decitabine) in combination with different inhibitors of enhancer of zeste homolog 2 (EZH2) on human lung carcinoma cells. *Journal of Cancer Research & Therapy*, 4: 42-49, **2016**.
- Nasu, M., Emi, M., Pastorino, S., Tanji, M., Powers, A., Luk, H., Baumann, F., Zhang, Y. A., Gazdar, A., Kanodia, S., Tiirikainen, M., Flores, E., Gaudino, G., Becich, M. J., Pass, H. I., Yang, H., and Carbone, M. High Incidence of Somatic BAP1 alterations in sporadic malignant mesothelioma. *J Thorac Oncol*, 10: 565-576, **2015**.
- Navada, S. C., Steinmann, J., Lubbert, M., and Silverman, L. R. Clinical development of demethylating agents in hematology. *J Clin Invest*, 124: 40-46, **2014**.
- Nicolini, F., Bocchini, M., Bronte, G., Delmonte, A., Guidoboni, M., Crino, L., and Mazza, M. Malignant Pleural Mesothelioma: State-of-the-Art on Current Therapies and Promises for the Future. *Front Oncol*, 9: 1519, **2020**.
- Orengo, A. M., Spoletini, L., Procopio, A., Favoni, R. E., De Cupis, A., Ardizzoni, A., Castagneto, B., Ribotta, M., Betta, P. G., Ferrini, S., and Mutti, L. Establishment of four new mesothelioma cell lines: characterization by ultrastructural and immunophenotypic analysis. *Eur Respir J*, 13: 527-534, **1999**.
- Orlichenko, L. S. and Radisky, D. C. Matrix metalloproteinases stimulate epithelial-mesenchymal transition during tumor development. *Clin Exp Metastasis*, 25: 593-600, **2008**.
- Otterstrom, C., Soltermann, A., Opitz, I., Felley-Bosco, E., Weder, W., Stahel, R. A., Triponez, F., Robert, J. H., and Serre-Beinier, V. CD74: a new prognostic factor for patients with malignant pleural mesothelioma. *Br J Cancer*, 110: 2040-2046, **2014**.
- Ouaissi, M., Silvy, F., Loncle, C., Ferraz da Silva, D., Martins Abreu, C., Martinez, E., Berthezene, P., Cadra, S., Le Treut, Y. P., Hardwigen, J., Sastre, B., Sielezneff, I., Benkoel, L., Delgrande, J., Ouasssi, A., Iovanna, J., Lombardo, D., and Mas, E. Further characterization of HDAC and SIRT gene expression patterns in pancreatic cancer and their relation to disease outcome. *PLoS One*, 9: e108520, **2014**.
- Pardoll, D. M. The blockade of immune checkpoints in cancer immunotherapy. *Nat Rev Cancer*, 12: 252-264, **2012**.
- Peng, D., Kryczek, I., Nagarsheth, N., Zhao, L., Wei, S., Wang, W., Sun, Y., Zhao, E., Vatan, L., Szeliga, W., Kotarski, J., Tarkowski, R., Dou, Y., Cho, K., Hensley-Alford, S., Munkarah, A., Liu, R., and Zou, W. Epigenetic silencing of TH1-type chemokines shapes tumour immunity and immunotherapy. *Nature*, 527: 249-253, **2015**.
- Portela, A. and Esteller, M. Epigenetic modifications and human disease. *Nat Biotechnol*, 28: 1057-1068, **2010**.
- Pulverer, W., Wielscher, M., Panzer-Grumayer, R., Plessl, T., Kriegner, A., Vierlinger, K., and Weinhausel, A. The stem cell signature of CHH/CHG methylation is not present in 271 cancer associated 5'UTR gene regions. *Biochimie*, 94: 2345-2352, **2012**.
- Qi, F., Okimoto, G., Jube, S., Napolitano, A., Pass, H. I., Laczko, R., Demay, R. M., Khan, G., Tiirikainen, M., Rinaudo, C., Croce, A., Yang, H., Gaudino, G., and Carbone, M. Continuous exposure to chrysotile asbestos can cause transformation of human mesothelial cells via HMGB1 and TNF-alpha signaling. *Am J Pathol*, 183: 1654-1666, **2013**.
- Rajak, H., Singh, A., Dewangan, P. K., Patel, V., Jain, D. K., Tiwari, S. K., Veerasamy, R., and Sharma, P. C. Peptide based macrocycles: selective histone deacetylase inhibitors with antiproliferative activity. *Curr Med Chem*, 20: 1887-1903, **2013**.

Richards, K. L., Zhang, B., Baggerly, K. A., Colella, S., Lang, J. C., Schuller, D. E., and Krahe, R. Genome-wide hypomethylation in head and neck cancer is more pronounced in HPV-negative tumors and is associated with genomic instability. *PLoS One*, 4: e4941, **2009**.

Richon, V. M. Cancer biology: mechanism of antitumour action of vorinostat (suberoylanilide hydroxamic acid), a novel histone deacetylase inhibitor. *Br J Cancer*, 95: S2–S6, **2006**.

Robertson, K. D. DNA methylation and chromatin - unraveling the tangled web. *Oncogene*, 21: 5361-5379, **2002**.

Roboz, G. J., Kantarjian, H. M., Yee, K. W. L., Kropf, P. L., O'Connell, C. L., Griffiths, E. A., Stock, W., Daver, N. G., Jabbour, E., Ritchie, E. K., Walsh, K. J., Rizzieri, D., Lunin, S. D., Curio, T., Chung, W., Hao, Y., Lowder, J. N., Azab, M., and Issa, J. J. Dose, schedule, safety, and efficacy of guadecitabine in relapsed or refractory acute myeloid leukemia. *Cancer*, 124: 325-334, **2018**.

Rodriguez-Paredes, M. and Lyko, F. The importance of non-histone protein methylation in cancer therapy. *Nat Rev Mol Cell Biol*, 20: 569-570, **2019**.

Ruiz, R., Raez, L. E., and Rolfo, C. Entinostat (SNDX-275) for the treatment of non-small cell lung cancer. *Expert Opin Investig Drugs*, 24: 1101-1109, **2015**.

Sacco, J. J., Kenyani, J., Butt, Z., Carter, R., Chew, H. Y., Cheeseman, L. P., Darling, S., Denny, M., Urbe, S., Clague, M. J., and Coulson, J. M. Loss of the deubiquitylase BAP1 alters class I histone deacetylase expression and sensitivity of mesothelioma cells to HDAC inhibitors. *Oncotarget*, 6: 13757-13771, **2015**.

Sage, A. P., Martinez, V. D., Minatel, B. C., Pewarchuk, M. E., Marshall, E. A., MacAulay, G. M., Hubaux, R., Pearson, D. D., Goodarzi, A. A., Dellaire, G., and Lam, W. L. Genomics and Epigenetics of Malignant Mesothelioma. *High Throughput*, 7, **2018**.

Santi, D. V., Norment, A., and Garrett, C. E. Covalent bond formation between a DNA-cytosine methyltransferase and DNA containing 5-azacytosine. *Proc Natl Acad Sci U S A*, 81: 6993-6997, **1984**.

Scarno, G., Pietropaolo, G., Di Censo, C., Gadina, M., Santoni, A., and Sciume, G. Transcriptional, Epigenetic and Pharmacological Control of JAK/STAT Pathway in NK Cells. *Front Immunol*, 10: 2456, **2019**.

Scherpereel, A., Mazieres, J., Greillier, L., Lantuejoul, S., Do, P., Bylicki, O., Monnet, I., Corre, R., Audigier-Valette, C., Locatelli-Sanchez, M., Molinier, O., Guisier, F., Urban, T., Ligeza-Poisson, C., Planchard, D., Amour, E., Morin, F., Moro-Sibilot, D., and Zalcman, G. Nivolumab or nivolumab plus ipilimumab in patients with relapsed malignant pleural mesothelioma (IFCT-1501 MAPS2): a multicentre, open-label, randomised, non-comparative, phase 2 trial. *Lancet Oncol*, 20: 239-253, **2019**.

Scherpereel, A., Wallyn, F., Albelda, S. M., and Munck, C. Novel therapies for malignant pleural mesothelioma. *Lancet Oncol*, 19: e161-e172, **2018**.

Schramm, A., Opitz, I., Thies, S., Seifert, B., Moch, H., Weder, W., and Soltermann, A. Prognostic significance of epithelial-mesenchymal transition in malignant pleural mesothelioma. *Eur J Cardiothorac Surg*, 37: 566-572, **2010**.

Schuettengruber, B., Chourrout, D., Vervoort, M., Leblanc, B., and Cavalli, G. Genome regulation by polycomb and trithorax proteins. *Cell*, 128: 735-745, **2007**.

Séput, C., Bellefroid, M., Rocks, N., Donati, K., Gerard, C., Gilles, C., Ludwig, A., Duysinx, B., Noel, A., and Cataldo, D. ADAM10 mediates malignant pleural mesothelioma invasiveness. *Oncogene*, 38: 3521-3534, **2019**.

Seto, E. and Yoshida, M. Erasers of histone acetylation: the histone deacetylase enzymes. *Cold Spring Harb Perspect Biol*, 6: a018713, **2014**.

Shen, H. and Laird, P. W. Interplay between the cancer genome and epigenome. *Cell*, 153: 38-55, **2013**.

Shi, B., Liang, J., Yang, X., Wang, Y., Zhao, Y., Wu, H., Sun, L., Zhang, Y., Chen, Y., Li, R., Zhang, Y., Hong, M., and Shang, Y. Integration of estrogen and Wnt signaling circuits by the polycomb group protein EZH2 in breast cancer cells. *Mol Cell Biol*, 27: 5105-5119, **2007**.

Shiio, Y. and Eisenman, R. N. Histone sumoylation is associated with transcriptional repression. *Proc Natl Acad Sci U S A*, 100: 13225-13230, **2003**.

Shinozaki-Ushiku, A., Ushiku, T., Morita, S., Anraku, M., Nakajima, J., and Fukayama, M. Diagnostic utility of BAP1 and EZH2 expression in malignant mesothelioma. *Histopathology*, 70: 722-733, **2017**.

Shivapurkar, N., Toyooka, S., Toyooka, K. O., Reddy, J., Miyajima, K., Suzuki, M., Shigematsu, H., Takahashi, T., Parikh, G., Pass, H. I., Chaudhary, P. M., and Gazdar, A. F. Aberrant methylation of trail decoy receptor genes is frequent in multiple tumor types. *Int J Cancer*, 109: 786-792, **2004**.

Sigalotti, L., Fratta, E., Bidoli, E., Covre, A., Parisi, G., Colizzi, F., Coral, S., Massarut, S., Kirkwood, J. M., and Maio, M. Methylation levels of the "long interspersed nucleotide element-1" repetitive sequences predict survival of melanoma patients. *J Transl Med*, 9: 78, **2011**.

Sigalotti, L., Fratta, E., Coral, S., and Maio, M. Epigenetic drugs as immunomodulators for combination therapies in solid tumors. *Pharmacol Ther*, 142: 339-350, **2014**.

Smith, Z. D. and Meissner, A. DNA methylation: roles in mammalian development. *Nat Rev Genet*, 14: 204-220, **2013**.

- Solbes, E. and Harper, R. W. Biological responses to asbestos inhalation and pathogenesis of asbestos-related benign and malignant disease. *J Investig Med*, 66: 721-727, **2018**.
- Stazi, G., Taglieri, L., Nicolai, A., Romanelli, A., Fioravanti, R., Morrone, S., Sabatino, M., Ragno, R., Taurone, S., Nebbioso, M., Carletti, R., Artico, M., Valente, S., Scarpa, S., and Mai, A. Dissecting the role of novel EZH2 inhibitors in primary glioblastoma cell cultures: effects on proliferation, epithelial-mesenchymal transition, migration, and on the pro-inflammatory phenotype. *Clin Epigenetics*, 11: 173, **2019**.
- Sudo, T., Mimori, K., Nishida, N., Kogo, R., Iwaya, T., Tanaka, F., Shibata, K., Fujita, H., Shirouzu, K., and Mori, M. Histone deacetylase 1 expression in gastric cancer. *Oncol Rep*, 26: 777-782, **2011**.
- Suraweera, A., O'Byrne, K. J., and Richard, D. J. Combination Therapy With Histone Deacetylase Inhibitors (HDACi) for the Treatment of Cancer: Achieving the Full Therapeutic Potential of HDACi. *Front Oncol*, 8: 92, **2018**.
- Szulwach, K. E., Li, X., Li, Y., Song, C. X., Wu, H., Dai, Q., Irier, H., Upadhyay, A. K., Gearing, M., Levey, A. I., Vasanthakumar, A., Godley, L. A., Chang, Q., Cheng, X., He, C., and Jin, P. 5-hmC-mediated epigenetic dynamics during postnatal neurodevelopment and aging. *Nat Neurosci*, 14: 1607-1616, **2011**.
- Szyf, M., Weaver, I. C., Champagne, F. A., Diorio, J., and Meaney, M. J. Maternal programming of steroid receptor expression and phenotype through DNA methylation in the rat. *Front Neuroendocrinol*, 26: 139-162, **2005**.
- Tahiliani, M., Mei, P., Fang, R., Leonor, T., Rutenberg, M., Shimizu, F., Li, J., Rao, A., and Shi, Y. The histone H3K4 demethylase SMCX links REST target genes to X-linked mental retardation. *Nature*, 447: 601-605, **2007**.
- Takai, D., Yagi, Y., Habib, N., Sugimura, T., and Ushijima, T. Hypomethylation of LINE1 retrotransposon in human hepatocellular carcinomas, but not in surrounding liver cirrhosis. *Jpn J Clin Oncol*, 30: 306-309, **2000**.
- Tan, J. Z., Yan, Y., Wang, X. X., Jiang, Y., and Xu, H. E. EZH2: biology, disease, and structure-based drug discovery. *Acta Pharmacol Sin*, 35: 161-174, **2014**.
- Tang, J., Yan, H., and Zhuang, S. Histone deacetylases as targets for treatment of multiple diseases. *Clin Sci (Lond)*, 124: 651-662, **2013**.
- Tellez, C. S., Grimes, M. J., Picchi, M. A., Liu, Y., March, T. H., Reed, M. D., Oganessian, A., Taverna, P., and Belinsky, S. A. SGI-110 and entinostat therapy reduces lung tumor burden and reprograms the epigenome. *Int J Cancer*, 135: 2223-2231, **2014**.
- Thiery, J. P., Acloque, H., Huang, R. Y., and Nieto, M. A. Epithelial-mesenchymal transitions in development and disease. *Cell*, 139: 871-890, **2009**.
- Thurneysen, C., Opitz, I., Kurtz, S., Weder, W., Stahel, R. A., and Felley-Bosco, E. Functional inactivation of NF2/merlin in human mesothelioma. *Lung Cancer*, 64: 140-147, **2009**.
- Turini, S., Bergandi, L., Gazzano, E., Prato, M., and Aldieri, E. Epithelial to Mesenchymal Transition in Human Mesothelial Cells Exposed to Asbestos Fibers: Role of TGF-beta as Mediator of Malignant Mesothelioma Development or Metastasis via EMT Event. *Int J Mol Sci*, 20, **2019**.
- Valenzuela-Fernandez, A., Cabrero, J. R., Serrador, J. M., and Sanchez-Madrid, F. HDAC6: a key regulator of cytoskeleton, cell migration and cell-cell interactions. *Trends Cell Biol*, 18: 291-297, **2008**.
- Vandermeers, F., Neelature Sriramareddy, S., Costa, C., Hubaux, R., Cosse, J. P., and Willems, L. The role of epigenetics in malignant pleural mesothelioma. *Lung Cancer*, 81: 311-318, **2013**.
- Vannini, A., Volpari, C., Filocamo, G., Casavola, E. C., Brunetti, M., Renzoni, D., Chakravarty, P., Paolini, C., De Francesco, R., Gallinari, P., Steinkuhler, C., and Di Marco, S. Crystal structure of a eukaryotic zinc-dependent histone deacetylase, human HDAC8, complexed with a hydroxamic acid inhibitor. *Proc Natl Acad Sci U S A*, 101: 15064-15069, **2004**.
- Varambally, S., Dhanasekaran, S. M., Zhou, M., Barrette, T. R., Kumar-Sinha, C., Sanda, M. G., Ghosh, D., Pienta, K. J., Sewalt, R. G., Otte, A. P., Rubin, M. A., and Chinnaiyan, A. M. The polycomb group protein EZH2 is involved in progression of prostate cancer. *Nature*, 419: 624-629, **2002**.
- Vaziri, H., Dessain, S. K., Ng Eaton, E., Imai, S. I., Frye, R. A., Pandita, T. K., Guarente, L., and Weinberg, R. A. hSIR2(SIRT1) functions as an NAD-dependent p53 deacetylase. *Cell*, 107: 149-159, **2001**.
- Wang, D., Quiros, J., Mahuron, K., Pai, C. C., Ranzani, V., Young, A., Silveria, S., Harwin, T., Abnousian, A., Pagani, M., Rosenblum, M. D., Van Gool, F., Fong, L., Bluestone, J. A., and DuPage, M. Targeting EZH2 Reprograms Intratumoral Regulatory T Cells to Enhance Cancer Immunity. *Cell Rep*, 23: 3262-3274, **2018**.
- Welch, B. T., Eiken, P. W., Atwell, T. D., Peikert, T., Yi, E. S., Nichols, F., and Schmit, G. D. A Single-Institution Experience in Percutaneous Image-Guided Biopsy of Malignant Pleural Mesothelioma. *Cardiovasc Intervent Radiol*, 40: 860-863, **2017**.
- Wilmott, J. S., Colebatch, A. J., Kakavand, H., Shang, P., Carlino, M. S., Thompson, J. F., Long, G. V., Scolyer, R. A., and Hersey, P. Expression of the class 1 histone deacetylases HDAC8 and 3 are associated with improved survival of patients with metastatic melanoma. *Mod Pathol*, 28: 884-894, **2015**.
- Woods, D. M., Sodre, A. L., Villagra, A., Sarnaik, A., Sotomayor, E. M., and Weber, J. HDAC Inhibition Upregulates PD-1 Ligands in Melanoma and Augments Immunotherapy with PD-1 Blockade. *Cancer Immunol Res*, 3: 1375-1385, **2015**.

- Wrangle, J., Wang, W., Koch, A., Easwaran, H., Mohammad, H. P., Vendetti, F., Vancrinkinge, W., Demeyer, T., Du, Z., Parsana, P., Rodgers, K., Yen, R. W., Zahnow, C. A., Taube, J. M., Brahmer, J. R., Tykodi, S. S., Easton, K., Carvajal, R. D., Jones, P. A., Laird, P. W., Weisenberger, D. J., Tsai, S., Juergens, R. A., Topalian, S. L., Rudin, C. M., Brock, M. V., Pardoll, D., and Baylin, S. B. Alterations of immune response of Non-Small Cell Lung Cancer with Azacytidine. *Oncotarget*, 4: 2067-2079, **2013**.
- Xie, Z., Ago, Y., Okada, N., and Tachibana, M. Valproic acid attenuates immunosuppressive function of myeloid-derived suppressor cells. *J Pharmacol Sci*, 137: 359-365, **2018**.
- Xu, C., Hua, F., Chen, Y., Huang, H., Ye, W., Yu, Y., and Shen, Z. MTA1 promotes metastasis of MPM via suppression of E-cadherin. *J Exp Clin Cancer Res*, 34: 151, **2015**.
- Xu, K., Wu, Z. J., Groner, A. C., He, H. H., Cai, C., Lis, R. T., Wu, X., Stack, E. C., Loda, M., Liu, T., Xu, H., Cato, L., Thornton, J. E., Gregory, R. I., Morrissey, C., Vessella, R. L., Montironi, R., Magi-Galluzzi, C., Kantoff, P. W., Balk, S. P., Liu, X. S., and Brown, M. EZH2 oncogenic activity in castration-resistant prostate cancer cells is Polycomb-independent. *Science*, 338: 1465-1469, **2013**.
- Yamada, Y., Jackson-Grusby, L., Linhart, H., Meissner, A., Eden, A., Lin, H., and Jaenisch, R. Opposing effects of DNA hypomethylation on intestinal and liver carcinogenesis. *Proc Natl Acad Sci U S A*, 102: 13580-13585, **2005**.
- Yamagishi, M. and Uchimar, K. Targeting EZH2 in cancer therapy. *Curr Opin Oncol*, 29: 375-381, **2017**.
- Yamanegi, K., Yamane, J., Kobayashi, K., Kato-Kogoe, N., Ohyama, H., Nakasho, K., Yamada, N., Hata, M., Nishioka, T., Fukunaga, S., Futani, H., Okamura, H., and Terada, N. Sodium valproate, a histone deacetylase inhibitor, augments the expression of cell-surface NKG2D ligands, MICA/B, without increasing their soluble forms to enhance susceptibility of human osteosarcoma cells to NK cell-mediated cytotoxicity. *Oncol Rep*, 24: 1621-1627, **2010**.
- Yanez, Y., Grau, E., Rodriguez-Cortez, V. C., Hervas, D., Vidal, E., Noguera, R., Hernandez, M., Segura, V., Canete, A., Conesa, A., Font de Mora, J., and Castel, V. Two independent epigenetic biomarkers predict survival in neuroblastoma. *Clin Epigenetics*, 7: 16, **2015**.
- Yang, B., Pan, Y. B., Ma, Y. B., and Chu, S. H. Integrated Transcriptome Analyses and Experimental Verifications of Mesenchymal-Associated TNFRSF1A as a Diagnostic and Prognostic Biomarker in Gliomas. *Front Oncol*, 10: 250, **2020**.
- Yao, Y., Hu, H., Yang, Y., Zhou, G., Shang, Z., Yang, X., Sun, K., Zhan, S., Yu, Z., Li, P., Pan, G., Sun, L., Zhu, X., and He, S. Downregulation of Enhancer of Zeste Homolog 2 (EZH2) is essential for the Induction of Autophagy and Apoptosis in Colorectal Cancer Cells. *Genes (Basel)*, 7, **2016**.
- Yap, T. A., Aerts, J. G., Popat, S., and Fennell, D. A. Novel insights into mesothelioma biology and implications for therapy. *Nat Rev Cancer*, 17: 475-488, **2017**.
- Yi, X., Guo, J., Guo, J., Sun, S., Yang, P., Wang, J., Li, Y., Xie, L., Cai, J., and Wang, Z. EZH2-mediated epigenetic silencing of TIMP2 promotes ovarian cancer migration and invasion. *Sci Rep*, 7: 3568, **2017**.
- Ying, S., Wang, Y., Lyu, L. Potential Roles of Matrix Metalloproteinases in Malignant Mesothelioma. *Asbestos-Related Diseases* book, edited by Takemi Otsuki, Intechopen, **2019**.
- You, J. S. and Jones, P. A. Cancer genetics and epigenetics: two sides of the same coin? *Cancer Cell*, 22: 9-20, **2012**.
- Yu, Q. and Stamenkovic, I. Cell surface-localized matrix metalloproteinase-9 proteolytically activates TGF-beta and promotes tumor invasion and angiogenesis. *Genes Dev*, 14: 163-176, **2000**.
- Yu, Z., Zeng, J., Liu, H., Wang, T., Yu, Z., and Chen, J. Role of HDAC1 in the progression of gastric cancer and the correlation with lncRNAs. *Oncol Lett*, 17: 3296-3304, **2019**.
- Yuan, L. W. and Gambie, J. E. Histone acetylation by p300 is involved in CREB-mediated transcription on chromatin. *Biochim Biophys Acta*, 1541: 161-169, **2001**.
- Zhang, W., Klinkebiel, D., Barger, C. J., Pandey, S., Guda, C., Miller, A., Akers, S. N., Odunsi, K., and Karpf, A. R. Global DNA Hypomethylation in Epithelial Ovarian Cancer: Passive Demethylation and Association with Genomic Instability. *Cancers (Basel)*, 12, **2020**.
- Zhang, X., Rao, A., Sette, P., Deibert, C., Pomerantz, A., Kim, W. J., Kohanbash, G., Chang, Y., Park, Y., Engh, J., Choi, J., Chan, T., Okada, H., Lotze, M., Grandi, P., and Amankulor, N. IDH mutant gliomas escape natural killer cell immune surveillance by downregulation of NKG2D ligand expression. *Neuro Oncol*, 18: 1402-1412, **2016**.
- Zingg, D., Debbache, J., Schaefer, S. M., Tuncer, E., Frommel, S. C., Cheng, P., Arenas-Ramirez, N., Haeusel, J., Zhang, Y., Bonalli, M., McCabe, M. T., Creasy, C. L., Levesque, M. P., Boyman, O., Santoro, R., Shakhova, O., Dummer, R., and Sommer, L. The epigenetic modifier EZH2 controls melanoma growth and metastasis through silencing of distinct tumour suppressors. *Nat Commun*, 6: 6051, **2015**.

## 7. ACKNOWLEDGEMENTS

First, I would like to express my gratitude to my tutor Prof. Michele Maio, director of the Center for Immuno-Oncology of the University Hospital of Siena, for giving me the opportunity to join his team. I wish to deeply thank Dr. Alessia Covre and Dr. Sandra Coral, who played an important role in my development, for the help provided during the writing of my thesis, and for the kindness. Also, thanks to Proff. Andrea Anichini and Giuseppe Palmieri for the contribution to the thesis review. I am very thankful to my past and present lab-mates: Maria, Ornella, Carolina and Laura for their lively company, and for the great support whenever I needed it; Carla for the intellectual and spiritual stimuli that have been extremely motivating.

The foremost thanks go to my special family for the support they have given to me from the first day of my academic career until the attainment of this title: Ernesto, Lella, Adriana, Daniela, and my brother Saverio, you represent that place where I always feel safe and beloved. Thanks to C1 to be there for me at any time. Final special mention to my lovely Michele, who always give me strength and words of advice, motivating me to do better.

**Table S1** – Gene expression analysis of 10 MPM cell lines, untreated or treated with 1 $\mu$ M guadecitabine, through the PanCancer IO 360 panel for nCounter SPRINT Profiler by NanoString Technologies.

	Sarcomatoid cells				Biphasic cells				Epithelioid cells		
	MesMM98	MesOC99	SiMes1	SiMes4	MMB	Mes1	Mes2	MPP89	MMCA	MesCM98	mFC
A2M	-10.34 <sup>a</sup>	0.03	-0.93	0.41	-0.16	-0.36	0.98	-0.23	7.11	6.10	<b>0.26<sup>b</sup></b>
ACVR1C	-0.65	4.45	7.73	1.76	-1.42	3.18	7.50	2.56	-7.68	7.63	<b>2.51</b>
ADAM12	-3.05	-0.18	2.02	0.54	-1.27	-2.92	1.66	-0.34	1.24	0.10	<b>-0.22</b>
ADGRE1	0.26	0.03	0.03	-0.18	-0.16	-0.36	-0.49	-3.10	-0.72	-0.28	<b>-0.50</b>
ADM	4.24	-2.07	1.91	1.24	1.45	-1.29	2.17	-0.83	-1.91	-0.28	<b>0.46</b>
ADORA2A	0.28	-4.78	1.66	1.11	1.76	-3.13	-3.21	-5.38	-1.37	2.79	<b>-1.03</b>
AKT1	-1.27	-1.58	-0.34	0.03	0.03	-2.17	-0.28	-1.99	-1.60	0.52	<b>-0.87</b>
ALDOA	1.29	-0.39	0.70	-0.47	0.08	-2.72	-0.78	-1.47	-1.71	0.52	<b>-0.49</b>
ALDOC	13.68	6.39	13.06	4.37	15.41	4.58	10.42	-0.62	13.03	10.24	<b>9.06</b>
ANGPT1	-6.49	9.26	0.03	7.89	6.03	7.71	4.89	-0.83	8.12	-6.05	<b>3.05</b>
ANGPT2	14.07	2.82	3.98	-0.18	-4.45	-0.36	2.41	-0.23	5.72	14.04	<b>3.78</b>
ANGPTL4	7.11	3.49	2.28	11.22	-0.16	3.91	-7.03	0.00	-0.80	-1.11	<b>1.89</b>
ANLN	-2.43	-3.72	3.18	-0.88	1.66	-2.02	3.16	-0.13	2.28	2.95	<b>0.40</b>
APC	0.47	0.62	1.11	0.91	0.49	-0.70	1.91	-1.81	-0.18	0.65	<b>0.35</b>
APH1B	0.28	0.52	0.39	-0.85	1.84	-0.80	1.06	-2.38	3.39	2.48	<b>0.59</b>
API5	0.05	-0.67	0.21	-0.65	-0.31	-1.99	0.05	-2.02	-2.35	-0.41	<b>-0.81</b>
APLN	0.26	0.03	0.03	-0.18	-0.16	-0.36	-0.49	-0.23	-0.72	-0.28	<b>-0.21</b>
APOE	-6.44	5.41	0.03	3.75	9.88	0.49	6.59	-1.68	-0.72	-0.28	<b>1.70</b>
APOL6	-0.57	-0.26	0.39	-0.23	0.23	-3.21	-0.96	-2.79	-4.14	-0.67	<b>-1.22</b>
AQP9	5.69	3.10	7.73	-0.18	-0.16	-0.36	-0.49	-0.23	-0.72	-7.91	<b>0.65</b>
AREG	17.95	12.41	2.56	4.16	14.95	6.28	14.74	-1.47	-2.61	1.14	<b>7.01</b>
ARG1	0.26	0.03	5.09	-0.18	-0.16	-0.36	-0.49	-0.23	-0.72	-0.28	<b>0.29</b>
ARG2	4.03	4.60	3.67	2.77	2.15	1.66	2.61	-1.14	1.37	6.16	<b>2.79</b>
ARID1A	0.88	-1.22	0.75	-1.03	0.62	-2.15	-0.23	-2.07	-1.29	0.10	<b>-0.56</b>
ARNT2	-3.91	-3.13	1.03	-1.78	-0.10	-2.87	-1.42	-2.53	-0.72	3.36	<b>-1.21</b>
ATF3	4.78	-0.26	1.24	0.98	1.73	1.42	1.06	-2.38	-0.13	6.03	<b>1.45</b>
ATM	-1.14	0.31	0.91	-0.65	0.72	-1.24	0.10	-1.73	-0.23	0.80	<b>-0.21</b>
AXIN1	0.80	-1.19	-0.98	-2.04	-0.03	-2.46	-0.41	-1.40	-2.64	0.10	<b>-1.02</b>
AXL	-4.24	-2.46	-1.58	-3.13	0.03	-3.80	-1.97	-2.38	-2.30	-0.91	<b>-2.27</b>
B2M	0.28	0.70	0.72	-0.91	0.28	-2.66	-0.36	-1.84	-1.73	-0.39	<b>-0.59</b>
BAD	-0.18	-0.47	-1.63	-2.17	0.98	-2.66	-0.98	-3.26	-2.43	0.80	<b>-1.20</b>
BAMBI	-1.19	0.00	0.57	-1.01	2.77	-3.57	-0.47	-2.07	-4.03	2.41	<b>-0.66</b>
BATF3	2.12	1.09	-0.49	-1.78	3.39	9.57	6.34	-5.64	-0.72	-0.28	<b>1.36</b>
BAX	0.00	0.44	-0.23	-1.19	0.13	-1.27	0.28	-2.61	-3.34	-0.91	<b>-0.87</b>
BBC3	0.26	1.24	-0.93	-0.75	0.65	1.84	-2.95	-3.83	-3.34	3.23	<b>-0.46</b>
BBS1	-0.88	-1.32	-0.03	-1.40	-0.23	-2.61	-0.62	-0.57	-1.97	-0.80	<b>-1.04</b>
BCAT1	-2.72	-2.35	1.16	-2.25	-0.21	-2.35	0.08	-3.16	6.70	18.10	<b>1.30</b>
BCL2	-6.36	-6.70	-2.84	-7.89	-1.55	-0.36	1.37	-2.38	5.09	-0.28	<b>-2.19</b>
BCL2L1	2.82	-0.08	0.47	0.80	1.66	-1.19	0.57	-1.73	-2.15	-1.68	<b>-0.05</b>
BCL6B	8.95	-5.22	0.03	-0.18	-0.16	-0.36	-0.49	-0.23	-0.72	-0.28	<b>0.13</b>
BID	-1.63	-1.53	-0.16	-1.03	-0.41	-3.39	-1.14	-2.20	-2.59	0.41	<b>-1.37</b>

	MesMM98	MesOC99	SiMes1	SiMes4	MMB	Mes1	Mes2	MPP89	MMCA	MesCM98	mFC
BIRC3	-0.39 <sup>a</sup>	-0.10	3.93	-2.79	0.39	8.87	-2.02	-8.51	2.66	0.03	<b>0.21<sup>b</sup></b>
BIRC5	-2.17	-4.01	1.11	-0.83	1.27	-2.04	2.72	-1.22	4.99	0.62	<b>0.04</b>
BLK	0.26	0.03	0.03	-0.18	-0.16	-0.36	-0.49	-0.23	-0.72	0.00	<b>-0.18</b>
BLM	-0.47	-3.23	2.77	-0.59	2.15	-1.32	2.74	-1.66	2.53	0.05	<b>0.30</b>
BMP2	0.47	3.80	1.55	2.53	4.19	5.64	1.63	-1.99	0.80	0.47	<b>1.91</b>
BNIP3	0.26	-0.57	-1.27	-1.60	0.41	-1.19	-1.50	-0.75	-2.07	0.08	<b>-0.82</b>
BNIP3L	-1.42	-0.36	-0.26	-0.41	0.34	-1.86	0.54	-2.82	-2.64	-0.18	<b>-0.91</b>
BRCA1	-2.12	-2.72	0.91	-0.70	2.07	-1.99	3.67	-1.63	3.18	2.64	<b>0.33</b>
BRCA2	-1.01	-1.47	3.57	2.07	2.15	1.55	5.15	-1.71	8.30	2.43	<b>2.10</b>
BRD3	-1.73	-2.43	-0.70	-1.24	0.65	-2.33	-1.14	-2.90	-1.78	-0.62	<b>-1.42</b>
BRD4	-0.31	-1.16	-1.06	-1.45	0.80	-1.94	0.34	-2.74	-2.17	0.16	<b>-0.95</b>
BRIP1	-2.38	-3.28	2.97	-0.44	2.07	-1.03	2.38	-1.34	-0.93	0.28	<b>-0.17</b>
BTLA	0.26	0.03	0.03	-0.18	-0.16	-0.36	-0.49	-0.23	-0.72	-0.28	<b>-0.21</b>
C1QA	0.26	-4.19	0.03	-0.18	-0.16	-0.36	-0.49	-0.23	-0.72	-0.28	<b>-0.63</b>
C1QB	0.26	0.03	0.03	-0.18	-0.16	-0.36	-6.34	-0.23	-0.72	-0.28	<b>-0.80</b>
C2	0.26	-6.03	5.95	-5.25	-4.68	-4.78	-4.32	4.97	3.41	1.50	<b>-0.90</b>
C5	-1.73	-3.23	8.30	-0.18	0.72	-7.06	2.07	-12.41	3.41	0.70	<b>-0.94</b>
C5AR1	0.26	0.03	0.03	-0.18	-0.16	-0.36	-0.49	-0.23	-0.72	-0.28	<b>-0.21</b>
C7	-2.33	-4.19	0.03	-0.18	-0.16	-0.36	-0.49	-0.23	6.70	-0.28	<b>-0.15</b>
CASP1	-0.41	1.99	2.77	-1.94	10.97	-1.27	0.05	-1.40	-3.47	0.78	<b>0.81</b>
CASP3	0.31	-0.80	-0.67	-0.28	1.63	-4.11	-0.03	-1.60	-1.81	0.70	<b>-0.67</b>
CASP8	-0.16	-0.39	-1.01	0.21	1.11	-2.22	-0.21	-3.72	-2.07	1.19	<b>-0.73</b>
CASP9	0.54	1.84	2.84	-0.10	-0.21	0.85	0.00	-2.12	-0.62	4.29	<b>0.73</b>
CBLC	0.26	-4.19	0.03	-0.18	-0.16	-3.44	-0.49	-0.23	-2.74	-1.22	<b>-1.24</b>
CCL13	0.26	-2.74	0.03	-0.18	1.09	-0.36	-0.49	-0.23	-0.72	-0.28	<b>-0.36</b>
CCL14	0.26	-2.74	0.03	-0.18	-0.16	-0.36	-0.49	-0.23	-0.72	-0.28	<b>-0.49</b>
CCL18	-0.23	-0.85	0.67	-0.36	0.80	-1.01	-1.01	0.03	-1.76	-1.22	<b>-0.49</b>
CCL19	0.26	0.03	0.03	-8.33	-3.44	-0.36	-0.49	-0.23	-0.72	4.58	<b>-0.87</b>
CCL2	0.28	1.16	3.78	1.22	1.32	-1.76	-2.33	-2.41	3.41	-0.28	<b>0.44</b>
CCL20	18.41	14.07	5.33	11.87	10.37	8.43	10.68	1.11	0.98	23.22	<b>10.45</b>
CCL21	0.26	-5.64	7.22	-0.18	8.41	-0.36	-0.49	-0.23	-7.14	1.97	<b>0.38</b>
CCL22	0.26	0.03	5.09	-0.18	-0.16	-0.36	-0.49	-0.23	7.47	10.01	<b>2.14</b>
CCL3/L1	8.59	5.07	0.03	-0.18	-0.16	-0.36	-0.49	1.32	-0.72	2.61	<b>1.57</b>
CCL4	0.26	0.03	0.03	-2.53	-3.44	2.59	0.98	-0.23	-0.72	-0.28	<b>-0.33</b>
CCL5	8.84	0.21	4.63	7.89	7.73	-1.47	-0.96	-0.62	-0.72	8.72	<b>3.42</b>
CCL7	6.47	1.09	12.59	-0.18	-0.16	2.97	0.98	-0.23	-0.72	-0.28	<b>2.25</b>
CCL8	0.26	-6.70	7.73	-0.18	7.22	0.21	-9.36	5.77	3.41	-0.28	<b>0.81</b>
CCNA1	11.59	17.59	1.01	3.44	3.28	-5.84	6.93	1.34	-0.72	-0.28	<b>3.83</b>
CCNB1	-2.72	-3.26	0.49	0.10	0.49	-2.51	0.88	-0.59	3.49	1.84	<b>-0.18</b>
CCND1	0.96	-2.15	-0.72	-1.27	1.11	-2.41	-0.21	-1.45	-3.91	-1.50	<b>-1.15</b>
CCND2	-1.60	7.32	-0.31	-0.72	3.98	6.83	6.05	-4.09	4.34	-0.28	<b>2.15</b>
CCND3	4.32	0.34	1.06	0.96	1.89	-2.33	-0.18	-0.52	-0.03	4.50	<b>1.00</b>

	MesMM98	MesOC99	SiMes1	SiMes4	MMB	Mes1	Mes2	MPP89	MMCA	MesCM98	mFC
CCNE1	2.95 <sup>a</sup>	-0.75	-0.28	-0.36	1.97	-1.47	3.67	-1.99	2.51	2.64	0.89 <sup>b</sup>
CCNO	3.85	2.41	-1.68	4.19	2.04	-2.56	3.54	-2.20	1.86	6.13	1.76
CCR2	0.26	-0.44	0.03	-0.18	-0.16	-0.36	-0.49	-0.23	0.34	1.97	0.07
CCR4	17.87	10.99	9.57	3.21	11.79	-4.89	4.06	-0.23	7.47	9.54	6.94
CCR5	-5.69	3.31	6.26	-0.18	-0.16	-1.29	-7.63	-4.55	0.34	6.70	-0.29
CD14	0.26	0.03	9.26	-0.18	-0.16	4.09	-0.49	-1.60	-0.72	-0.28	1.02
CD163	0.26	3.96	0.03	-0.18	-5.69	-0.36	-4.32	-0.23	-4.29	5.77	-0.51
CD19	11.64	8.53	0.03	-6.10	1.68	1.78	-6.34	6.36	-0.23	2.92	2.03
CD1C	0.26	0.03	0.03	-2.53	-0.16	-0.36	-0.49	-0.23	-0.72	3.52	-0.07
CD2	0.49	-0.96	-0.03	-0.08	0.83	-1.63	-0.47	-2.69	-3.10	-0.65	-0.83
CD209	0.26	0.03	0.03	-2.53	1.09	-0.36	-0.49	-0.23	-0.72	3.52	0.06
CD244	0.26	-4.19	11.56	-0.18	-0.16	-7.22	-0.49	0.34	-0.72	1.97	0.12
CD247	-1.53	0.03	3.98	7.45	-0.16	-0.36	-0.49	-0.23	-0.72	1.81	0.98
CD27	0.26	0.03	0.03	-0.18	-0.16	-0.36	-0.49	-0.23	-0.72	-0.28	-0.21
CD274	-0.21	0.31	0.88	1.55	5.84	10.01	6.96	-2.51	-4.37	0.10	1.86
CD276	-0.49	-2.66	-0.31	-0.10	0.59	-2.53	-0.54	-1.32	-2.59	-0.52	-1.05
CD28	0.26	0.03	0.03	-2.53	-0.16	-0.36	-0.49	-0.23	-0.72	-0.28	-0.45
CD300A	0.26	0.03	0.03	-0.18	-0.16	-0.36	-0.49	-0.23	-0.72	-0.28	-0.21
CD36	0.26	-6.03	0.03	11.22	-0.16	0.54	-0.49	0.67	10.94	3.52	2.05
CD38	0.26	3.31	8.59	-0.18	3.10	-4.42	-3.72	-1.22	-0.72	-8.77	-0.38
CD3D	6.21	0.36	3.28	0.67	-0.16	-1.53	-0.49	-3.16	-5.48	-1.68	-0.20
CD3E	8.38	-8.59	-1.45	-4.14	2.20	-1.06	-4.16	-1.16	0.00	8.02	-0.20
CD3G	0.26	-6.03	0.03	-0.18	-1.42	-0.36	-0.49	-0.23	6.70	-0.28	-0.20
CD4	0.26	-0.36	0.03	-0.18	-0.16	-0.36	-0.49	-0.23	-0.72	-0.28	-0.25
CD40	10.89	6.57	5.95	-0.26	-0.16	-0.39	10.29	-2.02	7.11	-1.60	3.64
CD40LG	0.26	0.03	0.03	-0.18	-0.16	-0.36	-0.49	-0.23	-0.72	-0.28	-0.21
CD44	-0.26	-0.41	-0.13	1.03	0.70	-0.83	-0.93	-2.04	-0.85	0.65	-0.31
CD45RA	0.26	0.03	0.03	-0.18	-0.16	-0.36	-0.49	-0.23	-0.72	-5.17	-0.70
CD45RB	5.46	-6.47	0.03	-0.83	-0.26	8.61	-3.26	-4.55	-0.44	2.61	0.09
CD45RO	0.26	0.03	3.98	5.66	3.05	-0.36	-0.49	-0.23	5.09	-0.28	1.67
CD47	-0.08	0.23	1.29	0.18	-0.03	-5.22	0.13	-1.11	-0.65	-1.22	-0.65
CD48	0.26	-5.22	0.03	-0.18	-0.16	-0.36	-0.49	-0.23	-0.72	-0.28	-0.74
CD5	3.80	0.03	3.28	-0.18	-0.16	-0.36	-0.49	-0.23	-0.72	-0.28	0.47
CD58	0.54	-1.58	-0.80	0.57	0.52	-2.04	0.16	-0.83	-1.45	-1.06	-0.60
CD6	0.26	0.03	0.03	-4.14	1.09	-0.36	-0.49	-0.23	-0.72	-0.28	-0.48
CD68	0.70	3.52	1.73	6.41	3.13	-0.08	10.66	-1.11	-0.41	-0.23	2.43
CD69	-3.23	0.49	1.22	1.24	9.13	6.47	0.67	-8.90	-7.14	2.28	0.22
CD7	0.26	5.07	0.03	-0.18	-0.16	-7.22	-0.98	-0.23	-0.72	-11.59	-1.57
CD70	6.75	4.97	15.10	15.80	-0.23	7.53	3.36	-0.13	-4.29	8.09	5.69
CD74	11.07	2.74	2.07	-0.28	4.34	4.91	3.91	6.98	0.36	-0.91	3.52
CD79A	0.26	-0.88	0.03	-0.93	-6.47	-7.22	-4.32	-0.23	-0.72	5.43	-1.51
CD79B	-3.23	0.03	0.03	3.75	-0.16	-0.36	-0.49	-0.23	-0.72	1.97	0.06

	MesMM98	MesOC99	SiMes1	SiMes4	MMB	Mes1	Mes2	MPP89	MMCA	MesCM98	mFC
CD80	0.26 <sup>a</sup>	0.03	0.03	-0.18	-0.16	-0.36	-0.49	-0.23	-0.72	-0.28	<b>-0.21<sup>b</sup></b>
CD84	0.26	0.03	0.03	-0.18	-0.16	-0.36	-0.49	-0.23	-0.72	-0.28	<b>-0.21</b>
CD86	0.26	0.03	0.03	-0.18	-0.16	-0.36	-0.49	-0.23	-0.72	3.52	<b>0.17</b>
CD8A	0.26	0.03	-3.05	-0.18	4.32	-0.36	6.75	-0.23	0.34	7.19	<b>1.51</b>
CD8B	-4.40	2.33	0.03	-4.14	2.09	-0.36	2.77	-0.23	-5.35	5.43	<b>-0.18</b>
CD96	0.26	-7.76	0.03	-2.53	-0.16	4.86	3.98	-4.55	-0.72	3.23	<b>-0.34</b>
CDC20	-0.78	0.10	0.91	-0.31	1.81	-2.38	3.03	0.08	4.53	2.66	<b>0.96</b>
CDC25C	-0.91	-5.20	1.47	-1.09	2.66	-2.64	4.47	-0.39	13.11	5.20	<b>1.67</b>
CDH1	7.27	8.77	4.42	9.78	0.62	-1.78	-1.22	0.00	-3.18	1.60	<b>2.63</b>
CDH11	-3.23	-2.04	0.13	-1.66	0.13	-2.17	-2.38	-2.15	-2.59	-0.83	<b>-1.68</b>
CDH2	-1.66	-2.72	-0.67	-1.22	-0.91	-1.01	-0.44	-2.46	-0.72	3.52	<b>-0.83</b>
CDH5	-4.40	0.03	0.03	3.57	2.09	4.86	-0.49	-0.23	-3.00	7.06	<b>0.95</b>
CDK2	-0.31	-2.56	0.96	-0.28	1.94	-1.27	1.32	-0.91	-0.08	1.91	<b>0.07</b>
CDK6	-1.06	-1.89	0.03	-0.36	-0.03	-0.91	0.78	-1.91	-2.02	-0.47	<b>-0.78</b>
CDKN1A	4.40	2.59	1.01	0.88	3.41	0.88	5.02	-1.27	-4.01	0.67	<b>1.36</b>
CDKN1C	-2.84	-0.23	1.76	3.59	3.28	12.34	4.53	-1.01	-1.53	-0.39	<b>1.95</b>
CDKN2A	-0.34	-0.16	0.52	-2.02	-1.68	-1.60	-1.37	-2.35	-2.82	-1.68	<b>-1.35</b>
CDKN2B	0.26	-6.03	0.03	-2.53	-0.16	-0.36	-6.34	-1.53	-1.94	3.28	<b>-1.53</b>
CEACAM3	-4.03	-3.75	0.96	-0.31	2.69	8.09	7.99	0.18	-0.72	-3.49	<b>0.76</b>
CEBPB	-1.24	-0.80	-0.59	-3.13	-0.80	-3.41	-1.86	-2.07	-2.92	0.88	<b>-1.60</b>
CENPF	-3.44	-3.67	2.77	-0.80	-0.31	1.47	4.24	-1.40	7.76	1.86	<b>0.85</b>
CEP55	0.00	-0.10	0.83	2.02	2.09	-2.15	3.47	-1.84	10.91	2.77	<b>1.80</b>
CES3	1.89	5.07	0.03	-0.18	1.09	-0.36	-0.49	-3.16	7.47	7.63	<b>1.90</b>
CHUK	1.55	-0.28	0.21	0.21	0.44	-2.15	0.93	-2.72	-1.81	-0.21	<b>-0.38</b>
CLEC14A	0.26	0.03	0.03	-0.18	-0.16	-0.36	-0.49	-0.23	-0.72	4.58	<b>0.27</b>
CLEC4E	0.26	-1.86	6.65	-10.94	-2.25	5.33	-8.90	8.28	2.72	9.28	<b>0.86</b>
CLEC5A	0.26	0.03	0.03	-0.18	-1.42	-0.36	-0.49	-0.23	-2.48	-0.28	<b>-0.51</b>
CLEC7A	0.26	0.03	0.03	-0.18	-0.16	-0.36	-0.49	-0.23	-0.72	-0.28	<b>-0.21</b>
CLECL1	0.26	0.03	0.03	-0.18	-0.16	-0.36	-0.49	-0.23	-0.72	-0.28	<b>-0.21</b>
CMKLR1	-7.11	0.03	0.03	-0.18	-0.16	-0.36	-0.49	0.00	-0.72	-0.28	<b>-0.93</b>
CNTRF	0.26	0.03	0.03	-0.18	-0.16	-0.36	-0.49	-0.23	-0.72	-0.28	<b>-0.21</b>
COL11A1	12.72	0.03	0.03	9.26	16.47	-2.33	6.23	5.77	-0.72	14.04	<b>6.15</b>
COL11A2	0.26	-4.19	-11.35	-0.18	-0.16	3.91	-4.32	-0.23	-0.72	-13.53	<b>-3.05</b>
COL17A1	13.76	4.24	-2.48	5.92	7.68	2.30	2.38	-8.33	-2.28	0.49	<b>2.37</b>
COL4A5	0.03	0.16	1.09	-0.78	0.16	-0.28	-0.65	-1.06	-0.39	0.67	<b>-0.11</b>
COL5A1	-3.23	-3.80	0.26	-0.47	0.41	-2.15	-0.41	-2.07	1.03	0.36	<b>-1.01</b>
COL6A3	6.44	14.87	3.31	11.53	11.15	4.86	17.33	-3.70	10.47	-0.28	<b>7.60</b>
COMP	9.31	7.73	-4.47	-0.18	-6.47	-0.36	-0.49	-0.23	-0.72	3.44	<b>0.76</b>
CPA3	-5.90	6.62	5.09	-0.18	11.07	1.09	-0.49	-3.34	-0.72	-0.28	<b>1.30</b>
CRABP2	2.07	3.62	0.75	4.32	3.41	0.03	4.32	-0.18	-3.75	-0.44	<b>1.41</b>
CSF1	-1.50	-0.98	1.50	-1.94	-2.38	-2.22	-6.03	-1.73	7.11	1.16	<b>-0.70</b>
CSF1R	0.10	1.66	5.95	10.68	-1.42	-3.44	8.92	5.38	3.91	3.83	<b>3.56</b>

	MesMM98	MesOC99	SiMes1	SiMes4	MMB	Mes1	Mes2	MPP89	MMCA	MesCM98	mFC
CSF2	3.34 <sup>a</sup>	11.38	0.62	8.64	-0.16	-3.44	0.98	4.29	-0.16	3.23	<b>2.87<sup>b</sup></b>
CSF2RB	0.26	0.03	0.03	-0.18	-0.16	-0.36	-0.49	-0.23	-0.72	-0.28	<b>-0.21</b>
CSF3	0.26	0.03	8.17	-0.18	-0.16	-0.36	-0.49	-2.43	-0.72	-0.28	<b>0.38</b>
CSF3R	0.26	-2.79	3.98	-0.18	4.32	-4.78	-0.49	2.87	-0.72	-0.28	<b>0.22</b>
CST2	0.26	5.92	-3.26	-0.18	-0.16	-0.36	-2.66	4.97	-0.72	-10.06	<b>-0.63</b>
CTAG1B	22.86	13.68	0.03	6.36	20.30	8.74	12.52	15.08	16.09	15.93	<b>13.16</b>
CTLA4	12.47	7.22	0.03	4.58	10.58	7.71	6.23	0.34	-0.72	-0.28	<b>4.81</b>
CTNNB1	-0.62	-1.60	-0.03	-0.13	0.16	-2.33	-0.34	-2.02	-1.97	-0.13	<b>-0.90</b>
CTSS	1.42	1.09	2.53	1.91	-0.28	-2.82	0.67	-1.22	-6.47	-3.03	<b>-0.62</b>
CTSW	0.26	0.03	0.03	-0.18	-0.16	-0.36	-0.49	-0.23	-0.72	4.58	<b>0.27</b>
CX3CL1	5.33	4.29	3.49	-0.18	10.78	-0.36	8.95	3.96	2.20	12.80	<b>5.13</b>
CX3CR1	0.26	0.03	0.03	-0.18	-0.16	-3.80	-0.49	-0.23	-0.72	-0.28	<b>-0.56</b>
CXCL1	8.64	6.98	1.63	-0.98	9.41	-1.14	-2.02	-2.35	-0.65	1.47	<b>2.10</b>
CXCL10	-1.53	1.24	4.11	6.52	-0.16	-4.40	-0.49	-3.75	6.23	10.63	<b>1.84</b>
CXCL11	5.12	2.09	1.66	10.27	6.03	-1.06	-9.36	-2.51	13.11	-1.89	<b>2.35</b>
CXCL12	-4.40	-0.36	0.03	-0.18	-0.16	-0.36	-0.49	-0.23	-0.72	3.52	<b>-0.34</b>
CXCL13	0.26	0.03	0.03	-0.18	-3.44	-0.36	-0.49	-0.23	3.41	-0.28	<b>-0.13</b>
CXCL14	2.61	-1.01	9.21	7.53	4.01	0.21	7.01	-0.23	3.91	-0.44	<b>3.28</b>
CXCL16	5.35	1.09	4.09	1.81	0.65	-1.81	1.42	-2.12	-2.59	1.29	<b>0.92</b>
CXCL2	3.21	2.84	1.22	-0.93	16.71	1.11	-0.72	-2.72	-1.03	3.36	<b>2.30</b>
CXCL3	2.90	3.21	0.88	1.84	6.65	0.54	-1.97	-3.39	0.00	4.89	<b>1.55</b>
CXCL5	0.26	0.03	10.11	-0.18	-0.16	-0.36	-0.49	-4.42	-0.72	-0.28	<b>0.38</b>
CXCL6	0.26	0.03	11.38	-0.18	-0.16	3.91	4.89	-1.68	4.27	1.37	<b>2.41</b>
CXCL8	7.34	8.09	0.70	0.23	12.70	-0.36	0.85	-1.60	0.34	1.66	<b>2.99</b>
CXCL9	0.26	-2.74	0.03	-0.18	-0.16	-0.36	-0.49	-0.23	-0.72	-0.28	<b>-0.49</b>
CXCR2	7.11	2.30	-4.40	-0.18	-0.16	-7.22	-4.01	-5.59	4.34	4.76	<b>-0.30</b>
CXCR3	0.26	0.03	0.03	-0.18	-0.16	0.54	0.98	-0.23	-0.72	-0.28	<b>0.03</b>
CXCR4	10.37	1.63	11.72	8.64	4.24	-1.66	2.38	3.96	-0.72	-0.28	<b>4.03</b>
CXCR6	0.26	0.03	-0.93	-0.18	-0.16	-0.36	-0.49	-0.23	-0.72	-0.28	<b>-0.31</b>
CXorf36	0.26	-4.19	0.03	-0.18	-0.16	-0.36	-0.49	-0.23	-0.72	-0.28	<b>-0.63</b>
CYBB	0.26	-2.74	0.03	-0.18	-0.16	0.54	-0.49	-0.23	-0.72	-0.28	<b>-0.40</b>
DAB2	-5.09	-1.16	0.91	-3.08	0.31	-2.07	-0.88	-1.81	-0.36	1.09	<b>-1.22</b>
DDB2	2.72	1.27	1.68	1.09	1.24	0.16	-1.27	-0.44	-1.68	1.22	<b>0.60</b>
DEFB134	0.26	0.03	0.03	-0.18	-0.16	-0.36	-0.49	-0.23	-0.72	-0.28	<b>-0.21</b>
DEPTOR	-4.78	0.21	4.55	-3.36	-2.33	3.98	1.03	-1.76	0.70	3.52	<b>0.18</b>
DKK1	2.02	0.18	-0.93	1.97	1.14	-0.96	5.95	-0.41	0.67	5.12	<b>1.47</b>
DLL1	0.05	-1.99	-1.29	-5.25	4.32	-0.28	-0.41	-3.91	-0.72	6.41	<b>-0.31</b>
DLL4	1.16	0.03	0.03	-0.18	-0.16	-0.36	4.06	0.52	-0.72	9.00	<b>1.34</b>
DNMT1	0.13	-2.61	0.72	-0.21	1.68	-1.97	1.06	-2.04	0.00	1.45	<b>-0.18</b>
DPP4	-4.29	5.79	0.57	-0.57	3.28	-0.75	4.06	-1.03	7.47	3.75	<b>1.83</b>
DTX3L	1.27	0.83	0.34	-0.10	0.85	-2.35	0.75	-2.79	-1.50	-0.83	<b>-0.35</b>
DTX4	3.31	-0.96	2.28	1.27	1.91	-0.93	1.89	-2.02	2.02	-0.13	<b>0.86</b>

	MesMM98	MesOC99	SiMes1	SiMes4	MMB	Mes1	Mes2	MPP89	MMCA	MesCM98	mFC
DUSP1	-1.03 <sup>a</sup>	-2.09	0.91	-1.37	0.91	-0.62	-1.76	-0.65	-3.62	0.10	-0.92 <sup>b</sup>
DUSP2	-3.57	-8.92	-7.84	-0.18	7.50	4.86	1.97	-1.16	6.05	6.10	0.48
DUSP5	4.16	1.19	0.26	-0.08	4.81	5.20	3.16	-0.44	-2.77	-0.44	1.51
E2F3	-0.52	-2.04	-0.67	-0.83	-0.05	-1.81	0.39	-2.15	-2.46	-1.45	-1.16
EDN1	-3.54	-3.62	3.54	4.29	2.61	-2.77	5.69	-2.25	-3.18	4.14	0.49
EGF	-4.40	0.57	0.03	0.78	8.09	-2.38	-2.28	-0.23	5.09	-0.28	0.50
EGFR	-1.42	0.49	-0.59	-2.28	-0.44	-2.97	-0.62	-3.13	-1.68	-0.80	-1.34
EGR1	0.75	-4.32	-0.21	-2.15	3.36	2.66	-0.65	-3.03	-1.73	2.95	-0.24
EIF2AK2	1.40	0.44	0.34	-0.57	-0.31	-2.82	-0.28	-2.33	-2.35	-0.88	-0.74
EIF2B4	1.01	-1.32	-0.62	-1.01	0.08	0.03	0.28	-2.09	-1.68	2.09	-0.32
EIF4EBP1	-4.94	-2.77	-3.00	-4.09	-0.18	-3.23	-0.88	-3.49	-3.05	-1.37	-2.70
EIF5AL1	0.26	0.03	0.03	-0.18	-0.16	-0.36	-0.49	-0.23	-0.72	-0.28	-0.21
ELOB	0.18	0.10	-0.36	-0.03	0.80	-2.95	0.23	-3.67	-2.15	0.18	-0.77
ENO1	-0.21	-1.66	0.67	-1.42	-0.21	-2.41	-0.88	-1.68	-1.27	-0.10	-0.92
ENTPD1	-1.73	0.03	2.30	-2.64	-2.79	0.57	-3.57	-1.86	1.16	1.53	-0.70
EOMES	13.11	-2.74	6.65	1.29	13.32	-0.36	4.29	-0.23	0.34	14.20	4.99
EPCAM	5.22	5.97	8.59	0.62	11.64	-7.34	15.70	-10.40	-0.57	2.33	3.18
EPM2AIP1	0.13	-0.52	1.78	-0.18	0.52	-2.28	-0.98	-2.17	-1.45	-0.34	-0.55
ERBB2	-0.28	-2.02	0.62	-0.34	0.72	-1.55	1.03	-1.76	-1.60	1.37	-0.38
ERO1A	-0.08	-0.88	0.41	0.21	0.23	-1.84	0.18	-1.81	-1.32	0.65	-0.42
ESR1	4.66	0.03	0.03	2.22	-0.16	-0.36	-5.35	4.97	-0.65	1.86	0.72
EXO1	-1.60	-3.10	0.18	-0.39	3.05	-1.34	3.91	-1.91	6.91	3.70	0.94
EZH2	-0.05	-2.46	2.87	1.11	1.14	-1.91	2.30	-1.14	0.88	2.33	0.51
F2RL1	15.39	2.74	1.89	10.68	4.29	-0.36	5.64	-3.05	-2.30	0.54	3.55
FADD	-1.91	-1.06	-0.96	-1.16	-0.16	-2.12	0.05	-3.31	-2.79	-0.88	-1.43
FAM124B	0.26	0.03	0.03	-0.18	-0.16	-0.36	-0.49	-0.23	-0.72	-0.28	-0.21
FAM30A	0.26	0.03	7.73	-0.18	-0.16	-0.36	-6.34	-0.23	0.34	-0.28	0.08
FANCA	0.31	-2.41	2.33	0.44	3.13	-1.73	2.17	-2.25	6.80	3.93	1.27
FAP	-8.66	-0.36	-0.72	-0.18	-0.16	-5.30	-0.49	-1.55	-3.49	-5.53	-2.65
FAS	4.47	6.34	1.71	4.29	9.13	4.40	2.12	-3.41	0.54	2.46	3.20
FASLG	0.26	0.03	0.03	-0.18	-0.16	-0.36	-0.49	-0.23	-0.72	4.58	0.27
FBP1	11.12	3.96	-4.40	-0.18	3.05	-0.36	-0.49	-8.33	9.16	5.51	1.90
FCAR	0.26	0.03	0.03	-0.18	-0.16	-0.36	-0.49	-0.23	-0.72	-0.28	-0.21
FCGR1A	-3.23	-4.19	0.03	-0.18	-0.16	-0.36	-0.49	-0.23	2.20	-6.05	-1.27
FCGR2A	-6.00	0.03	0.03	-0.18	-0.16	0.54	-0.49	-0.23	-0.72	-3.98	-1.12
FCGR2B	0.26	0.03	-0.93	-0.18	-0.16	-6.57	-0.49	-0.23	-2.48	-0.28	-1.10
FCGR3A/B	0.26	0.03	0.03	-0.18	-0.16	-0.36	-0.49	-0.23	-0.72	-0.28	-0.21
FCGRT	-1.09	-2.97	0.59	-0.47	-1.22	-4.22	-2.33	-2.04	-0.72	8.72	-0.57
FCN1	0.26	0.03	-3.05	-0.18	4.32	-4.78	-0.49	-0.23	2.20	-0.28	-0.22
FCRL2	-6.00	0.03	2.38	-0.18	-0.16	-0.36	-0.49	-0.23	-0.72	-0.28	-0.60
FGF13	-3.62	-2.28	0.03	7.32	-0.16	-0.36	5.84	-10.40	-3.49	1.22	-0.59
FGF18	0.26	-4.22	9.85	-1.27	1.47	0.80	-2.22	-0.23	-0.72	-0.28	0.34

	MesMM98	MesOC99	SiMes1	SiMes4	MMB	Mes1	Mes2	MPP89	MMCA	MesCM98	mFC
FGF9	0.26 <sup>a</sup>	-2.74	0.03	-0.18	-0.16	-6.00	-0.49	-3.16	-0.72	-0.28	-1.34 <sup>b</sup>
FGFR1	-0.83	-1.45	0.08	-1.40	-0.85	-4.11	-0.39	-1.89	-0.72	5.43	-0.61
FLNB	-1.16	-1.14	0.21	-0.16	0.65	-1.91	-0.31	-1.40	-3.91	-0.72	-0.99
FLT1	8.95	1.84	5.90	3.10	9.13	-0.36	9.67	-2.02	2.20	-0.28	3.81
FOSL1	-1.76	0.49	-3.34	-1.32	-1.01	-1.14	-1.94	-2.22	-5.82	-3.16	-2.12
FOXP3	0.26	5.53	0.03	-0.18	-3.44	-0.36	-0.49	-0.23	-0.72	4.58	0.50
FPR1	-12.39	0.03	-2.07	-1.94	-3.88	-6.52	3.44	-1.58	-2.48	-0.28	-2.77
FPR3	1.16	-2.92	0.03	-0.18	-0.16	-4.78	-0.49	-0.88	0.34	6.10	-0.18
FSTL3	-0.47	-0.54	2.25	-0.16	0.26	-2.72	-0.21	-0.85	-0.78	2.35	-0.09
FUT4	0.16	-1.22	-0.41	-2.43	7.16	0.80	2.74	0.47	0.10	-0.78	0.66
FYN	-0.31	0.16	-1.14	2.38	0.96	-1.84	1.14	-3.31	-1.84	1.45	-0.24
FZD8	1.66	-0.88	-0.72	0.93	1.27	3.28	3.70	-1.01	0.85	1.50	1.06
FZD9	10.68	8.17	0.03	-0.18	-0.16	-0.36	-0.49	-0.70	0.34	7.19	2.45
GAS1	-6.59	-4.78	3.59	-10.94	3.39	-0.52	-10.78	-3.21	-0.72	7.19	-2.34
GBP1	-2.04	-1.24	3.44	0.65	-0.28	-4.42	-0.39	-1.11	-3.57	0.59	-0.84
GBP2	-5.79	1.22	10.06	-0.23	2.12	-0.80	4.89	-1.03	-2.53	0.98	0.89
GBP4	-4.01	3.65	1.24	7.89	6.39	-3.23	-1.55	-0.70	-7.42	-2.22	0.00
GHR	4.66	0.05	3.98	0.75	-1.01	-1.29	-1.50	-0.85	0.34	-0.28	0.48
GIMAP4	0.26	-6.03	-4.40	-1.78	-0.16	-7.76	-0.49	-0.23	-7.55	0.54	-2.76
GIMAP6	0.26	0.03	5.95	-0.18	3.05	-0.36	-0.49	-0.23	-0.72	-0.28	0.70
GLI1	-0.44	-1.32	-6.83	-4.86	0.98	0.54	-2.48	-7.58	-0.72	5.43	-1.73
GLS	-3.41	-3.21	0.93	-3.18	-0.39	-1.63	-0.88	-1.29	-2.90	-0.08	-1.60
GLUD1	-0.93	0.88	0.05	0.67	0.65	-2.66	0.57	-1.84	-2.38	-0.91	-0.59
GLUL	-0.88	0.28	-0.10	0.80	1.01	-2.43	0.13	-1.22	-0.59	-0.28	-0.33
GMIP	0.26	0.36	0.03	-0.18	-0.16	-0.36	-0.49	-0.23	-4.29	1.97	-0.31
GNG4	-6.59	0.39	-7.06	10.27	1.55	-4.24	-0.21	-4.78	6.23	-0.28	-0.47
GNLY	0.26	0.03	2.38	-0.18	-0.16	-0.36	2.77	2.07	-0.72	1.97	0.80
GOT1	0.36	0.05	-0.62	0.08	0.91	-2.28	1.32	-1.84	-2.74	3.08	-0.17
GOT2	-0.05	-1.32	0.44	-0.67	0.03	-2.87	-0.13	-1.84	-1.63	0.39	-0.77
GPC4	-1.53	-1.91	5.95	1.86	1.34	-0.54	2.69	-1.63	3.28	1.53	1.10
GPR160	3.78	-0.72	0.44	0.52	0.54	-2.09	4.60	-1.63	1.16	3.49	1.01
GPSM3	1.84	-0.49	1.68	0.47	4.32	2.09	0.52	-2.79	2.61	2.15	1.24
GZMA	0.26	0.03	0.03	-0.18	-0.16	-0.36	-0.49	-0.23	4.34	-0.28	0.29
GZMB	0.26	0.03	0.03	-0.18	-0.16	-0.36	-0.49	-0.23	-0.72	-0.28	-0.21
GZMH	0.26	0.03	0.03	-0.18	-0.16	-0.36	-0.49	-0.23	-0.72	-0.28	-0.21
GZMK	-7.97	0.03	0.36	-0.18	-7.09	-0.36	-2.66	-7.03	-0.72	5.43	-2.02
GZMM	0.26	0.03	0.03	-0.18	-0.16	-0.36	-0.49	-0.23	-0.72	1.97	0.01
H2AFX	1.97	-1.71	1.19	0.59	1.27	-2.04	1.32	-0.21	-1.01	2.59	0.40
HAVCR2	-4.16	2.82	0.03	-9.72	3.10	-5.79	6.75	-4.71	3.91	8.72	0.09
HCK	6.47	-2.74	0.03	-0.18	-0.16	-0.36	9.18	-3.16	-0.72	-0.28	0.81
HDAC11	3.49	-0.13	0.41	0.47	0.88	-0.98	0.67	-2.12	-0.85	2.28	0.41
HDAC3	-1.03	-2.53	-0.31	-1.42	-0.13	-2.84	-0.96	-2.77	-2.69	-0.31	-1.50

	MesMM98	MesOC99	SiMes1	SiMes4	MMB	Mes1	Mes2	MPP89	MMCA	MesCM98	mFC
HDAC4	-5.15 <sup>a</sup>	-4.68	-2.17	-4.91	0.28	-3.96	-0.47	-2.74	-3.57	8.02	-1.93 <sup>b</sup>
HDAC5	0.00	0.00	-0.57	-0.83	0.47	0.44	0.18	-1.42	-0.31	1.29	-0.08
HDC	0.26	0.03	0.03	-0.18	-0.16	-0.36	-0.49	-0.23	-0.72	-0.28	-0.21
HELLS	0.54	-3.72	0.80	-0.44	2.66	-1.71	2.28	-1.91	1.06	3.08	0.26
HERC6	4.34	3.80	0.75	2.38	0.52	-1.27	3.41	-4.29	-2.74	0.75	0.77
HES1	2.72	-2.64	0.26	-2.53	1.01	-1.37	-1.27	-1.37	-2.56	0.70	-0.71
HEY1	3.75	2.02	1.97	1.37	9.70	7.14	3.31	-1.34	0.47	3.93	3.23
HIF1A	-1.19	-0.91	1.16	0.31	0.23	-0.67	0.13	-0.88	-1.60	-1.32	-0.47
HK1	-0.31	0.44	0.80	-0.57	0.57	3.83	-0.34	-1.58	1.99	0.08	0.49
HK2	0.62	2.72	1.37	-0.67	-0.05	-1.97	0.10	-1.45	-1.45	-0.88	-0.17
HLA-A	-0.16	1.40	-0.21	-1.58	-0.08	-2.33	-1.01	-2.20	-3.31	-0.16	-0.96
HLA-B	0.98	2.09	0.23	-0.26	0.75	-2.77	0.13	-1.81	-2.33	0.44	-0.25
HLA-C	-0.13	1.06	-0.05	-1.09	-0.03	-2.56	-0.18	-1.76	-2.77	0.70	-0.68
HLA-DMA	-1.63	-3.57	1.32	0.78	2.38	-1.14	-1.66	-5.84	1.42	-1.22	-0.92
HLA-DMB	12.16	0.03	0.03	-0.18	-0.16	-0.36	-0.49	-0.23	5.09	0.41	1.63
HLA-DOA	6.47	-6.70	0.03	-0.18	-5.69	3.91	-7.63	-0.23	-0.72	-2.28	-1.30
HLA-DOB	-3.23	0.03	0.03	-0.18	-0.16	-0.36	-0.49	-0.23	5.09	4.58	0.51
HLA-DPA1	-12.72	0.03	0.03	-0.18	-0.16	-0.36	-0.49	-2.04	-0.72	-3.59	-2.02
HLA-DPB1	1.16	-6.03	0.03	-0.18	-0.16	-0.36	-4.32	-1.60	-7.14	-0.28	-1.89
HLA-DQA1	0.26	0.03	0.03	-0.18	-0.16	-0.36	-0.49	-0.23	-0.72	-2.28	-0.41
HLA-DQA2	0.26	0.03	0.03	-0.18	-0.16	-0.36	-0.49	-0.23	-0.72	-0.28	-0.21
HLA-DQB1	0.26	0.03	0.03	-0.18	-0.16	-0.36	-0.49	-0.23	-0.72	-0.28	-0.21
HLA-DRA	0.26	0.03	0.03	-6.67	-0.16	-0.36	-0.49	-0.23	4.34	-5.20	-0.85
HLA-DRB1	0.26	0.03	7.73	-8.33	1.78	-0.36	-0.49	-0.23	3.41	-3.75	0.01
HLA-DRB5	0.26	0.03	0.03	-0.18	-0.16	-0.36	-0.49	-0.23	-0.72	-0.28	-0.21
HLA-E	-0.21	1.24	0.54	-0.78	1.03	-2.69	-0.03	-1.37	-2.17	-0.31	-0.47
HLA-F	-1.60	4.22	-0.03	-0.18	0.88	-2.92	-0.47	-1.97	-2.90	0.23	-0.47
HMGA1	0.47	0.70	-1.37	-0.23	2.41	-0.83	0.08	-2.15	-2.43	0.31	-0.31
HMGB1	-2.28	-5.30	0.47	0.10	1.14	-2.79	1.91	-2.07	-0.80	-2.20	-1.18
HNF1A	0.26	-2.74	0.03	-0.18	1.09	-0.36	7.22	-0.23	-0.72	-3.80	0.05
HRAS	1.42	-1.32	-1.29	-0.75	-0.21	-2.09	-0.57	-3.36	-2.53	-1.42	-1.21
HSD11B1	-0.39	0.03	7.71	9.26	-0.16	-0.36	-0.49	-1.97	-0.72	-0.28	1.26
ICAM1	1.78	4.01	0.80	0.18	1.84	0.44	-0.28	-1.91	4.71	4.37	1.59
ICAM2	12.31	0.03	0.03	-0.18	-0.16	-0.36	-0.49	-0.23	-6.21	4.63	0.94
ICAM3	1.78	0.57	-2.30	-1.42	-0.10	-0.78	-1.24	-1.73	-2.20	0.75	-0.67
ICAM5	0.26	3.57	2.38	-5.25	-4.63	-1.94	-0.49	-1.81	-2.48	9.00	-0.14
ICOS	0.26	0.03	0.03	-0.18	-0.16	-0.36	-0.49	-0.23	-0.72	-0.28	-0.21
ICOSLG	-4.84	1.09	0.93	-1.89	-0.75	-0.26	-3.47	-3.98	-1.94	3.31	-1.18
ID4	0.65	0.36	4.50	-0.10	2.25	-1.06	-1.11	-0.23	18.34	11.95	3.55
IDO1	-1.60	2.53	8.59	8.28	-0.16	5.33	-0.49	-1.47	-0.72	1.97	2.22
IER3	1.81	-2.41	0.41	-0.65	-0.10	-0.65	-1.19	-1.91	-2.33	2.66	-0.43
IFI16	-1.01	1.55	0.59	-0.93	0.00	-2.35	1.06	-2.04	-2.56	2.82	-0.29

	MesMM98	MesOC99	SiMes1	SiMes4	MMB	Mes1	Mes2	MPP89	MMCA	MesCM98	mFC
IFI27	8.12 <sup>a</sup>	3.98	1.66	0.78	11.22	5.74	0.10	-1.53	-0.34	0.13	<b>2.99<sup>b</sup></b>
IFI35	3.75	2.56	0.16	1.78	-0.41	-2.72	0.83	-3.13	-0.96	0.91	<b>0.28</b>
IFI6	7.55	6.36	0.05	1.63	2.28	-1.22	2.46	-1.89	0.85	1.99	<b>2.01</b>
IFIH1	3.85	3.00	1.40	0.83	1.01	-1.40	1.42	-2.97	-1.55	2.35	<b>0.79</b>
IFIT1	5.28	4.91	0.62	3.39	1.24	-1.53	-3.03	-2.74	-1.84	-0.62	<b>0.57</b>
IFIT2	2.02	0.52	1.34	3.39	3.62	-1.06	-1.37	-2.97	-5.02	-1.29	<b>-0.08</b>
IFIT3	5.15	4.27	1.40	4.42	1.47	-2.59	-0.49	-2.56	-2.53	-0.59	<b>0.79</b>
IFITM1	6.54	5.30	1.29	4.66	7.71	2.41	2.38	-1.27	-0.59	-0.98	<b>2.74</b>
IFITM2	-2.69	-0.83	0.41	1.58	4.42	-1.73	0.96	-1.66	-3.28	-0.52	<b>-0.33</b>
IFNA1	1.40	-0.05	9.39	-7.32	-6.03	2.28	-0.93	-2.07	-7.76	8.72	<b>-0.24</b>
IFNAR1	-0.26	-1.29	0.36	-0.05	0.49	-3.26	-1.03	-3.18	-2.77	-0.03	<b>-1.10</b>
IFNG	-1.53	3.96	0.03	-0.18	-0.16	-7.22	-0.49	-0.23	0.34	-0.28	<b>-0.58</b>
IFNGR1	-0.70	-0.88	1.58	-0.18	-0.03	-1.40	-1.01	-1.78	-0.39	0.03	<b>-0.48</b>
IFNGR2	-0.91	-1.73	1.16	-0.10	1.37	-1.89	-1.53	-1.71	-1.60	-1.86	<b>-0.88</b>
IGF2R	0.13	-1.71	-1.76	-2.07	-0.59	-2.15	-0.91	-2.64	-1.63	0.96	<b>-1.24</b>
IHH	0.26	0.03	0.03	-2.53	1.09	2.59	-7.63	-0.23	-7.24	0.00	<b>-1.37</b>
IKBKB	0.83	0.88	1.84	0.00	0.78	-1.24	-1.86	-2.20	-0.05	-0.28	<b>-0.13</b>
IKBKG	0.65	-0.70	0.70	0.36	-0.05	-1.84	1.29	-2.43	-0.21	1.84	<b>-0.04</b>
IL10	-6.59	-4.19	0.03	-0.18	-0.16	-4.78	-0.49	-0.23	-0.72	4.58	<b>-1.28</b>
IL10RA	0.26	-0.36	0.03	-2.53	-0.16	-0.36	-3.91	-0.23	-0.72	9.28	<b>0.13</b>
IL11	4.89	7.22	1.06	6.00	5.17	-3.18	4.06	-1.50	-2.09	2.69	<b>2.43</b>
IL11RA	0.13	-1.50	2.84	-0.67	0.85	-0.62	3.34	-2.17	-0.91	0.88	<b>0.22</b>
IL12RB2	6.13	7.73	0.03	-0.18	-0.16	-0.36	7.99	-0.23	-0.72	-0.28	<b>1.99</b>
IL15	-0.18	1.19	3.59	0.78	5.09	1.06	-1.32	-2.77	0.52	2.59	<b>1.06</b>
IL16	0.26	0.03	0.03	-0.18	-0.16	-0.36	-0.49	4.97	-0.72	-0.28	<b>0.31</b>
IL17A	0.26	-1.89	0.03	-4.14	-6.47	-0.36	-8.15	-0.23	-0.72	1.97	<b>-1.97</b>
IL18	-1.27	0.28	1.99	-1.89	2.20	-3.44	-0.57	-0.98	0.05	0.78	<b>-0.28</b>
IL18R1	-5.53	-0.59	-1.37	-2.66	-4.14	-2.04	-3.54	-2.95	-3.44	0.52	<b>-2.58</b>
IL1A	4.73	2.64	-0.93	-0.52	1.63	0.88	4.86	-3.00	0.47	3.34	<b>1.41</b>
IL1B	0.98	1.71	-2.84	-1.66	-0.16	-2.46	-0.49	-2.51	-0.39	-0.98	<b>-0.88</b>
IL1R2	9.91	-6.03	0.03	-0.49	-0.16	9.31	-9.70	2.56	0.80	8.92	<b>1.52</b>
IL1RN	0.26	-0.36	0.03	0.62	-0.16	-5.79	-0.49	-6.39	-1.81	2.84	<b>-1.13</b>
IL2	-5.28	0.03	0.03	-0.18	-0.16	-0.36	-0.49	-3.16	2.20	6.10	<b>-0.13</b>
IL21R	0.26	0.03	0.03	-0.18	6.88	-0.36	-0.49	-0.23	-0.72	5.43	<b>1.06</b>
IL22RA1	3.67	-1.66	8.95	-0.18	5.92	-2.69	2.72	-1.89	1.11	6.36	<b>2.23</b>
IL24	0.47	7.73	0.52	8.95	3.85	-5.79	7.06	0.41	10.47	9.28	<b>4.30</b>
IL2RA	0.26	0.03	0.03	-0.18	6.67	-0.36	-0.49	-0.23	-0.72	7.63	<b>1.26</b>
IL2RB	8.59	0.03	0.03	-0.18	-0.16	-0.36	11.28	-2.12	-0.72	4.99	<b>2.14</b>
IL2RG	11.51	15.05	0.03	12.13	3.05	7.71	14.84	-0.23	-0.72	9.00	<b>7.24</b>
IL32	-0.75	4.16	-0.41	-0.96	2.43	0.21	0.28	-2.46	-1.63	6.00	<b>0.69</b>
IL33	-5.90	0.03	-0.36	-2.38	-0.16	-0.36	-0.49	0.26	-5.48	-0.28	<b>-1.51</b>
IL34	-6.67	1.84	2.15	10.03	0.57	-4.16	-2.38	-7.03	0.34	3.83	<b>-0.15</b>

	MesMM98	MesOC99	SiMes1	SiMes4	MMB	Mes1	Mes2	MPP89	MMCA	MesCM98	mFC
IL4	0.26 <sup>a</sup>	-2.74	0.03	-5.25	-0.16	-0.36	-4.32	-0.23	-0.72	-0.28	-1.38 <sup>b</sup>
IL6	4.71	2.87	0.36	-1.09	-2.53	6.18	2.30	-3.23	0.67	10.47	<b>2.07</b>
IL6R	8.38	4.47	5.95	0.03	7.34	-1.19	8.82	-0.23	4.55	8.82	<b>4.69</b>
IL7R	-3.91	2.82	3.41	2.69	4.29	2.48	2.66	-1.50	-0.72	13.11	<b>2.53</b>
INHBA	0.00	2.87	0.44	2.04	10.37	2.07	4.63	-1.50	3.10	5.07	<b>2.91</b>
IRF1	1.16	1.11	0.62	-0.31	0.34	-3.44	-0.28	-2.43	-1.81	-0.18	<b>-0.52</b>
IRF2	-0.47	-0.13	0.83	-0.91	-0.16	-3.26	-0.88	-1.73	-1.71	2.17	<b>-0.62</b>
IRF3	1.32	1.58	0.41	0.47	1.50	0.83	1.40	-2.77	-2.25	2.72	<b>0.52</b>
IRF4	0.26	-6.03	5.66	-0.18	-0.16	-2.53	-2.59	-3.57	2.20	-0.28	<b>-0.72</b>
IRF5	-5.90	-0.80	6.65	-1.29	0.34	-3.00	-0.98	0.57	-3.21	6.10	<b>-0.15</b>
IRF7	4.19	3.39	-1.32	2.20	4.32	6.08	3.49	-4.50	-2.28	3.52	<b>1.91</b>
IRF8	0.26	5.53	0.03	1.58	-0.16	-0.36	4.89	-0.36	-0.72	-0.28	<b>1.04</b>
IRF9	2.59	1.94	0.36	-0.85	0.39	-2.82	-0.85	-3.00	0.16	3.49	<b>0.14</b>
ISG15	9.93	5.51	0.67	5.64	4.63	-0.78	1.27	-1.78	-2.72	0.57	<b>2.29</b>
ITGA1	-2.69	6.62	1.45	5.66	-0.16	-0.36	8.82	-1.24	6.70	1.76	<b>2.66</b>
ITGA2	0.98	-0.49	0.08	2.35	2.25	-3.28	-0.83	-1.55	-2.22	-0.23	<b>-0.29</b>
ITGA4	7.68	3.18	3.98	-0.18	10.37	3.70	8.92	-1.40	-0.72	5.43	<b>4.10</b>
ITGA6	-0.80	0.72	-1.09	3.44	2.51	-1.68	4.29	-2.09	-2.95	-1.94	<b>0.04</b>
ITGAE	-0.93	-2.82	-1.11	-0.41	-0.10	-2.82	0.93	-3.26	-1.37	0.10	<b>-1.18</b>
ITGAL	0.26	0.03	0.03	-0.18	-0.16	-0.36	-0.49	-0.23	-0.72	-0.28	<b>-0.21</b>
ITGAM	0.26	0.03	0.03	-4.14	-3.44	6.83	-3.91	-0.23	-0.72	4.58	<b>-0.07</b>
ITGAV	-1.32	-0.80	0.85	0.13	0.10	-0.41	-0.23	-2.72	-1.06	0.75	<b>-0.47</b>
ITGAX	-1.94	4.27	-8.64	-2.77	-0.85	3.72	-1.09	-0.59	-5.48	-0.28	<b>-1.37</b>
ITGB2	2.07	0.88	0.23	-0.70	11.61	4.91	0.54	-1.40	5.09	3.39	<b>2.66</b>
ITGB3	-3.49	-3.96	4.29	0.62	3.36	-3.03	0.62	-0.85	-1.34	-4.97	<b>-0.87</b>
ITGB8	-0.91	-1.14	6.23	0.10	2.20	-0.18	5.64	-1.11	-2.46	2.64	<b>1.10</b>
ITPK1	-0.16	-1.71	0.13	-1.60	-0.47	-2.43	-0.26	-2.07	-2.33	-0.36	<b>-1.13</b>
JAG1	2.48	0.36	1.40	3.41	0.49	0.80	1.55	-3.57	-2.87	0.65	<b>0.47</b>
JAG2	0.26	-2.07	5.09	-4.14	5.28	-1.06	-0.49	8.61	-4.94	-6.72	<b>-0.02</b>
JAK1	-1.81	-0.80	0.44	-0.93	-0.03	-1.97	-0.16	-2.07	-2.28	-1.03	<b>-1.06</b>
JAK2	0.08	-0.21	1.97	1.01	0.23	-1.14	0.78	-1.91	-0.23	-0.49	<b>0.01</b>
JAK3	0.26	0.03	2.38	-0.18	-0.16	-0.36	3.98	-0.21	8.69	-0.28	<b>1.41</b>
KAT2B	0.96	-1.22	1.78	0.21	-0.80	-2.22	-1.19	-3.31	1.53	3.70	<b>-0.06</b>
KDR	-1.53	0.78	7.73	-0.13	2.53	0.62	-2.46	2.02	-0.72	-0.28	<b>0.86</b>
KIF2C	-1.81	-2.51	1.16	0.85	1.68	-2.17	4.34	-0.54	3.52	2.69	<b>0.72</b>
KIR2DL3	-6.00	-2.74	-5.38	-0.18	-0.16	-1.29	-0.49	-4.55	-0.72	-0.28	<b>-2.18</b>
KIR3DL1	0.26	0.03	0.03	-0.18	7.68	5.64	-0.49	-0.23	2.20	4.58	<b>1.95</b>
KIR3DL2	0.26	0.03	0.03	-0.18	-0.16	-0.36	-0.49	-0.23	-0.72	-0.28	<b>-0.21</b>
KIT	7.68	0.41	0.03	9.80	10.97	4.60	6.23	-3.91	3.41	1.97	<b>4.12</b>
KLRB1	0.26	0.03	-5.38	-0.18	-0.16	-0.36	-0.49	-0.23	-0.72	-0.28	<b>-0.75</b>
KLRD1	0.26	-2.72	1.19	-3.03	-6.47	-0.36	-0.49	-5.46	0.34	-0.28	<b>-1.70</b>
KLRK1	0.26	0.03	0.03	-0.18	-0.16	-0.36	-0.49	-0.23	-0.72	2.61	<b>0.08</b>

	MesMM98	MesOC99	SiMes1	SiMes4	MMB	Mes1	Mes2	MPP89	MMCA	MesCM98	mFC
KRAS	-0.70 <sup>a</sup>	-1.89	-0.41	0.08	0.34	-1.45	0.98	-1.27	-0.23	-0.36	<b>-0.49<sup>b</sup></b>
LAG3	4.63	1.94	6.10	1.06	9.67	1.58	-3.93	-0.39	-3.10	0.23	<b>1.78</b>
LAIR1	0.26	0.03	9.85	-0.18	-0.16	-9.39	-0.49	-0.23	-0.72	4.58	<b>0.35</b>
LAMA1	2.20	1.14	0.39	1.19	1.40	-2.95	3.52	-2.28	0.18	-2.17	<b>0.26</b>
LAMB3	1.81	6.36	4.45	7.37	13.11	3.28	6.96	-2.92	-4.89	-0.65	<b>3.49</b>
LAMC2	-1.76	5.97	-0.49	0.96	12.34	1.73	4.71	-2.20	-5.04	-1.11	<b>1.51</b>
LCK	4.09	-2.72	0.03	-2.59	-0.26	2.59	4.16	2.07	0.34	3.16	<b>1.09</b>
LDHA	0.75	-1.60	1.53	1.29	-0.26	-2.66	-0.28	-1.22	-2.95	0.67	<b>-0.47</b>
LDHB	-0.05	-1.53	0.67	-0.52	-0.26	-3.00	-1.29	-1.27	-1.86	-0.08	<b>-0.92</b>
LGALS9	0.26	11.35	3.98	-0.18	-0.16	-0.36	-0.49	-0.85	-2.35	-0.23	<b>1.10</b>
LIF	0.16	-0.67	-0.93	-1.37	0.26	-1.78	-2.84	-2.48	-3.31	0.18	<b>-1.28</b>
LILRA1	0.26	-4.19	0.03	-4.97	4.32	-2.53	-2.77	-0.23	-6.41	-0.28	<b>-1.68</b>
LILRA3	-4.50	2.28	0.03	-7.89	-0.80	2.56	-2.20	-0.85	-5.17	-1.37	<b>-1.79</b>
LILRA5	0.26	0.03	2.38	-7.37	5.28	3.91	-0.49	-0.23	-0.72	-0.28	<b>0.27</b>
LILRB2	0.26	-4.19	0.03	-0.18	-0.16	0.54	-0.49	-0.23	-0.72	-0.28	<b>-0.54</b>
LILRB4	0.26	0.03	0.03	-0.18	-0.16	-0.36	-0.49	-0.23	-0.72	-0.28	<b>-0.21</b>
LOXL2	-2.30	-1.66	-0.57	-2.64	-2.59	-3.39	-0.49	-1.86	9.31	-2.09	<b>-0.83</b>
LRRC32	2.61	-0.13	0.03	-11.87	2.09	5.33	-6.10	3.16	-6.41	7.19	<b>-0.41</b>
LTB	0.26	4.97	3.62	0.57	8.46	-0.36	0.67	1.45	-0.72	-0.28	<b>1.86</b>
LTBP1	-0.75	-6.59	-0.85	-0.80	-0.28	-2.04	1.60	-2.30	-1.55	2.30	<b>-1.13</b>
LY9	0.26	-0.36	0.03	-0.18	-0.16	-0.36	-0.49	-6.39	-0.72	1.81	<b>-0.66</b>
LY96	-4.34	10.11	2.04	1.27	4.55	-1.16	6.00	-1.53	-0.72	12.00	<b>2.82</b>
LYZ	-5.28	-1.01	0.03	-0.18	-0.16	-0.36	-0.49	-0.23	-0.72	-0.28	<b>-0.87</b>
MAGEA1	1.94	0.80	12.83	15.21	17.46	0.88	6.96	-1.66	8.43	10.55	<b>7.34</b>
MAGEA12	2.72	6.88	0.03	8.28	9.67	2.59	10.97	-1.53	12.31	2.51	<b>5.44</b>
MAGEA3/A6	0.72	3.85	3.98	11.84	16.76	8.09	16.81	-2.12	-2.64	0.18	<b>5.75</b>
MAGEA4	19.73	16.32	10.11	14.84	15.93	9.57	13.34	-0.23	15.62	15.41	<b>13.07</b>
MAGEB2	8.17	18.70	11.30	6.65	18.44	14.51	16.63	-0.57	16.58	20.53	<b>13.09</b>
MAGEC1	5.61	10.11	0.03	-0.18	6.67	-0.36	-0.49	-0.23	9.39	6.10	<b>3.66</b>
MAGEC2	0.88	17.38	0.03	17.53	16.22	12.88	10.97	-9.85	16.58	18.10	<b>10.07</b>
MAML2	-1.84	-2.41	1.32	-1.89	-0.28	-1.60	1.60	-2.02	-1.99	-1.16	<b>-1.03</b>
MAP3K12	-0.96	0.18	6.47	-2.53	2.15	2.59	7.99	-11.07	-0.72	-0.28	<b>0.38</b>
MAP3K5	-0.57	2.07	0.96	-0.49	1.32	-1.42	-0.41	-1.68	1.37	-0.67	<b>0.05</b>
MAP3K7	0.13	-0.23	0.36	0.21	0.03	-2.25	0.26	-2.41	-2.56	-0.78	<b>-0.72</b>
MAP3K8	-3.57	-0.88	2.59	-2.12	-0.83	-3.31	-1.66	-0.49	-0.98	3.10	<b>-0.81</b>
MAPK10	0.26	0.03	0.03	-6.10	1.09	-0.36	-0.49	-0.23	-5.33	2.97	<b>-0.81</b>
MARCO	1.73	0.03	4.78	10.03	3.05	-0.36	5.35	-0.23	6.72	9.52	<b>4.06</b>
MB21D1	2.02	-0.10	1.32	12.26	1.60	-0.18	1.78	-2.07	-2.17	-0.36	<b>1.41</b>
MELK	-1.29	-3.39	-0.05	-0.31	2.09	-2.59	2.51	-2.25	2.74	0.88	<b>-0.17</b>
MET	0.05	0.83	0.21	1.34	3.34	1.01	4.19	-1.37	-1.94	0.59	<b>0.83</b>
MFGE8	0.75	0.72	2.07	1.11	3.13	-1.09	4.03	-1.53	-1.66	1.89	<b>0.94</b>
MFNG	5.69	-2.74	5.09	2.22	6.67	-1.29	2.77	-0.23	-1.34	-2.92	<b>1.39</b>

	MesMM98	MesOC99	SiMes1	SiMes4	MMB	Mes1	Mes2	MPP89	MMCA	MesCM98	mFC
MGMT	-1.22 <sup>a</sup>	-3.41	-1.34	-3.36	-1.45	-3.21	-1.84	-1.91	-3.83	-0.05	-2.16 <sup>b</sup>
MICA	-0.23	-0.67	1.24	0.57	1.34	-2.79	0.72	-0.75	-0.49	1.84	0.08
MICB	4.60	2.87	0.98	1.81	2.12	-1.47	5.17	-0.78	3.03	1.66	2.00
MKI67	-2.97	-4.58	1.89	0.62	1.58	-1.89	3.31	-0.88	3.70	0.54	0.13
MLANA	0.26	3.96	0.03	-0.18	-0.16	-0.36	-0.49	-0.23	-0.72	4.58	0.67
MLH1	-0.57	-0.91	0.80	-1.03	0.75	-1.27	0.96	-2.95	-2.02	2.15	-0.41
MMP1	2.07	16.37	9.57	15.21	9.67	-0.36	18.85	-1.42	-0.72	-0.28	6.89
MMP7	0.13	0.03	0.03	-0.18	-0.16	-0.36	-0.49	-0.23	0.34	-4.63	-0.55
MMP9	7.60	-8.59	6.65	3.75	-0.18	-0.36	1.45	-5.48	4.34	8.02	1.72
MMRN2	-1.58	0.03	0.03	-0.18	7.22	-3.44	-4.32	-0.23	-1.42	2.15	-0.18
MRC1	0.26	0.03	0.03	-0.18	1.09	-0.03	-2.66	-0.23	4.34	5.43	0.81
MRE11	-0.75	-1.63	1.34	0.08	0.98	-0.98	1.16	-1.94	-1.53	1.66	-0.16
MS4A1	0.70	-4.97	-10.58	-7.37	-8.51	-1.06	-9.00	-0.23	0.00	-1.55	-4.26
MS4A2	0.26	0.03	0.03	-0.18	-0.16	-0.36	-0.49	-0.23	-0.72	-0.28	-0.21
MS4A4A	-7.97	0.03	0.03	-0.18	-4.45	-4.78	-5.46	-0.23	12.41	9.54	-0.11
MS4A6A	0.26	-2.74	0.03	-0.18	1.09	-0.36	-0.49	4.97	-0.72	-0.28	0.16
MSH2	1.09	-2.35	0.98	-0.23	1.68	-2.92	1.45	-1.99	-0.70	5.33	0.23
MSH6	-1.22	-2.20	0.00	-0.13	0.83	-2.30	1.11	-1.66	-0.54	0.59	-0.55
MTOR	0.47	-1.34	0.08	-1.32	0.36	-1.94	-0.36	-0.41	-1.55	-0.28	-0.63
MX1	17.35	4.42	0.75	3.36	2.25	-2.59	0.47	-4.16	1.53	4.03	2.74
MXI1	-1.19	-0.52	-0.10	-1.19	-0.26	-0.96	0.39	-3.28	-3.05	0.36	-0.98
MYC	-2.56	-1.47	-0.54	-2.15	-0.54	-2.77	-0.88	-2.46	-3.96	-1.09	-1.84
MYCT1	-3.23	-2.74	0.03	-0.18	-0.16	-0.36	-0.49	-0.23	-0.72	-0.28	-0.84
MYD88	0.54	0.80	0.57	0.18	1.71	-0.31	0.75	-1.63	-5.02	-0.08	-0.25
NBN	-1.42	-0.88	1.27	-1.42	0.08	-0.52	-0.65	-2.46	-1.11	0.36	-0.68
NCAM1	-4.58	-2.82	0.03	-0.59	-2.53	-2.04	-0.49	-3.98	-0.72	-0.28	-1.80
NCR1	0.26	0.03	0.03	-0.18	-0.16	-0.36	-0.49	-0.23	-0.72	-0.28	-0.21
NDUFA4L2	0.26	1.16	-3.05	-0.18	2.56	3.91	-0.49	-0.23	-0.72	-0.28	0.29
NECTIN1	2.02	1.89	2.79	2.15	1.66	-2.48	1.91	-1.19	-0.85	-1.50	0.64
NECTIN2	-0.08	-0.28	0.49	-0.49	1.16	-2.79	-1.42	-1.66	-2.77	0.31	-0.75
NEIL1	2.77	-5.07	-0.93	-0.18	-0.16	1.91	1.78	-2.17	0.85	2.97	0.18
NF1	-1.03	-1.76	0.18	-0.34	-0.05	-2.41	0.13	-1.86	-2.02	0.18	-0.90
NFAM1	0.26	0.03	0.03	-0.18	-0.16	-0.36	-0.49	-0.23	-0.72	-0.28	-0.21
NFATC2	6.44	2.20	3.41	6.36	12.80	-1.50	6.00	-2.56	3.34	13.55	5.00
NFIL3	-0.41	-0.85	-0.98	-1.40	-0.62	-0.85	0.67	-2.25	-1.50	0.05	-0.81
NFKB1	-0.59	-0.31	0.59	-1.68	0.44	-1.99	-0.52	-3.59	-2.09	-0.08	-0.98
NFKB2	1.27	0.70	0.65	-0.70	0.96	-2.15	-0.80	-2.46	-2.59	1.86	-0.33
NFKBIA	-0.34	0.39	1.50	0.13	1.32	-2.17	-1.50	-1.76	-0.93	-0.08	-0.34
NFKBIE	1.40	0.49	0.31	-0.34	0.18	-0.93	-0.62	-3.05	-2.43	0.72	-0.43
NGFR	13.16	13.11	8.59	2.02	9.13	-0.36	1.45	-0.23	10.94	-1.60	5.62
NID2	-2.53	5.07	7.22	12.49	-0.18	6.83	-0.34	1.01	14.97	16.11	6.06
NKG7	0.26	0.03	0.03	-0.18	-0.16	-0.36	-0.49	1.94	-0.72	-0.28	0.01

	MesMM98	MesOC99	SiMes1	SiMes4	MMB	Mes1	Mes2	MPP89	MMCA	MesCM98	mFC
NLRC5	1.22 <sup>a</sup>	-0.39	3.54	0.59	3.00	-2.04	-0.52	-0.85	0.44	1.29	0.63 <sup>b</sup>
NLRP3	1.27	0.03	0.03	3.75	-0.16	-0.36	-0.49	-2.20	-2.20	-0.34	-0.07
NOD2	7.11	-7.27	5.95	-0.18	5.28	-2.53	-0.52	-0.49	8.69	4.66	2.07
NOS2	0.26	0.03	0.03	-0.18	-0.16	-0.36	-0.49	-0.23	-0.72	-0.28	-0.21
NOTCH1	2.43	2.04	3.28	-0.54	2.48	1.34	-0.28	-3.78	-4.68	-0.52	0.18
NOTCH2	-3.00	-2.74	-0.16	-1.63	-0.08	-3.28	-1.29	-2.53	-2.87	-1.27	-1.89
NRAS	-0.21	-0.80	0.26	0.28	0.03	-1.99	0.93	-1.91	-2.04	-1.11	-0.66
NT5E	-1.09	1.03	0.65	1.09	2.30	-1.29	-0.62	-1.24	-0.34	0.65	0.11
OAS1	4.84	5.66	0.59	3.34	-0.16	-1.11	0.08	-3.00	-2.97	2.69	1.00
OAS2	4.91	7.03	0.78	12.39	-0.16	-1.99	-0.98	-2.72	-0.65	0.26	1.89
OAS3	7.89	3.54	0.62	1.68	2.46	-1.58	1.94	-2.33	-2.09	1.45	1.36
OASL	9.72	-0.44	0.28	5.66	12.80	-5.38	-3.54	-1.78	-1.32	3.62	1.96
OLFML2B	-1.29	-3.13	0.03	-4.14	-5.20	-3.70	-0.49	-0.23	5.09	-0.28	-1.33
OLR1	1.94	3.10	2.97	4.68	2.69	-3.08	0.96	-0.70	-0.13	2.07	1.45
OTOA	0.26	-6.03	0.03	-0.18	-0.16	-0.36	-0.49	-0.23	-0.72	-0.28	-0.82
P2RY13	0.26	0.03	0.03	-0.18	-0.16	-0.36	-0.49	-0.23	-0.72	-0.28	-0.21
P4HA1	0.88	-0.31	1.55	0.98	1.45	-1.94	1.16	-1.73	0.47	0.75	0.33
P4HA2	-0.44	0.23	-0.31	1.34	0.59	-2.20	1.16	-1.97	-0.80	1.22	-0.12
PALMD	0.26	0.03	0.03	-0.18	-0.16	-0.36	-0.49	0.44	0.03	4.47	0.41
PARP12	3.83	3.44	0.91	0.98	1.32	-1.97	0.57	-2.35	-0.05	0.72	0.74
PARP4	-0.80	-0.70	0.49	-0.65	-0.08	-1.94	-0.34	-2.17	-0.65	0.85	-0.60
PARP9	2.72	2.17	1.06	0.59	1.63	-2.38	0.28	-2.46	-1.71	-0.31	0.16
PC	-3.36	-1.32	9.62	2.64	10.16	2.09	-0.93	-0.08	-0.36	2.82	2.13
PCK2	-4.34	-2.12	-2.02	-3.13	0.05	-0.47	-0.39	-4.22	-2.41	-2.28	-2.13
PDCD1	0.26	6.83	0.03	5.66	3.05	3.91	-0.49	-0.23	-0.72	-2.28	1.60
PDCD1LG2	-1.37	1.06	-0.16	1.14	2.28	-1.45	4.34	-1.76	-2.33	-0.13	0.16
PDGFA	0.91	-0.62	-1.03	-0.21	0.52	-0.34	1.94	-1.97	-0.67	5.84	0.44
PDGFB	-9.26	-7.73	3.65	0.91	-0.39	-0.26	-2.48	-1.58	-2.46	-5.38	-2.50
PDGFRB	-3.98	-4.78	3.98	3.83	2.02	-0.96	3.57	-1.84	5.72	-1.73	0.58
PDK1	-0.13	-0.72	1.01	-0.03	0.00	-2.07	1.45	-1.42	-1.73	1.22	-0.24
PDZK1IP1	2.61	0.03	3.52	-1.34	-0.18	0.54	-2.33	-0.23	6.21	0.59	0.94
PECAM1	12.31	3.70	6.65	14.15	-0.16	-0.36	-0.49	1.66	2.20	9.00	4.86
PF4	-5.28	-0.36	0.03	-2.53	-0.16	3.91	-6.34	-0.23	2.20	1.97	-0.68
PFKFB3	3.21	1.66	1.40	0.36	2.02	1.94	2.43	-1.42	-0.88	2.09	1.28
PFKM	-1.42	-1.68	0.28	-3.23	-1.16	-3.03	-3.08	-3.23	-1.32	0.65	-1.72
PGPEP1	2.04	1.32	-1.16	0.67	-0.98	-0.36	-1.53	-4.89	-1.32	2.53	-0.37
PIAS4	-0.47	-0.47	0.41	0.00	0.16	-2.59	0.78	-1.22	-1.42	1.86	-0.29
PIK3CA	-1.32	-0.67	0.93	0.31	0.23	-1.86	0.83	-2.46	-2.02	-1.42	-0.74
PIK3CD	0.31	2.33	-0.78	-1.40	-0.05	-3.96	0.18	-2.87	-0.34	3.05	-0.35
PIK3CG	7.99	0.03	0.03	-6.10	6.03	2.59	-0.49	-1.14	3.96	1.97	1.48
PIK3R1	-1.76	-2.07	0.34	1.42	1.24	-0.34	0.26	-2.59	0.57	-0.31	-0.32
PIK3R2	-2.43	-1.86	0.47	-2.72	-0.57	-3.47	-1.37	-3.34	-1.78	0.93	-1.61

	MesMM98	MesOC99	SiMes1	SiMes4	MMB	Mes1	Mes2	MPP89	MMCA	MesCM98	mFC
PIK3R5	4.68 <sup>a</sup>	0.03	0.03	-0.18	-0.16	-0.36	-0.49	-1.68	-0.72	-0.28	0.09 <sup>b</sup>
PKM	-0.10	-0.26	0.00	0.10	-0.18	-2.56	-1.37	-1.71	-1.50	-0.41	-0.80
PLA1A	0.26	2.33	0.03	-0.18	3.05	-0.36	-0.49	-0.23	5.09	1.97	1.15
PLA2G2A	0.26	-0.36	0.03	-0.18	-0.16	2.59	0.98	-0.23	3.41	-0.28	0.61
PLOD2	-1.14	-2.02	1.73	1.03	-0.23	-1.42	0.28	-1.76	0.08	1.40	-0.20
PMS2	-1.14	-0.93	-0.52	-1.50	-0.36	-2.66	0.16	-2.20	-1.27	0.00	-1.04
PNOC	-7.11	-6.70	-4.47	-7.60	-0.16	4.86	-1.89	4.97	5.72	4.58	-0.78
POLD1	0.96	-3.59	3.34	-1.19	2.53	-0.23	0.91	-1.55	-0.36	3.54	0.43
PPARG	-0.96	-1.86	-2.90	-2.48	-0.16	-6.21	1.60	-2.66	15.28	17.02	1.67
PPARGC1B	0.31	1.60	-0.98	1.76	-1.91	-7.01	-1.68	-8.33	5.72	-2.20	-1.27
PRF1	0.26	0.03	0.03	-0.18	-0.16	-0.36	-0.49	-0.23	-0.72	-0.28	-0.21
PRKAA2	1.11	-0.39	1.97	-0.28	0.52	-0.96	-0.13	-4.91	-0.72	-0.28	-0.41
PRKACB	-2.43	-2.22	1.86	0.21	-0.57	-2.46	0.05	-1.76	-0.85	2.30	-0.59
PRKCA	-0.80	-2.82	0.28	-2.46	-1.32	-3.39	-0.59	-2.20	-2.97	-0.08	-1.63
PRKX	-3.23	-0.13	0.03	-6.80	-0.16	7.16	-0.49	-0.23	-0.72	-0.28	-0.49
PRLR	1.16	2.33	7.73	8.28	-0.16	-0.36	-0.49	-0.18	-0.72	-0.28	1.73
PROM1	0.26	9.57	0.03	-0.18	8.09	6.83	13.34	-0.23	0.34	-0.28	3.78
PRR5	-2.79	-0.18	1.73	-0.80	1.40	-3.28	0.23	-2.66	-1.19	0.59	-0.70
PSMB10	0.49	0.05	1.55	-0.49	1.03	-2.22	-0.54	-3.03	-5.07	-2.09	-1.03
PSMB5	-0.13	-0.85	0.91	-0.67	0.34	-1.84	-0.70	-1.03	-1.47	0.47	-0.50
PSMB8	1.24	0.54	0.31	-1.99	0.00	-2.43	-0.21	-2.77	-2.07	0.80	-0.66
PSMB9	-0.44	2.61	0.93	-0.96	0.67	-3.31	-1.29	-1.94	-2.28	0.34	-0.57
PTCD2	-0.49	-0.18	-1.19	-2.61	-0.41	-0.78	-0.72	-3.05	-2.72	-1.09	-1.32
PTEN	-0.67	-1.40	1.53	-0.16	-0.10	-1.16	0.16	-2.38	-2.20	-0.80	-0.72
PTGER4	1.19	-1.16	0.03	0.44	4.32	-1.50	-0.49	-1.09	-3.93	5.33	0.31
PTGS2	0.91	-0.49	8.92	1.14	6.57	-0.34	-0.10	-2.17	-5.35	-1.24	0.78
PTPN11	-1.06	-1.42	0.34	-1.24	-0.13	-1.55	0.21	-2.04	-2.17	-0.49	-0.96
PTPRC	0.26	-2.74	0.03	-6.10	-0.16	-0.36	-7.03	-0.23	-0.72	6.70	-1.04
PVR	-1.27	0.34	-0.67	-2.48	1.16	-1.78	0.85	-1.60	-1.86	0.39	-0.69
PVRIG	-6.00	3.21	2.74	0.03	9.93	4.63	0.67	1.47	1.99	3.78	2.24
RAD50	-0.98	-1.97	0.88	-1.19	0.31	0.08	0.88	-2.51	-1.84	0.78	-0.56
RAD51	-1.06	-3.62	-0.05	0.39	3.28	-2.20	3.72	-1.24	3.93	4.50	0.77
RAD51C	0.85	-0.91	-0.98	-1.60	0.54	-1.66	0.83	-2.87	-2.64	0.67	-0.78
RASAL1	5.22	0.78	0.03	1.53	5.53	-3.44	7.01	-5.59	3.67	8.46	2.32
RASGRF1	11.72	12.03	15.78	8.66	6.65	3.49	12.80	-3.00	2.72	3.16	7.40
RB1	-0.03	-2.28	0.65	-0.44	-0.28	-2.20	0.10	-1.66	-1.86	-0.47	-0.85
RBL2	0.16	0.44	1.50	0.65	0.52	-2.15	-0.26	-1.24	0.00	1.09	0.07
RELA	-0.28	-0.26	-0.39	-0.96	0.08	-1.55	-0.08	-2.07	-2.15	-0.39	-0.80
RELB	1.24	1.60	0.08	-1.22	0.85	-1.97	-0.41	-3.08	-1.78	1.37	-0.33
RELN	-1.53	3.85	0.03	0.31	-0.16	-0.49	7.63	-6.44	-0.72	-0.28	0.22
REN	10.89	0.03	0.03	-0.18	-0.16	-0.36	-0.49	-0.23	11.07	8.72	2.93
RICTOR	-1.22	-0.98	0.91	0.21	0.49	-1.66	-0.10	-1.71	-1.40	-1.14	-0.66

	MesMM98	MesOC99	SiMes1	SiMes4	MMB	Mes1	Mes2	MPP89	MMCA	MesCM98	mFC
RIPK1	1.01 <sup>a</sup>	0.00	0.16	-0.34	0.67	-1.29	-0.18	-1.60	-1.73	-0.65	-0.40 <sup>b</sup>
RIPK2	-1.01	1.76	0.00	-1.47	0.49	-3.13	-0.23	-3.21	-1.14	1.73	-0.62
RIPK3	0.26	0.03	0.03	-0.18	-0.16	-0.36	-0.49	-0.23	-4.29	-0.28	-0.57
RNLS	8.95	5.92	3.59	0.59	1.32	-0.21	1.47	-0.21	11.07	9.28	4.18
ROBO4	0.26	3.96	0.03	5.66	12.21	-0.36	12.62	-4.66	-0.72	-0.28	2.87
ROCK1	-0.98	-1.42	1.03	1.03	0.13	-0.83	0.26	-2.59	-1.78	-0.78	-0.59
ROR2	-1.32	-0.72	0.54	-3.31	-0.16	-1.63	7.22	-3.05	-0.72	4.58	0.14
RORC	-6.00	0.03	0.03	-0.18	1.29	4.86	-7.55	-0.23	-0.72	-0.28	-0.88
RPL23	-2.74	-1.32	0.00	-0.54	0.34	-2.69	-1.86	-2.17	-2.30	-0.54	-1.38
RPL7A	-2.41	-1.60	0.39	-0.62	0.39	-2.41	-1.47	-1.58	-3.13	-1.01	-1.34
RPS6KB1	-0.44	-1.14	1.19	0.28	0.34	-1.78	0.16	-1.89	-2.09	0.10	-0.53
RPTOR	0.18	-1.27	0.49	-4.22	-0.28	-3.88	-2.04	-2.90	-3.34	-1.19	-1.84
RRM2	0.34	-3.65	3.00	1.01	3.62	-1.58	3.52	-1.50	5.33	4.14	1.42
RSAD2	5.90	2.59	1.34	1.97	4.24	-2.66	-1.45	-2.38	-0.34	0.57	0.98
RUNX3	13.11	11.53	0.03	-0.18	0.26	-0.41	0.21	-2.53	-0.72	-0.28	2.10
S100A12	0.26	5.92	0.03	-2.53	-0.16	-0.36	-0.49	-0.23	-0.72	-0.28	0.14
S100A8	0.26	0.03	0.03	-0.18	-0.16	-0.36	1.81	-0.23	13.29	12.70	2.72
S100A9	0.26	6.62	2.38	13.45	-0.16	2.59	-0.49	2.35	4.19	1.76	3.29
SAMD9	0.88	2.64	2.48	1.89	0.70	0.72	1.84	-1.76	-4.58	1.55	0.64
SAMSN1	-12.39	-0.36	5.09	-0.18	1.09	-0.36	-0.49	-1.73	-0.72	1.97	-0.81
SBNO2	-0.75	-0.31	0.18	-2.25	0.47	-2.87	-2.17	-2.30	-2.30	0.16	-1.22
SELE	0.26	0.03	-5.38	-0.18	-0.16	-0.36	-0.49	-0.23	-0.72	-0.28	-0.75
SELL	0.26	0.03	0.03	-0.18	-0.16	-0.36	0.98	-0.23	-0.72	-0.28	-0.06
SELP	0.26	-5.22	-0.93	-2.53	-0.16	2.59	-0.49	-0.23	2.20	8.02	0.35
SERPINA1	7.42	3.18	15.05	9.18	10.37	-2.79	15.31	-1.68	16.42	8.33	8.08
SERPINB5	11.33	18.41	11.48	8.43	-0.16	5.09	-0.93	-0.57	-2.53	-1.47	4.91
SERPINH1	-4.40	-2.56	-0.26	-1.55	-0.23	-2.09	-0.16	-1.99	-3.18	1.03	-1.54
SFRP1	2.64	-1.94	2.84	3.08	6.67	-2.41	10.09	-1.84	1.19	0.41	2.07
SFRP4	0.26	6.62	0.03	10.03	-0.16	2.59	-0.49	-0.23	-0.72	-0.28	1.76
SFXN1	0.08	-1.19	0.34	0.36	0.62	-2.82	0.23	-1.29	-0.72	-0.08	-0.45
SGK1	1.27	-1.22	-0.70	2.28	1.06	-0.54	2.79	-1.53	1.29	0.96	0.57
SH2D1A	-1.53	0.03	0.03	-0.18	3.05	3.91	-0.49	-0.23	0.34	-0.28	0.46
SHC2	10.37	-2.41	0.28	-3.00	-1.68	-4.29	-0.93	-2.20	-0.72	-0.28	-0.49
SIGLEC1	-3.23	7.73	0.03	-4.14	1.09	-0.54	-4.32	-0.23	5.09	-0.28	0.12
SIGLEC5	0.26	0.03	0.03	-0.18	-0.16	-0.36	-0.49	-0.23	-0.72	-0.28	-0.21
SIGLEC8	0.26	0.03	0.03	-0.18	-0.16	-0.36	-4.32	-0.23	-0.72	-10.06	-1.57
SIRPA	-2.22	-1.86	1.47	-1.47	1.68	-0.83	0.31	-1.86	-3.44	-1.66	-0.99
SIRPB2	9.62	0.03	0.03	-0.18	-0.16	-0.36	-0.49	-0.23	0.59	5.95	1.48
SLAMF7	0.57	3.57	-2.25	2.22	9.13	0.85	0.85	8.92	-2.64	2.79	2.40
SLC11A1	-6.00	5.07	-6.18	-0.18	-0.16	-0.36	-0.49	-0.23	-8.07	6.10	-1.05
SLC16A1	0.41	-0.57	1.06	-0.98	0.21	-2.30	0.10	-1.91	-1.94	-0.08	-0.60
SLC1A5	-3.78	-1.78	-2.09	-3.16	-0.05	-1.53	-1.16	-3.26	-3.62	-1.71	-2.21

	MesMM98	MesOC99	SiMes1	SiMes4	MMB	Mes1	Mes2	MPP89	MMCA	MesCM98	mFC
SLC2A1	3.70 <sup>a</sup>	-0.13	2.66	0.98	-0.98	-0.80	2.35	-1.09	-0.10	0.00	0.66 <sup>b</sup>
SLC7A5	-0.39	-1.37	-1.11	-3.54	-1.29	-2.33	-0.16	-3.93	-4.58	-3.10	-2.18
SMAD5	-1.29	-1.32	1.16	-0.62	0.28	-2.38	0.57	-2.64	-1.86	-1.53	-0.96
SMAP1	0.10	-1.32	-0.16	-0.39	0.62	-2.77	0.26	-2.02	-1.34	1.24	-0.58
SNAI1	1.32	2.95	1.47	0.36	1.55	-1.55	2.25	-0.05	0.85	5.35	1.45
SNCA	1.24	-1.76	0.85	0.54	-0.75	-4.78	-2.33	-1.86	-0.72	-0.28	-0.99
SOCS1	2.15	1.99	2.64	1.89	7.27	5.35	1.09	-2.74	-1.09	2.25	2.08
SOX10	0.26	0.03	0.03	-0.18	-0.16	-0.36	-0.49	-0.23	-0.72	3.52	0.17
SOX11	1.27	-4.84	5.09	-1.40	-0.39	-4.60	2.84	-0.23	2.20	-0.28	-0.03
SOX2	0.26	0.03	0.03	-2.53	-0.16	-0.36	-0.49	-0.23	-0.72	6.10	0.19
SPIB	0.26	0.03	0.03	-0.18	4.32	-0.36	7.22	-0.23	-0.72	-0.28	1.01
SPP1	4.78	14.61	0.03	7.27	-0.16	-0.36	-0.49	-0.83	-0.72	-0.28	2.38
SPRY4	3.96	-0.41	-1.71	3.65	7.01	-1.53	0.28	-1.37	-2.22	-1.14	0.65
SREBF1	1.14	-0.96	0.75	-0.57	-0.10	-2.30	-1.60	-2.74	-2.15	0.10	-0.84
SRP54	1.50	0.21	0.80	0.85	0.88	-1.37	1.76	-1.06	-2.02	0.88	0.24
STAT1	4.19	0.72	0.85	1.01	0.34	-1.55	0.31	-2.51	-0.80	3.00	0.56
STAT2	0.21	1.29	0.67	-1.14	0.31	-2.79	-0.23	-1.86	-2.17	0.72	-0.50
STAT3	0.44	-0.10	2.02	0.49	0.70	-2.43	0.03	-1.55	-1.27	0.18	-0.15
STAT4	4.03	-0.03	3.16	-0.18	3.93	-0.36	9.44	-4.97	2.30	0.52	1.78
STC1	4.24	6.62	4.94	2.22	-0.16	-4.50	-0.49	-0.54	4.37	11.30	2.80
SYK	0.26	0.03	0.03	10.86	-0.16	-0.36	-0.49	-0.23	-0.80	3.44	1.26
TAF3	0.93	-2.04	-3.03	-2.09	0.21	-3.54	0.98	-4.78	1.34	7.71	-0.43
TAP1	3.75	3.52	1.11	1.19	1.06	-3.28	-1.09	-1.81	-0.08	1.19	0.56
TAP2	1.66	0.47	-0.08	-1.03	0.65	-2.95	-0.28	-2.77	-2.82	-0.36	-0.75
TAPBP	-1.47	-0.72	0.39	-1.66	0.00	-2.38	-1.78	-2.15	-2.07	-0.70	-1.25
TAPBPL	-0.18	-1.45	0.70	-2.09	0.75	-3.57	-1.40	-1.94	-1.63	-1.06	-1.19
TBX21	-3.49	4.94	3.98	-0.18	4.01	7.71	-3.23	7.89	-2.48	-0.28	1.89
TBXAS1	-3.23	-3.83	-0.47	-4.14	-0.16	-0.36	-0.49	1.06	-0.72	-0.28	-1.26
TCF3	-0.13	-1.81	-1.03	-0.13	0.34	-1.78	0.34	-2.87	-2.20	0.96	-0.83
TCL1A	1.16	0.03	0.03	-0.18	-0.16	-0.36	-0.49	-0.23	-0.72	-0.28	-0.12
TDO2	-4.89	4.06	-0.93	-4.14	-0.93	-0.36	-4.53	-5.17	-3.78	5.43	-1.52
TGFB1	-2.12	-1.73	-0.39	-0.03	-0.39	-1.11	-0.59	-2.22	-1.71	-1.24	-1.15
TGFB2	-4.66	-1.01	1.03	-0.10	-0.31	1.14	5.22	-1.14	-1.97	1.71	-0.01
TGFB3	10.19	-2.41	0.03	6.36	8.82	0.75	-2.97	-4.55	5.09	3.52	2.48
TGFBR1	-2.20	-0.78	1.14	-0.18	-0.18	-0.65	0.59	-0.88	0.26	0.85	-0.20
TGFBR2	-2.51	-0.83	0.28	-0.03	-0.08	-0.98	-0.93	-2.53	-0.13	-0.26	-0.80
THBD	9.70	1.01	-0.72	9.54	-0.16	-0.36	8.92	-2.41	-3.36	-3.05	1.91
THBS1	-1.11	-4.60	1.22	3.65	-0.21	5.51	2.35	-1.78	-2.59	-0.26	0.22
THY1	-1.73	-2.53	5.09	19.32	10.50	-2.64	3.08	2.56	-4.29	3.52	3.29
TICAM1	-1.84	-0.16	0.57	0.16	-1.16	-1.14	-2.33	-8.09	-4.99	0.72	-1.83
TIE1	-1.34	-7.76	0.03	6.36	-0.16	-0.36	0.98	-1.68	-0.72	3.52	-0.11
TIGIT	0.26	7.22	0.03	-0.18	-0.16	-0.36	-0.49	-0.23	2.20	6.70	1.50

	MesMM98	MesOC99	SiMes1	SiMes4	MMB	Mes1	Mes2	MPP89	MMCA	MesCM98	mFC
TLR1	1.14 <sup>a</sup>	0.96	0.03	0.88	0.18	-3.44	-4.53	-0.23	8.41	9.78	1.32 <sup>b</sup>
TLR2	10.68	2.69	4.09	2.09	2.07	2.82	-1.29	0.10	0.28	0.52	2.41
TLR3	2.38	0.96	1.66	2.33	-0.16	-2.33	0.91	-11.07	-4.76	1.86	-0.82
TLR4	3.00	2.59	9.62	3.96	15.26	6.54	17.69	-1.50	-0.54	9.00	6.56
TLR5	-0.44	-3.13	8.17	-3.47	8.12	-2.87	-1.78	4.37	-1.71	7.19	1.45
TLR7	0.26	0.03	0.03	-0.18	-0.16	-0.36	-0.49	-0.23	-0.72	-0.28	-0.21
TLR8	0.26	-2.74	0.03	-2.53	-0.16	0.54	-0.49	-0.23	-7.14	-0.28	-1.28
TLR9	1.94	-1.37	7.22	-10.50	-0.26	7.29	-5.46	-2.51	1.06	3.52	0.09
TMEM140	5.41	11.53	11.74	3.75	-0.16	-4.81	0.98	-3.10	7.47	3.52	3.63
TMEM173	-1.71	-0.59	3.28	1.16	0.65	-1.99	1.37	-1.50	-0.96	0.05	-0.02
TNF	8.97	2.43	14.97	-0.75	10.42	5.35	4.22	-0.23	8.12	3.21	5.67
TNFAIP3	4.34	2.41	1.89	1.27	3.75	-1.84	1.01	-1.76	-3.39	2.61	1.03
TNFAIP6	-13.73	9.18	8.82	-0.18	-0.16	-0.36	-0.49	-3.34	-0.72	-0.28	-0.13
TNFRSF10B	0.80	0.13	-0.21	-0.83	-0.10	-1.19	-0.72	-2.64	-3.26	0.52	-0.75
TNFRSF10C	7.42	8.74	4.91	6.93	9.31	3.65	-2.07	-3.72	0.54	16.94	5.27
TNFRSF10D	3.85	1.22	0.03	0.52	15.21	2.69	12.80	-2.02	-1.37	-0.39	3.25
TNFRSF11A	1.22	-0.85	-0.72	0.05	8.82	-3.93	8.92	-1.29	0.05	0.05	1.23
TNFRSF11B	-8.48	2.25	10.11	2.22	-0.16	2.46	-5.46	-0.85	-0.57	2.25	0.38
TNFRSF14	1.01	-1.37	0.62	3.34	4.32	0.13	1.40	-1.42	-3.88	-1.34	0.28
TNFRSF17	0.26	-0.36	0.03	-0.18	-0.16	-0.36	-0.49	-0.23	-0.72	-0.28	-0.25
TNFRSF18	-7.58	-5.22	2.38	-0.18	2.09	-0.59	-1.34	-0.23	0.34	8.38	-0.20
TNFRSF1A	-2.02	-1.76	0.47	-1.40	-0.05	-2.74	-1.91	-1.63	-1.11	-1.06	-1.32
TNFRSF1B	2.64	3.16	6.18	7.29	10.58	-0.62	3.13	0.23	-0.72	-5.17	2.67
TNFRSF25	-2.46	-2.84	-0.93	-0.18	-3.44	-1.29	8.92	-0.72	-5.09	1.97	-0.61
TNFRSF4	-6.59	5.92	7.22	-0.18	5.28	3.91	-0.49	1.06	-9.16	5.43	1.24
TNFRSF8	-8.66	0.03	0.03	-0.18	-0.16	-0.36	-0.49	-0.23	-0.72	-0.28	-1.10
TNFRSF9	-1.19	6.75	0.59	-1.45	0.59	-3.47	-1.66	-5.25	0.34	16.01	1.13
TNFSF10	2.25	8.41	6.28	12.39	-0.16	6.83	-0.49	-0.10	2.43	4.40	4.22
TNFSF12	-5.51	0.03	-2.07	-0.18	1.09	-2.20	-0.49	-1.91	3.41	3.52	-0.43
TNFSF13	0.26	3.96	0.03	3.75	-0.16	-0.36	-0.49	-0.23	-5.48	6.26	0.75
TNFSF13B	-8.66	-2.07	3.31	-2.30	1.78	-0.83	0.16	0.67	-3.75	4.47	-0.72
TNFSF18	0.57	-0.44	1.99	3.83	-3.28	-2.69	6.13	-5.51	18.31	15.85	3.48
TNFSF4	-1.55	3.00	-3.28	5.61	11.79	7.29	3.96	-3.03	3.41	-3.98	2.32
TNFSF8	-1.53	0.03	0.03	-0.18	-0.16	-0.36	-0.49	-0.23	6.70	-0.28	0.35
TNFSF9	2.59	1.94	8.59	-3.83	7.68	-2.30	6.23	0.34	0.34	6.18	2.78
TNKS	-1.16	-1.58	0.96	-0.78	-0.26	-3.18	-0.26	-2.41	-2.25	-0.34	-1.13
TP53	-1.55	-2.72	-0.41	-1.63	1.06	-2.43	-1.50	-1.73	-3.93	0.03	-1.48
TPI1	0.83	-1.03	-0.70	-0.85	-0.10	-2.61	-0.23	-1.45	-1.97	0.67	-0.74
TPM1	-3.96	-4.47	-0.96	-0.57	0.00	-3.18	-1.53	-2.84	-2.38	1.01	-1.89
TPSAB1/B2	3.62	0.70	0.03	4.84	1.37	-1.53	5.15	-8.09	-0.59	0.00	0.55
TRAF1	1.47	1.32	-1.01	4.55	3.21	1.14	-4.47	0.26	8.69	5.77	2.09
TRAT1	0.26	0.57	0.03	-0.18	-0.16	-0.36	-0.49	-0.23	-3.96	1.86	-0.27

	MesMM98	MesOC99	SiMes1	SiMes4	MMB	Mes1	Mes2	MPP89	MMCA	MesCM98	mFC
TREM1	-1.53 <sup>a</sup>	0.03	3.98	-0.18	-0.16	-0.36	-0.49	-0.23	2.20	8.02	<b>1.13<sup>b</sup></b>
TREM2	5.53	5.04	-7.37	14.28	-0.16	-0.36	-0.49	-0.23	-0.72	4.58	<b>2.01</b>
TRIM21	1.42	1.58	0.59	1.40	0.21	-2.09	-0.31	-3.39	-0.93	-0.75	<b>-0.23</b>
TSLP	-0.16	-0.36	4.14	-2.87	-0.16	-11.20	9.67	4.97	-2.53	3.83	<b>0.53</b>
TTC30A	1.27	-1.40	-0.57	-1.14	-0.52	-2.74	-0.34	-1.58	1.19	2.38	<b>-0.34</b>
TWF1	0.23	-0.65	0.13	-0.54	-0.16	-2.07	-0.21	-1.76	-1.76	0.08	<b>-0.67</b>
TWIST1	5.33	-9.26	0.03	-0.18	-0.16	-3.65	-2.66	-3.16	-0.72	6.10	<b>-0.83</b>
TWIST2	-1.53	-0.36	0.03	-0.18	-0.16	-0.36	-0.49	-0.23	-0.72	-0.28	<b>-0.43</b>
TYMP	1.94	3.26	-0.62	1.55	4.14	3.34	-0.16	-2.56	4.76	1.47	<b>1.71</b>
TYMS	2.15	-2.38	1.66	0.54	2.64	-1.09	1.94	-0.98	5.22	2.30	<b>1.20</b>
UBA7	-1.73	-0.93	2.53	0.36	8.46	-3.49	2.77	-1.53	2.74	0.05	<b>0.92</b>
UBE2C	-2.79	-1.73	-0.05	1.01	1.11	-1.55	1.50	-0.65	3.18	1.16	<b>0.12</b>
UBE2T	-1.11	-3.96	2.43	-1.01	1.89	-0.65	1.86	-0.98	1.68	3.59	<b>0.38</b>
ULBP2	4.27	4.89	2.09	3.52	3.83	2.43	4.97	-0.91	1.19	0.67	<b>2.69</b>
VCAM1	-5.97	11.02	12.47	2.22	7.27	9.05	12.62	-2.51	-0.72	1.97	<b>4.74</b>
VCAN	-2.46	-1.11	9.57	25.76	1.09	6.59	11.95	-1.73	-0.72	-0.28	<b>4.86</b>
VEGFA	-4.45	-2.17	-1.55	-3.49	-1.19	-0.83	-0.83	-3.49	-2.92	-1.42	<b>-2.23</b>
VEGFB	-1.99	-1.68	-0.78	-2.66	-1.40	-3.57	-1.29	-2.02	-2.82	0.18	<b>-1.80</b>
VEGFC	-3.80	-0.85	-1.19	0.26	-0.31	-2.64	-1.55	-3.08	-1.09	0.91	<b>-1.33</b>
VHL	-0.31	-0.67	0.47	-2.64	0.80	-2.02	-1.27	-2.25	-1.11	-0.54	<b>-0.95</b>
VSIR	-1.55	0.47	1.50	-1.09	1.97	-2.97	0.83	-1.06	-2.82	0.54	<b>-0.42</b>
VTCN1	-0.10	-1.45	0.39	-0.75	0.78	-2.15	1.19	-0.21	1.63	1.97	<b>0.13</b>
WDR76	-1.32	-3.93	1.03	-0.59	3.54	-2.46	2.77	-1.84	2.20	2.20	<b>0.16</b>
WNT10A	4.68	0.03	5.35	-3.41	2.43	-6.26	-1.86	0.44	-3.78	0.34	<b>-0.20</b>
WNT11	9.91	-1.86	0.03	-0.18	-0.16	-0.36	9.67	2.07	-0.72	-0.28	<b>1.81</b>
WNT2	0.26	-8.92	0.03	-0.18	-0.16	5.64	-0.49	-0.23	-0.72	7.63	<b>0.28</b>
WNT2B	1.66	-2.33	1.09	5.41	0.16	-4.73	-2.69	-2.46	3.49	5.90	<b>0.55</b>
WNT3A	-4.40	3.96	0.03	-6.10	-0.16	-0.36	-0.49	-0.23	0.34	-0.28	<b>-0.77</b>
WNT4	0.26	-0.36	4.97	-4.14	-0.16	-3.96	-0.49	-0.23	-0.72	0.93	<b>-0.39</b>
WNT5A	-1.22	0.47	15.18	0.00	0.21	-1.78	-0.08	-1.45	-2.43	-1.19	<b>0.77</b>
WNT5B	-4.22	-5.22	-0.13	0.65	-3.03	-1.66	7.63	-1.11	-8.28	2.46	<b>-1.29</b>
WNT7B	3.31	-3.21	5.69	-0.80	2.66	1.03	-1.06	-0.75	-2.74	-1.29	<b>0.28</b>
XCL1/2	8.95	0.03	0.03	-0.18	5.28	-0.36	2.77	-0.23	-4.45	-4.11	<b>0.77</b>
ZAP70	3.34	5.07	0.03	-0.18	-0.16	-0.36	-0.49	-0.23	-0.72	9.78	<b>1.61</b>
ZC3H12A	-1.29	0.21	1.99	-2.25	2.82	-4.11	-2.30	-2.53	-2.87	-0.93	<b>-1.13</b>
ZEB1	-1.89	-1.45	0.67	-0.65	0.08	-2.15	0.13	-1.37	-1.50	-0.10	<b>-0.82</b>
ZEB2	-1.29	0.05	0.21	-0.52	-0.62	-1.89	0.62	-2.53	-0.72	-0.28	<b>-0.70</b>

<sup>a</sup>, values are reported as fold change (FC), calculated as the ratio between values derived from guadecitabine-treated *versus* untreated cell lines. <sup>b</sup>, FC are expressed as average (mFC) of results from MPM cell lines belonging to each histotype.



FONDAZIONE IRCCS  
ISTITUTO NAZIONALE  
DEI TUMORI

20133 Milano - via Venezian, 1 - tel. 02.2390.1 - codice fiscale 80018230153 - partita i.v.a. 04376350155

Milan, 11 November 2020

Review of the thesis entitled: "*Modelling of cancer immune phenotype by new epigenetic drugs: a strategy to improve efficacy of immunotherapy*", by PhD candidate Dott.ssa Sara Cannito.

To whom it may concern

Major goals of the thesis. The main goal of this thesis was to characterize the immunomodulatory activity of the epigenetic drug guadecitabine on mesothelioma cell lines representing different histotypes. Dr Cannito developed the work by exploiting gene expression assays as well as computational tools to infer main pathways and master regulators of the immune-related activity of guadecitabine. The work also tested the effects of combinatorial treatments of guadecitabine with HDAC and EZH2 inhibitors. In this section of the thesis Dr. Cannito assessed the effects of these combinatorial treatments on immune-related and EMT-related genes, apoptosis and cell migration.

Main results. Mesothelioma cell line treatment with Guadecitabine resulted in significant modulation of immune-related canonical pathways in several of the cell lines (crosstalk between dendritic cells and natural killer cells, and response to infections and inflammation). Master regulatory factors explaining the modulatory effects of guadecitabine included those related to the interferon (IFN)- $\gamma$  signalling pathway (such as IFNL1, STAT1, IRF3 and TNFSF14). In agreement with the biological activity of guadecitabine in different tumor types, most frequently/strongly upregulated genes included the cancer-testis class, TNF family genes, ligands of the NKG2D receptor, IFN-responsive genes, chemokines and receptors, adhesion molecules, members of the toll-like receptor system and inhibitory receptors. Associations between modulation of some genes and the histological subtype of mesothelioma were also found. Combinatorial treatments with different epigenetic drugs in association with guadecitabine led to significant upregulation of HLA antigens (detected by flow cytometry analysis) and adhesion molecules, although most of the effects seen by combination of drugs were not markedly different from the results seen by guadecitabine alone. These results were replicated on expression (by RT-PCR) of cancer testis genes, where again guadecitabine showed to be the most effective drugs with little, if any, additional effects observed in the combinatorial treatments. A strong upregulation of PD-L1 was observed only by the guadecitabine + VPA association. Analysis of modulatory effects of drug combinations on NKG2D ligands (MICA, MICB, and ULBP2, by quantitative PCR) showed that the VPA + guadecitabine association was the most effective treatment. Expression of cadherin genes was histotype-related and either single epigenetic drugs or their combinations exerted little modulatory activity.

Specific comments. The rationale supporting this research work is well presented in the introduction section. The experimental plan is well described. Some of the results are in agreement with the expected immunomodulatory effects described for these drugs in different tumor types, but analysis of mesothelioma lines is a novel approach. Results are analyzed carefully and described with great detail. Some conclusive outline (in graphical/tabular form) of the main findings, possibly to be placed at the end of the results section could be helpful to summarize major effects that support the rationale for clinical translation of these drugs in the mesothelioma immunotherapy field.

Sincerely,

Dr. Andrea Anichini,  
Director, SSD Immunobiology of Human Tumors  
Dept. of Research  
Fondazione IRCCS Istituto Nazionale dei Tumori, Milan, Italy



Gent.ma Cannito,

ho preso visione della sua tesi e mi complimento per l'ottimo lavoro eseguito.

La tesi merita l'ammissione alla discussione pubblica.

Ecco il mio breve commento analitico sul lavoro di tesi:

*The work of dr. Sara Cannito was focused on evaluating the changes in gene expression profiles among 10 malignant pleural mesothelioma (MPM) cell lines treated with DNA the hypomethylating agent guadecitabine. Overall, this latter compound promoted the overexpression of immune-related effectors in MPM cells (the stratification of data according to histological classification seems instead to be a pure speculation due to the limited amount of the cell subtypes). The experimental plan is appropriate and well presented. The conclusions are consistent with the obtained results. In the Introduction section, a Table summarizing all different drugs and inhibitors with their correspondent targets should be helpful for readers.*

Resto a disposizione per eventuali altri commenti od implementazioni da inserire.

Saluti

---

Prof. Giuseppe Palmieri, MD, PhD  
CNR Research Director

Institute Genetic Biomedical Research (IRGB), Branch Sassari, Head  
Unit of Cancer Genetics, Head - National Research Council (CNR)  
Italian Melanoma Intergroup (IMI), Former President

Traversa La Crucca, 3 - Baldinca Li Punti  
07100 Sassari, ITALY  
Tel. +39 079 2841303  
Mobile +39 339 2800855  
Fax +39 079 2841301  
email 1: gpalmieri@yahoo.com  
email 2: giuseppe.palmieri@cnr.it  
PEC: gspalmieri@pec.it  
Skype: giuseppe.palmieri.icb.cnr.it